

2

# Synthesis of a Biologically Active Tethered Growth Factor Surface and Comparison with Soluble Delivery

by

Philip R. Kuhl

B.S. Engineering (1992)

The Cooper Union for the Advancement of Science and Art

Submitted to the Department of Chemical Engineering  
in Partial Fulfillment of the Requirements for the Degree of

DOCTOR OF PHILOSOPHY

IN CHEMICAL ENGINEERING

at the

MASSACHUSETTS INSTITUTE OF TECHNOLOGY


September, 1997

© Massachusetts Institute of Technology 1997. All rights reserved.

Author \_\_\_\_\_

August 26, 1997

Certified by \_\_\_\_\_

  
Linda G. Griffith, Associate Professor  
Thesis Supervisor

Accepted by \_\_\_\_\_

Robert E. Cohen, St. Laurent Professor of Chemical Engineering  
Chairman, Committee for Graduate Students

APR 13 1998

LIBRARIES

# Synthesis of a Biologically Active Tethered Growth Factor Surface and Comparison with Soluble Delivery

by  
Philip R. Kuhl

Submitted to the Department of Chemical Engineering  
on August 26, 1997 in partial fulfillment of the requirements for the degree of  
Doctor of Philosophy in Chemical Engineering

## ABSTRACT

Major impediments to the clinical use of growth factors, polypeptide signaling molecules that promote or inhibit cell growth, are their rapid diffusion away from targeted *in vivo* sites, internalization by cells, and subsequent down regulation of growth factor receptors. In an effort to overcome these limitations, a model biomaterial surface was developed consisting of a glass slide with epidermal growth factor (EGF) covalently linked via long, flexible polymer tethering molecules.

The polymer chosen for these studies was star poly(ethylene oxide) (star PEO). PEO grafting on aminated glass surfaces generally diminished nonspecific protein adsorption onto the glass.  $^{125}\text{I}$ -EGF was grafted onto these surfaces and primary rat hepatocytes were seeded to assess the biological activity of tethered EGF. DNA synthesis was measured by incubation with bromodeoxyuridine (BrdU), a DNA precursor analog, and immunocytochemical detection with enzyme-linked antibodies. A larger fraction of cells synthesized DNA when seeded on tethered growth factor surfaces as compared to unmodified surfaces or controls with only nonspecifically adsorbed EGF at surface densities comparable to the tethered case. The response was equivalent to that observed in response to soluble EGF. The biological activity also varied with the size of the star PEO molecules grafted. Large star PEO tethering molecules caused the hepatocytes to assume a completely rounded morphology when stimulated by EGF in either the soluble or tethered forms. Nonspecifically adsorbed EGF had no such activity.

In order to generalize the tethering method for polymer substrates, and to provide more control of ligand density and spacing on the surface, EGF was covalently coupled to star PEO along with a bifunctional crosslinking molecule, ethylene diamine. The purified protein-polymer conjugate, EGF-PEO-Amine, was internalized by a fibroblast cell line at the same rate as unmodified EGF. This macromolecule was grafted to agarose activated with tresyl chloride or glutaraldehyde, and to glutaraldehyde-treated, aminated glass. Hepatocytes seeded on the latter underwent DNA synthesis at a faster rate than on control surfaces in the absence of EGF. At the highest surface density of EGF examined using this method,  $0.4 \text{ ng/cm}^2$ , the fraction of cells synthesizing DNA was comparable to that for saturating concentrations of soluble EGF ( $10 \text{ ng/ml}$ ). The signaling efficiencies of rat hepatocyte EGF receptors bound to either soluble or tethered EGF were compared. When cell response as a function of initial or steady state receptor occupancy was compared for the two cases, tethered and soluble EGF appeared to signal the cells with the same efficiency. Although it is not clear at this time during what time period ligand-receptor binding truly drives the rate of cell proliferation in this system, existing data indicates that events shortly after receptor binding are most influential. These results imply that the tethered EGF system described herein is as efficient as soluble EGF at stimulating DNA synthesis in rat hepatocytes.

Thesis Supervisor: Linda G. Griffith, Associate Professor

for Sandra

## Contents

Chapter 1 Introduction .....	11
1.1 Motivation.....	11
1.2 Tethered Growth Factors - the state of the art .....	12
1.3 Overview.....	14
Chapter 2 Preparation and Characterization of PEO Tether-Grafted Surfaces .....	16
2.1 Introduction.....	16
2.2 Surface and Polymer Preparation .....	17
2.2.1 Overview .....	17
2.2.2 Materials .....	18
2.2.3 Preparation of Slides for Grafting .....	18
2.2.4 Activation of polymer for surface grafting.....	19
2.2.5 Polymer grafting to aminated glass: protein adsorption experiments.....	19
2.2.6 Polymer grafting to aminated glass: biological activity experiments.....	19
2.3 Protein Adsorption Experiments .....	20
2.3.1 BSA Adsorption .....	20
2.3.2 EGF Adsorption .....	22
2.3.2 Methods and Results .....	22
2.4 Conclusions.....	23
Chapter 3 Tethered Growth Factor Surface Preparation and Chemical Characterization .....	32
3.1 Introduction.....	32
3.2 Validation of Coupling Chemistry .....	32
3.2.1 Background .....	32
3.2.2 Methods and Results .....	33
3.3 EGF Tethering to PEO-Grafted Glass: The Surface First Method .....	34
3.4 Silanol Blocking.....	35
3.5 EGF Coupling to PEO in Solution: The Solution First Method .....	36
3.5.1 Motivation .....	36
3.5.2 Validation of EGF-PEO coupling .....	37
3.5.3 Prevention of PEO gelation during coupling with bifunctional amine .....	38

3.5.4 Synthesis and purification of EGF-PEO-Amine .....	38
3.6 Grafting of EGF-PEO-Amine to Agarose.....	40
3.7 EGF-PEO-Amine Grafting to Aminated Glass Slides .....	41
3.8 EGF-PEO-Amine Iodination and Grafting to Glass .....	42
3.8.1 Methods and Results .....	42
3.8.2 Grafting to Primaria-coated plastic .....	42
3.9 Direct EGF Grafting to Aminated Glass.....	43
3.10 EGF Stability in Solution.....	43
3.11 EGF Aggregation.....	44
3.12 Conclusions .....	45
Chapter 4 Biological Activity Experiments .....	60
4.1 Introduction.....	60
4.1.1 Overview .....	60
4.1.2 The EGF Molecule .....	60
4.1.3 Cell Responses to EGF Stimulation.....	61
4.2 Receptor Binding and Internalization of Soluble EGF and EGF-PEO Conjugate .....	63
4.2.1 Overview .....	63
4.2.2 Equilibrium receptor binding of soluble EGF by rat hepatocytes .....	63
4.2.2.1 Background.....	63
4.2.2.2 Materials and Methods.....	64
4.2.2.3 Results.....	64
4.2.3 Internalization of soluble receptor ligands .....	65
4.2.3.1 Motivation.....	65
4.2.3.2 Background.....	65
4.2.3.3 Materials and Methods.....	67
4.2.3.4 Results and Discussion.....	68
4.3 DNA Synthesis in Response to Tethered EGF .....	69
4.3.1 Overview .....	69
4.3.2 Materials .....	69
4.3.3 Surface first method.....	69
4.3.3.1 Methods .....	69
4.3.3.2 Results and Discussion.....	70
4.3.4 Solution first method.....	71
4.3.4.1 Overview.....	71

4.3.4.2	Materials and Methods.....	71
4.3.4.3	Results.....	72
4.4	DNA Synthesis in Response to Adsorbed EGF.....	72
4.4.1	Background .....	72
4.4.2	Methods.....	74
4.4.3	Results and Discussion .....	74
4.5	Cell morphology experiments .....	75
4.5.1	Overview .....	75
4.5.2	Methods.....	75
4.5.3	Results and Discussion .....	76
4.6	EGF desorption during cell culture .....	77
4.6.1	Surface first method.....	77
4.6.2	Solution-first method.....	77
4.7	Conclusions.....	78
Chapter 5	Comparison of Soluble and Tethered EGF Signaling Efficiency .....	92
5.1	Introduction.....	92
5.1.1	Overview .....	92
5.1.2	Background .....	92
5.2	Model.....	95
5.2.1	Model Overview .....	95
5.2.2	Linear model for cell response vs. initial equilibrium receptor occupancy.....	97
5.2.3	Calculation of initial equilibrium complex number (soluble case), $[C^s_{PM}]_{eq}$ .....	98
5.2.4	Calculation of steady state complex number (soluble case), $[C^s_{TOT}]_{ss}$ .....	99
5.2.5	Tethered ligand-receptor binding model. ....	100
5.2.6	Estimation of receptor binding for tethered EGF.....	102
5.3	Results.....	103
5.4	Discussion .....	108
5.4.1	Discussion Overview.....	108
5.4.2	Membrane Localization .....	112
5.4.2.1	EGFR Distribution in Hepatocytes in Vivo .....	112
5.4.2.2	Focal Adhesion Contacts (FACs) and hemidesmosomes.....	112
5.4.2.3	Membrane Localization Summary.....	113

5.5 Conclusions.....	113
Chapter 6 Future Directions .....	123
6.1 Overview.....	123
6.2 Membrane domain considerations in biomaterials.....	123
6.3 Polymer-enhanced drug delivery.....	124
6.4 Receptor-ligand binding to engineered biomaterials .....	125
6.5 Compartmentalized Signal Transduction.....	126
Appendix.....	128
A1 Analysis of Desorption Controls in Immobilized IL-2 System.....	128
A2 Protein Assays .....	128
A2.1 Background.....	128
A2.2 Protein Assay Experiments .....	129
A3 DNA Synthesis .....	130
A3.1 Background.....	130
A3.2 Thymidine Experiments .....	130
A3.3 DNA synthesis as a function of time using the BrdU assay .....	131
A4 Quantitative Cell Spreading Assay.....	131
A4.1 Introduction .....	131
A4.2 Materials.....	132
A4.3 Methods .....	133
A4.3.1 Microscopy.....	133
A4.3.2 Colored Histological Stains .....	133
A4.3.3 Fluorescence Experiments.....	133
A4.4 Results.....	133
References .....	143

## List of Figures

Figure 2.1 Silane chemistry used to covalently attach organic functional groups to glass substrates.....	24
Figure 2.2 Tresyl chloride chemistry. ....	25
Figure 2.3 XPS of star PEO-grafted slide before (A) and after (B) brief rinse with water.....	26
Figure 2.4 BSA adsorption on slides grafted with star and linear PEO. ....	27
Figure 2.5 BSA adsorption on PEO-grafted slides. ....	28
Figure 2.6 EGF adsorption to and desorption from aminated glass slides.....	29
Figure 2.7 Effect of Triton X-100 on adsorption of EGF to aminated glass slides. ....	30
Figure 2.8 Effect of pH on EGF adsorption to aminated glass slides. ....	31
Figure 3.1 Schematic of EGF surface first tethering protocol to glass-grafted PEO.....	46
Figure 3.2 Solution first EGF tethering protocol.....	47
Figure 3.3 BSA grafting to tresyl chloride activated agarose beads.....	48
Figure 3.4 Desorption profile for tethered EGF surfaces and controls during washes. ....	49
Figure 3.5 EDA blocking of reactive silanols.....	50
Figure 3.6 Gel filtration of reaction products after coupling of EGF to star PEO 3510.....	51
Figure 3.7 EGF-PEO-EDA grafting to tresyl-agarose.....	52
Figure 3.8 EGF-PEO-EDA grafting to glutaraldehyde-treated agarose.....	53
Figure 3.9 EGF-PEO-Amine grafting to aminated glass slides.....	54
Figure 3.10 EGF-PEO-Amine grafting to aminated glass dishes post iodination. ....	55
Figure 3.11A EGF-PEO-Amine grafting to Primaria-coated tissue culture plastic.....	56
Figure 3.11B EGF-PEO-Amine grafting to Primaria-coated tissue culture plastic.....	57
Figure 3.12 EGF grafting to glutaraldehyde-treated, aminosilane derivatized glass. ....	58
Figure 3.13 Typical chromatogram of 125I-EGF.....	59
Figure 4.1 EGF-induced rounding of A-431 cells.....	81
Figure 4.2 Equilibrium binding data for rat hepatocytes. ....	82
Figure 4.3 Internalization plot for EGF and EGF-PEO-Amine (both in soluble form). ....	83
Figure 4.4 DNA synthesis activity of cells exposed to soluble or tethered EGF. ....	84
Figure 4.5A Soluble and tethered EGF dose response data (isolation 1).....	85
Figure 4.5B Soluble and tethered EGF dose response data (isolation 2).....	86



Figure 4.5C Soluble and tethered EGF dose response data (isolation 3).....	87
Figure 4.6 DNA synthesis dose response to soluble EGF by cells seeded on glass with or without adsorbed EGF.....	88
Figure 4.7 Extent of cell spreading on surfaces grafted with star PEO (f=70, Ma=5200) from 1% solution and exposed to soluble or tethered EGF. ....	89
Figure 4.8 Extent of cell spreading vs. PEO grafting density. ....	90
Figure 4.9 Desorption of EGF from glass slides in culture.....	91
Figure 5.1 Model for RTK signal transduction through the Ras-activated protein kinase cascade.....	115
Figure 5.2 Size scales for determination of local EGF concentration in the tethered case.....	116
Figure 5.3 Dose response data for soluble EGF in terms of fraction of total receptors occupied at initial binding equilibrium. ....	117
Figure 5.4 Dose response data for tethered EGF in terms of fraction of total receptors occupied after cells have attached to the surface but before significant spreading.....	118
Figure 5.5 Curve fits to tethered EGF dose response data (isolation 1) with various values of $K_D^t$ .....	119
Figure 5.6 Cell surface and internalized receptor-ligand complex number at steady state as a function of ligand concentration rat hepatocytes stimulated by EGF.....	120
Figure 5.7 Dose response data for soluble EGF stimulation of primary rat hepatocytes as a function of steady state surface and internalized, undegraded receptor-ligand complexes.....	121
Figure 5.8 Dose response data for tethered EGF (isolation 3) in terms of fraction of total receptors occupied twenty hours after seeding .....	122
Figure A.1 Typical standard curve for the Bio-Rad DC Protein Assay.....	135
Figure A.2 Typical Standard Curve for Flourescamine Assay. ....	136
Figure A.3 Standard curves for OPA assay.....	137
Figure A.4 DNA synthesis activity in rat hepatocytes as a function of time after seeding. ....	138
Figure A.5 Phase contrast images of unstained cells and cells stained with hematoxylin+eosin.....	139
Figure A.6 Fluorescence and phase contrast images of cells stained with CMFDA at the indicated concentrations.....	140

Figure A.7 Fluorescence and phase contrast images of cells stained with 50M DAF. ....	141
Figure A.8 Fluorescence and phase contrast images of cells stained with 10M Hoechst. ....	142

## List of Tables

Table 2.1 Experimental conditions for BSA adsorption experiments.....	21
Table 3.1 EGF Grafting and Adsorption Data -mean +/- sd in ng/cm2.....	35
Table 3.2 PEO gelation experiments.....	38
Table 3.5 Anion Exchange Buffers for conjugate purification.....	40
Table 3.3 Stability of 125I-EGF under various storage conditions. ....	44
Table 3.4 Dissociation of EGF aggregates.....	45
Table 4.1 Internalization rate constant for EGF at three different EGF concentrations. ....	68
Table 5.1 Steady state model parameter values for EGF-hepatocyte system.....	100
Table 5.2 Effect of tethered ligand dissociation constant on $m_{eq}^t$ values. ....	105
Table 5.3 Effect of $[R]_{T,0}$ on $m_{eq}^s$ and $m_{eq}^t$ .....	105
Table 5.4 Signaling efficiencies of receptors bound to soluble and tethered EGF. ....	107
Table A.1 Cell proliferation Assay Results. ....	131

## Chapter 1

### Introduction

#### 1.1 Motivation

Since the 1960's many peptide signaling molecules that promote or inhibit cell growth have been isolated. These factors produce profound effects on cell behavior, including proliferation, migration and changes in protein synthesis and secretion. As a result they have been considered promising agents to promote wound healing (ten Dijke and Iwata 1989; Meyer-Ingold 1993). Nevertheless, and despite intensive effort, to date few growth factors have been developed into clinical products. These include erythropoietin and granulocyte-macrophage colony stimulating factor (GMCSF), which stimulate specific cell types and hence can be delivered systemically (Lawrence and Diegelmann 1994).

Clinical use of growth factors is complicated by problems of delivery on the cellular level. Since growth factors often stimulate more than a single cell type, systemic delivery of these agents to treat wound healing is impractical due to overgrowth of non-targeted cells. Even when delivered locally, the problem of diffusion of the polypeptide away from the targeted site persists (Buckley *et al.* 1985). This problem is enhanced by down-regulation of the growth factor receptor and intracellular degradation of the growth factor following endocytosis.

Growth factors are only one component of the extracellular milieu from which cells receive signals. Signaling molecules are present in insoluble form as components of the extracellular matrix (ECM). Structural ECM proteins such as collagen and fibronectin provide signals to cells in addition to physical support (Juliano 1996) and ligands for many growth factor receptors including fibroblast growth factor, GMCSF, and IL-3 are bound reversibly to the ECM, often through proteoglycans (reviewed in Ruoslahti and Yamaguchi

1991). Consistent with this physiological paradigm, researchers attempting to synthesize materials as matrices for cell growth have immobilized ECM proteins and their polypeptide analogs on solid supports to increase cell attachment and spreading thereon (Massia and Hubbell 1991). In such systems cytokines and other signaling molecules have been added to the medium and have thus been part of the fluid phase.

In the present work this paradigm was inverted with respect to a single growth factor, with the goal of developing a system in which the problems of diffusion away from the targeted site, internalization of the factor and thereby down-regulation of the receptor could be overcome, and a tunable delivery of signal to specifically targeted cells could be achieved.

## **1.2 Tethered Growth Factors - the state of the art**

Proteins may be caused to associate with a solid substrate through covalent or non-covalent means, for example, to retain an enzyme on a solid packing for later re-use. The general term for this procedure is immobilization, a process which may result in partial or complete denaturation of the protein. Attachment may be accomplished by creating one or more covalent bonds between the protein and the surface with or without the use of a polymer linker. Creation of a covalent linkage between a solid substrate and a ligand molecule via a polymer linker is known as tethering.

Immobilization of growth factors has been studied as an approach to cell stimulation since at least 1969 (Cuatrecasas). Generally the main limitation of the studies has been a failure to account for stimulation of cells by desorption of nonspecifically adsorbed protein. Two recent bodies of work will be discussed below.

Y. Imanishi and co-workers studied cell growth on surfaces to which insulin and various adhesion molecules were covalently linked (Ito *et al.* 1992; Liu *et al.* 1992; Ito *et al.* 1993; Zheng *et al.* 1994; Ito *et al.* 1996). Insulin was immobilized on poly (ethylene terephthalate) (PET) and poly (methyl methacrylate) (PMMA) using water soluble

carbodiimide (WSC) after basic hydrolysis of the polymer to create carboxyl groups. Membranes were then washed in PBS and desorption of nonspecifically adsorbed protein during the washes was monitored using a colorimetric assay with a sensitivity of 1  $\mu\text{g/ml}$ . Desorption was reportedly complete after 24 hours. Growth of mouse fibroblast STO cells seeded on the insulin-immobilized membranes was measured indirectly by lactate dehydrogenase assay. Growth induction of the fibroblast cells was observed on the polymer films having immobilized insulin; however, no data was provided on desorption of nonspecifically adsorbed insulin or hydrolysis of the immobilization linkage during the cell culture period. Hydrolysis of the covalent linkage is a well-recognized limitation of the WSC immobilization method, and the limited sensitivity of the colorimetric assay implies that desorption of less than 1  $\mu\text{g}$  insulin from the surface would not be detected. This is significant since the same authors showed that significant stimulation of mouse fibroblast STO cells occurs at an insulin concentration of 1  $\mu\text{g/ml}$ . Hence, it remains unclear whether the growth induction observed was truly due to immobilized growth factor.

Horwitz *et al.* (1993) reported that immobilized IL-2 preserved the viability of an IL-2 dependent cell line. This cell line required a minimum concentration of 6.7  $\text{pg/ml}$  of IL-2 to maintain cell viability. Glutaraldehyde cross-linking was used to immobilize 0.6 - 28  $\text{ng/cm}^2$  IL-2 on activated polystyrene membranes. Desorption controls were made by plating cells on top of microporous filter paper placed on top of the immobilized growth factor membranes. The researchers reported that the filter paper allowed efficient diffusion of IL-2, but they did not provide any protein adsorption data for the filter paper. Adsorption of IL-2 to the filter paper would invalidate the control since it would prevent desorbing IL-2 from reaching the cells, while no such barrier would exist for the experimental samples. As described in Appendix A1, complete adsorption of IL-2 to the filter paper is highly probable in their system.

In addition to maintenance of cell viability, IL-2 normally causes cell proliferation. The immobilized system described by Horwitz *et al* did not mimic this biological activity.

The question therefore remains whether tethered growth factor is capable of activating the same signaling pathways as the soluble molecule.

### 1.3 Overview

In this work, epidermal growth factor (EGF), a well studied growth factor with several known biological activities (see section 4.1.3) was tethered to a solid support using long flexible polymers to facilitate receptor binding. A glass substrate was chosen as a model system to facilitate observation of cells in contact with the tethered growth factor, and because chemical modification of glass for polymer grafting is well established. This system was chosen to avoid the limitations of previous studies described above. Most cell types possess receptors for EGF, and require nanomolar concentrations (on the order of 10 ng/ml) of the growth factor for stimulation. This is in contrast to the pg/ml concentrations of IL-2 required to maintain viability of the cell line used by Horwitz *et al.* In this work the surface density of tethered EGF was closely matched to the number of cell surface receptors to avoid stimulation by a small fraction of leachate. Numerous chemistries are available for linking EGF to polymers. Murine EGF has the advantage that it possesses only one primary amine, the N-terminus, and thus chemistries that target primary amines (like the one used in this study) result in tethered molecules of a single conformation.

Chapters 2 and 3 detail two methods for tethering EGF, one in which the polymer tethers are grafted first and then the EGF is linked to the surface (the surface-first method) and a second in which a protein-polymer conjugate is synthesized and the macromolecule is linked to the surface (the solution-first method). These chapters also detail experiments to characterize protein adsorption onto these surfaces, a phenomenon which is important for cell attachment in the case of extracellular matrix (ECM) proteins and for cell signaling in the case of growth factor adsorption since nonspecifically adsorbed molecules can eventually desorb and stimulate cells. Other factors which were important for the

development of the experimental system are described including EGF aggregation and stability of the iodinated protein in solution.

Chapter 4 describes biological activity experiments for tethered EGF surfaces synthesized by both methods, for EGF nonspecifically adsorbed to glass, and for soluble EGF and EGF-polymer conjugate. Details on important assays for this system can be found in the appendix. The data demonstrate that tethered EGF stimulates the same biological activities as soluble EGF, but that EGF is rendered inactive when it is nonspecifically adsorbed to glass. In addition, binding parameters for soluble EGF to rat hepatocytes are obtained and the rate of internalization of soluble EGF-polymer conjugate is found to be comparable to that for soluble EGF.

A quantitative comparison of the efficiency of rat hepatocyte EGF receptors bound by soluble EGF to those bound by tethered EGF is given in Chapter 5, after development of the appropriate models. The analysis indicates that EGF receptors produce mitogenic signals with comparable efficiencies when bound by soluble or tethered ligand. Finally, Chapter 6 presents ideas for further research in the field of engineered biomaterials.

## Chapter 2

# Preparation and Characterization of PEO Tether-Grafted Surfaces

### 2.1 Introduction

Poly(ethylene oxide) is widely recognized as an unusual polymer due to its lack of interaction with proteins (Merrill 1993). It is therefore an ideal candidate for use as a tether to link EGF to a solid surface, since a surface with grafted PEO would adsorb little protein and present an inert background to cells. This chapter describes the preparation of glass surfaces with grafted poly(ethylene oxide) and protein adsorption experiments that were performed on these surfaces. EGF was subsequently linked to some of these surfaces (Chapter 3) and used in biological activity experiments (Chapter 4).

Protein adsorption onto biomaterials for implantation is of critical importance for biocompatibility since adsorption after contact with blood and body fluids is widely believed to be the first step leading to all subsequent cellular interactions. Poly(ethylene oxide) (PEO) renders surfaces resistant to protein adsorption and is a component of many FDA-approved implantable devices (Amiji and Park 1992; Lee *et al.* 1989; Gombotz *et al.* 1991; Desai and Hubbell 1991). This effect is believed to be due to steric repulsion (Jeon *et al.* 1991). Many approaches have been described for covalent grafting of PEO to surfaces (Gombotz *et al.* 1991). PEO can be synthesized in the linear form, having one free hydroxyl at the end of each arm, or in the star form, having many arms and thereby many points of attachment (Rempp *et al.* 1990). In this chapter data on protein adsorption onto surfaces grafted with various forms of PEO at different concentrations is presented.

Characterization of protein adsorption on the tethered growth factor surfaces developed in this study was important for several reasons. Adsorption of EGF during surface preparation was potentially problematic since nonspecifically adsorbed growth



factor could desorb during cell culture and stimulate cells, confounding interpretation of observed biological effects in the presence of the tethered growth factor. Experiments were performed to assess the extent of nonspecific EGF adsorption to glass and to develop optimal wash conditions for its removal. On the other hand, adsorption of ECM proteins to the surfaces is required for cell adhesion, as described in Chapter 3. A surface was required, then, that permitted sufficient ECM adsorption for cell attachment but did not adsorb excess EGF.

X-ray photoelectron spectroscopy (XPS), sometimes also referred to as electron spectroscopy for chemical analysis (ESCA) was used to assess the stability and composition of the aminated and PEO-grafted glass substrates. XPS involves bombarding a surface with X-rays, causing the release of core electrons. The kinetic energies of the released electrons are measured by a detector and their binding energies are calculated. This permits unambiguous determination of the of the elements present in the sample, as well as information concerning the chemical bonding character of the elements. The X-rays penetrate only 10-100 angstroms into the surface, permitting the determination of the elemental composition of the surface. While translation of XPS spectra into quantitative measures of surface-bound molecules is difficult, the relative amounts of various species can be readily determined to assess the extent of surface changes with time.

## **2.2 Surface and Polymer Preparation**

### 2.2.1 Overview

The preparation of the polymer-grafted substrates may be described briefly as follows: Glass slides were amine-derivatized using standard silane chemistry (Figure 2.1); then, linear or star PEO of different molecular weights was tresyl activated (Figure 2.2) and grafted to the glass surfaces. These slides were then ready for protein adsorption measurements or re-activation and EGF coupling.

### 2.2.2 Materials

Borosilicate glass slides, used in all protein adsorption and DNA synthesis experiments, were from Fischer. Glass microscope slides with hydrophobic Teflon masks (5 mm diameter “wells”) were used for the cell rounding experiments; they were purchased from Cel-Line Associates, Inc., Newfield, NJ. EDA (N-(2-aminoethyl)(3-aminopropyl) trimethoxysilane) was from Huls America, Inc. Star poly(ethylene oxide) produced by living anionic polymerization from divinyl benzene cores were provided by Rempp (Rempp et al. 1990; Lutz and Rempp 1988). Two lots of star molecules were used in these studies. Star 3510 had an average of 70 arms per star with arm molecular weight 5,200. Star BS10.2 had 180 arms/star with arm molecular weight of 10,000 Da. All chemicals used in the surface preparation were reagent grade. All water was purified with a 4-cartridge Milli-Q system to 18 megaohm purity.

### 2.2.3 Preparation of Slides for Grafting

Substrates were prepared as described previously by Stenger *et al.* (1992) (Figure 2.1). Glass microscope slides were cleaned by immersion in 1:1 methanol:HCl for at least 30 minutes. They were rinsed twice in water and immersed in 1:1 water:concentrated sulfuric acid for at least 30 minutes. After another rinse in water, the slides were placed in boiling water for 15-30 minutes. Under a nitrogen atmosphere, the freshly cleaned slides were placed in a solution of freshly mixed acidic methanol (1.0 mM acetic acid in methanol), 5.0 % H<sub>2</sub>O, and 1 % EDA for 15 minutes, and then rinsed three times in methanol. Following the final rinse the slides were either baked on a 120 °C hot plate for 5-10 minutes or placed in a 120 °C oven for 5-10 minutes. The slides were stored in a desiccator at room temperature and used within 12 weeks. XPS analysis of the surface indicated the presence of nitrogen on the surface; values of 4-6 at% were consistently achieved, and were stable after soaking for 14 days in pH 7 carbonate buffer (Allgor 1995).

#### 2.2.4 Activation of polymer for surface grafting

Star poly(ethylene oxide) was dissolved in methylene chloride (10 wt%) and dried over molecular sieves at 4 °C. Dry triethylamine (110 µl/g polymer) and tresyl chloride (75 µl/g polymer-2.5-fold molar excess over star arms) were added to the dry polymer solution. After 90 minutes the solvent was evaporated under vacuum and the polymer was re-dissolved in acidified methanol (0.06M HCl in methanol) at room temperature and then allowed to precipitate at -20 °C. This precipitation procedure was repeated six times to remove unreacted tresyl chloride. The solvent was then evaporated and the dried, activated polymer stored under nitrogen at room temperature in a glove box or in a tightly capped glass vessel at -70°C. Storage in air quickly resulted in the formation of crosslinks in the activated polymer, which resulted in the formation of a gel upon addition of water. This process was retarded by storage under a nitrogen atmosphere in a glove box at room temperature, but gel formation was observed after approximately 9 months of storage under these conditions. It was found that low temperature storage (-70°C, nitrogen atmosphere) retarded crosslinking of the activated polymer such that no gel formation was observed even after storage for one year .

#### 2.2.5 Polymer grafting to aminated glass: protein adsorption experiments

Tresyl-activated PEO of different sizes and molecular weights (see Table 2.1) were grafted by incubation for 24 hours in PBS, pH 7.4. Linear PEO L18500 and L2000 were grafted to the same surfaces sequentially. PEO-grafted surfaces for these preliminary experiments were provided by Susan Allgor of Professor Merrill's laboratory.

#### 2.2.6 Polymer grafting to aminated glass: biological activity experiments

Tresyl-activated star PEO (star 3510) was grafted to aminated slides from solutions containing 0.1%, 1%, and 5% (wt/vol) polymer and tresyl-activated star BS10.2 was grafted from a 3.6% solution. Star polymer was used to permit ligand clustering. After

polymer grafting slides were again analyzed by XPS. A typical high resolution C-1s scan (which provides information as to the chemical bonding of carbon atoms on the surface) is shown in Figure 2.3. The presence of the C-O ether peak indicates the presence of PEO. These surfaces were used in biological activity experiments as described in chapter 4.

## **2.3 Protein Adsorption Experiments**

### 2.3.1 BSA Adsorption

Bovine serum albumin (BSA) adsorption experiments were performed on aminated glass slides grafted with PEO in the linear (L3400) and star form (S3509) (see Table 2.1) to determine to what extent adsorption of large proteins representative of ECM molecules was inhibited on the two surfaces. BSA was chosen because it is a reference protein commonly used in protein adsorption studies and for its low cost. Aminated glass slides, with no grafted PEO, were used as controls. Petri dishes were passivated with 6.2  $\mu\text{g/ml}$   $^{14}\text{C}$ -BSA in PBS, the solutions were removed and fresh solutions (same concentrations) were added. The slides were incubated in the BSA solution for 24 hours resting on the bottom of the petri dishes under static conditions. The slides were then removed from the dishes, excess liquid was removed with an aspirator, and the slides were placed in scintillation vials. Results are shown in Figure 2.4; they indicate that star PEO grafting significantly inhibited protein adsorption, but the results for the linear molecule were not statistically different from controls ( $p=0.15$ ).

**Table 2.1** Experimental conditions for BSA adsorption experiments.

Polymer	Concentration in Grafting Solution (wt/vol %)	Concentration of BSA in Adsorbing Solution ( $\mu\text{g/ml}$ )
L3400	5.1	6.2
S5309 (55 arms/star, $M_a=10,000$ )	4.3	6.2
L18500 and L2000	6.2	6.1

To further characterize the inhibition of protein adsorption by these two forms of PEO, protein adsorption experiments were performed on aminated glass slides grafted with linear PEO (L3400), with star PEO (S3509) and a combination of two sizes of linear PEO (L18500 and L2000). Large molecules of PEO may be expected to leave gaps on the surface after they are grafted; by filling these gaps with shorter segments of linear PEO, protein adsorption could presumably be reduced further. The slides were incubated overnight in  $6.1 \mu\text{g/ml}$   $^{14}\text{C}$ -BSA in PBS in petri dishes. The slides were affixed to the petri dishes using epoxy, allowing the protein solution to contact one side of the slides in these experiments. Results are shown in Figure 2.5. In this experiment, all three surface treatments inhibited BSA adsorption, with the combination of large and small linear molecules inhibiting protein adsorption to a modestly greater extent than the star form or the single linear form. These results have important implications for the biological activity experiments discussed in Chapter 4. Star PEO grafting did not completely inhibit BSA adsorption, implying that cell adhesion could be enhanced by allowing nonspecific adsorption of matrix proteins rather than covalent grafting along with the tethered growth factor. As shown below, the BSA adsorption results also indicate that nonspecific adsorption of EGF can be expected on these surfaces.

### 2.3.2 EGF Adsorption

To help determine optimal conditions for minimizing the adsorption of EGF and for maximizing its desorption during subsequent wash steps, experiments were performed to test how adsorption was affected by changes in pH and addition of surfactant during adsorption and during washes.

### 2.3.2 Methods and Results

It is widely believed that proteins adsorb less strongly onto hydrophilic as compared to hydrophobic surfaces. Aminated glass slides are hydrophilic, so it was expected that most EGF adsorbed to the surface during coupling could be washed off. To test this hypothesis,  $^{125}\text{I}$ -EGF was adsorbed onto aminated glass slides for two hours and then the slides were counted in a gamma counter and soaked repeatedly in aqueous buffer with counting between each solution transfer.

Slides incubated with 17 ng/ml  $^{125}\text{I}$ -EGF (sp. act. 116  $\mu\text{Ci}/\mu\text{g}$ ) in PBS and washed in pH 7 buffer retained 33% of the EGF initially adsorbed after 3 days (Figure 2.6). A subsequent 1 day wash in PBS containing 1% Triton X-100, a surfactant, resulted in desorption of 1/2 the remaining adsorbed EGF (Figure 2.6).

To further characterize the effects of the surfactant on the adsorption and desorption of the protein, adsorption experiments were conducted in the presence and absence of 1% Triton X-100. Slides were exposed to an average of 2.4 ng/ml  $^{125}\text{I}$ -EGF for 24 hours. A lower concentration was used in this experiment to conserve protein. This does not affect the validity of the results since the limit of detection for this system is approximately 10  $\text{pg}/\text{cm}^2$  and a comparative measure of protein adsorption on different surfaces is required. One group of slides was incubated with the EGF in PBS with 1% Triton X-100 and washed in PBS with 1% Triton X-100, and one was incubated with the EGF in PBS without surfactant and washed in 1% Triton X-100. Less EGF adsorbed initially to slides in the presence of surfactant, but after one day of soaking in the surfactant-containing

buffer the percent adsorbed was the same (Figure 2.7). These experiments showed that surfactant addition in the wash buffer was as effective at minimizing protein adsorption as surfactant addition during the adsorption step.

The pH of the protein-containing solution can greatly influence protein adsorption behavior. Proteins adsorb most strongly to hydrophobic substrates near their isoelectric point (pI), the pH at which the overall electrostatic charge of the protein is zero. The pI of EGF is 4.63. Experiments were performed to determine whether adsorption of EGF to glass, a hydrophilic substrate, is affected by changes in pH. Slides were pre-adsorbed in 1% Triton X-100 solutions and incubated in 1.2 ng/ml EGF (with surfactant) overnight at pH 5 and pH 7. The amount of EGF adsorbed to the various slides after one wash is shown in Figure 2.8. More EGF adsorbed to the glass slide at the lower pH, consistent with observations for hydrophobic substrates.

## 2.4 Conclusions

The silane coating was found to be stable for at least two weeks in aqueous buffer by XPS. The stability of the star PEO was determined by measuring the removal of grafted  $^{125}\text{I}$ -EGF from the surface, as will be discussed. Activated star PEO was successfully grafted to aminated glass as shown by XPS. This grafting procedure, as well as that utilizing linear PEO chains, reduced protein adsorption as compared to ungrafted controls (Figures 2.4 and 2.5). These results agree with earlier studies showing that covalent attachment of PEO reduces protein adsorption (Gombotz *et al.* 1991). EGF adsorption onto aminated glass slides was studied. Nonspecific adsorption could be reduced to very low levels by repeated washing (Figure 2.6), by using a nonionic surfactant in the wash solution (Figure 2.7), and by adsorption at near neutral pH (Figure 2.8). These results informed subsequent attempts to desorb EGF after surface grafting reactions.

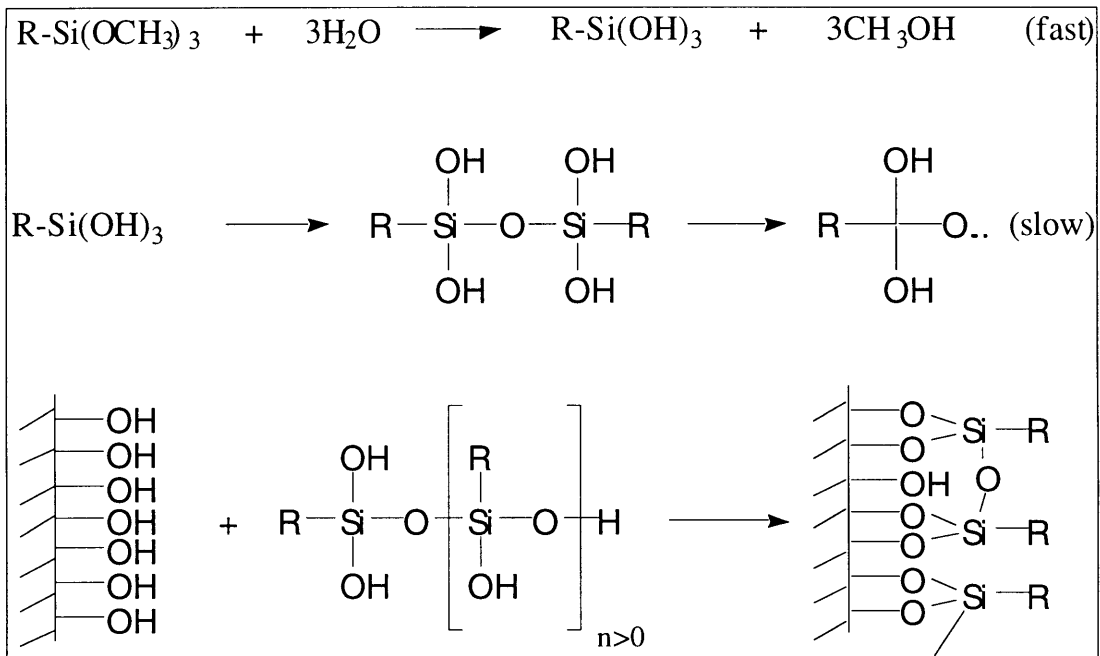
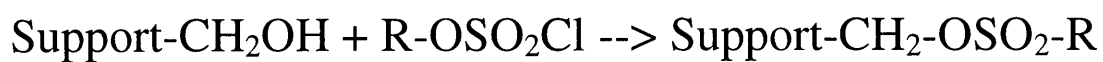


**Figure 2.1** Silane chemistry used to covalently attach organic functional groups to glass substrates.  $\text{R}=(\text{CH}_2)_3\text{NH}(\text{CH}_2)_2\text{NH}(\text{CH}_2)_2\text{NH}_2$  for these studies.



- **Activation**



- **Coupling**

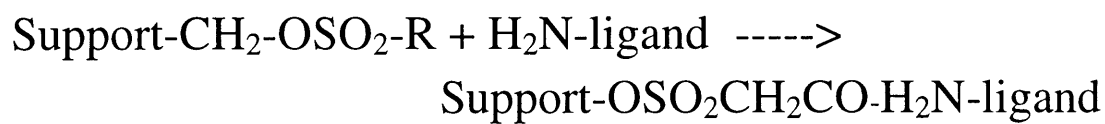


**Figure 2.2** Tresyl chloride chemistry.

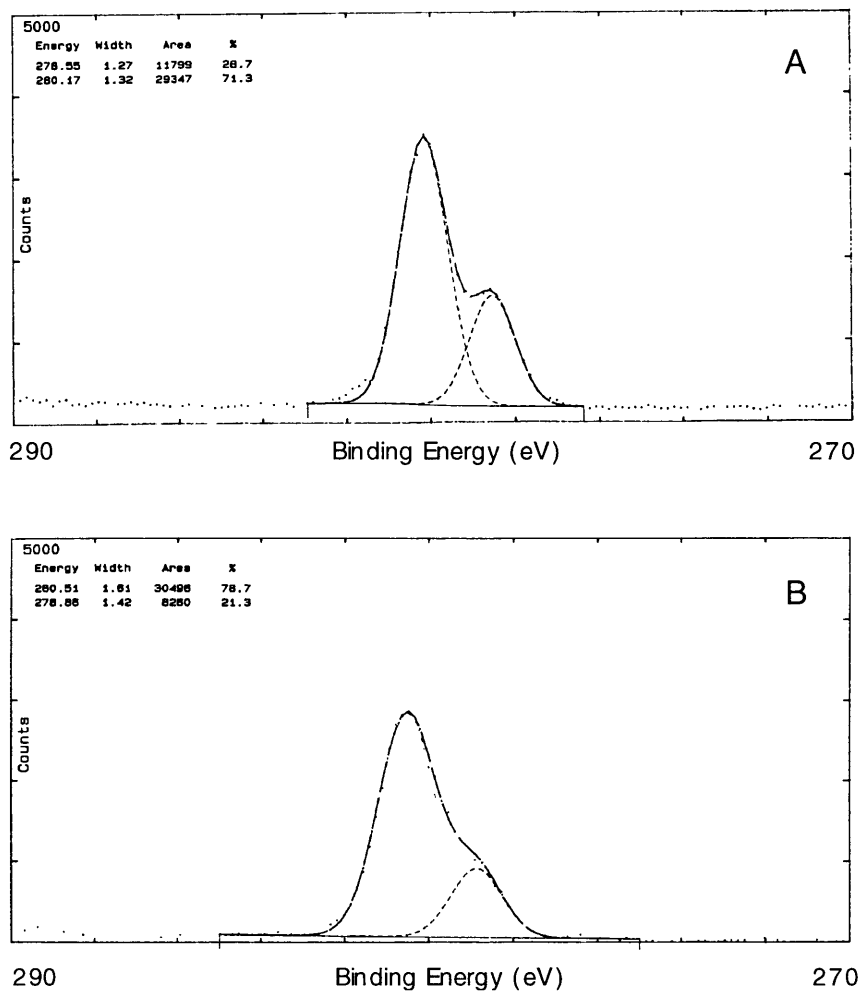


**Figure 2.3** XPS of star PEO-grafted slide before (A) and after (B) brief rinse with water. High resolution C(1s) scan.

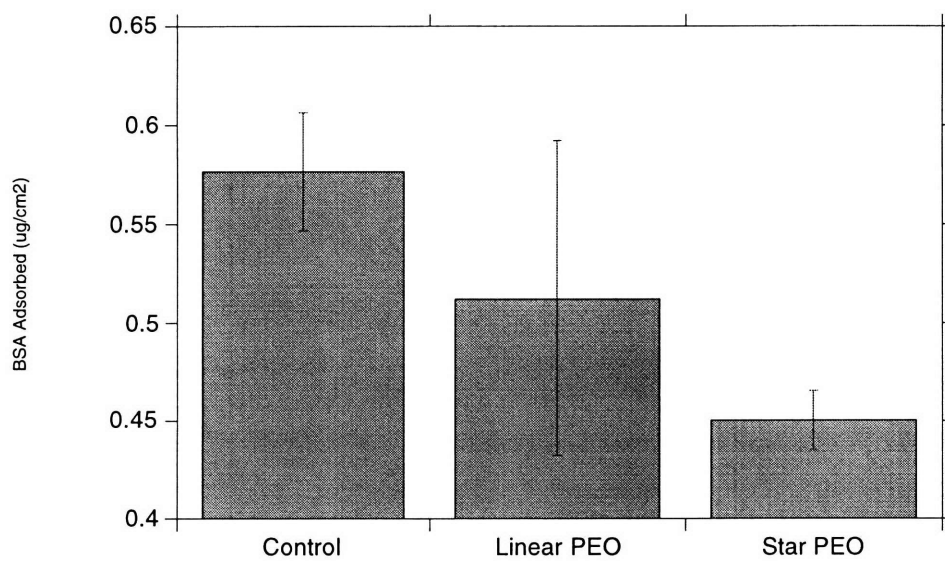


**Figure 2.4** BSA adsorption on slides grafted with star and linear PEO. Aminated glass slides were used as controls. Slides were incubated with  $6.2 \mu\text{g}/\text{ml}$   $^{14}\text{C}$ -BSA in PBS for 24 hours. The protein solution contacted both sides of the slides.

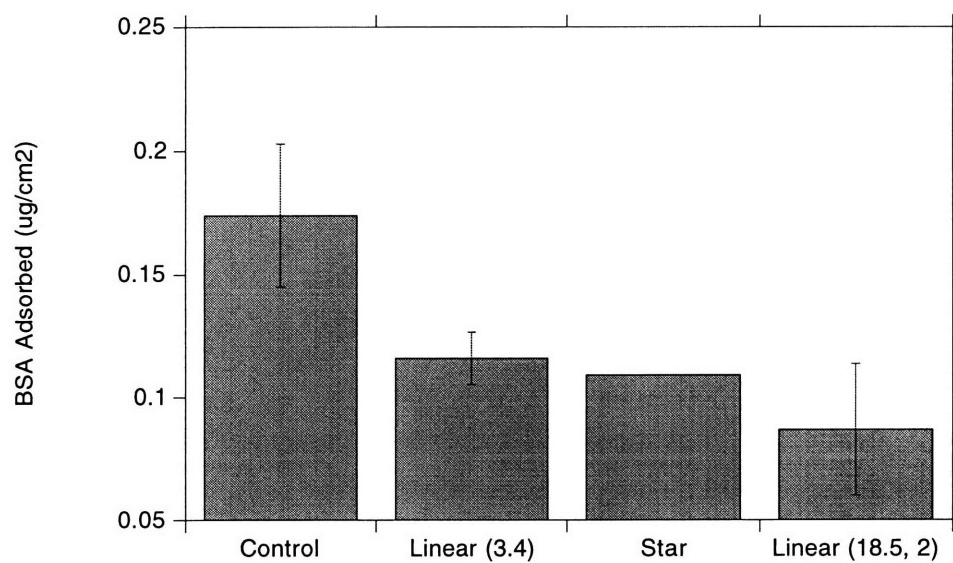


**Figure 2.5** BSA adsorption on PEO-grafted slides. Adsorption was measured on aminated glass slides (control) and on aminated glass slides grafted with linear PEO (3400 MW), with star PEO (186 arms/star, 5500 arm MW) and a combination of two sizes of linear PEO (2,000 and 18,500 MW, 1:1 molar ratio). Slides were incubated with 6.1  $\mu\text{g/ml}$   $^{14}\text{C}$ -BSA (one side only) in PBS overnight.

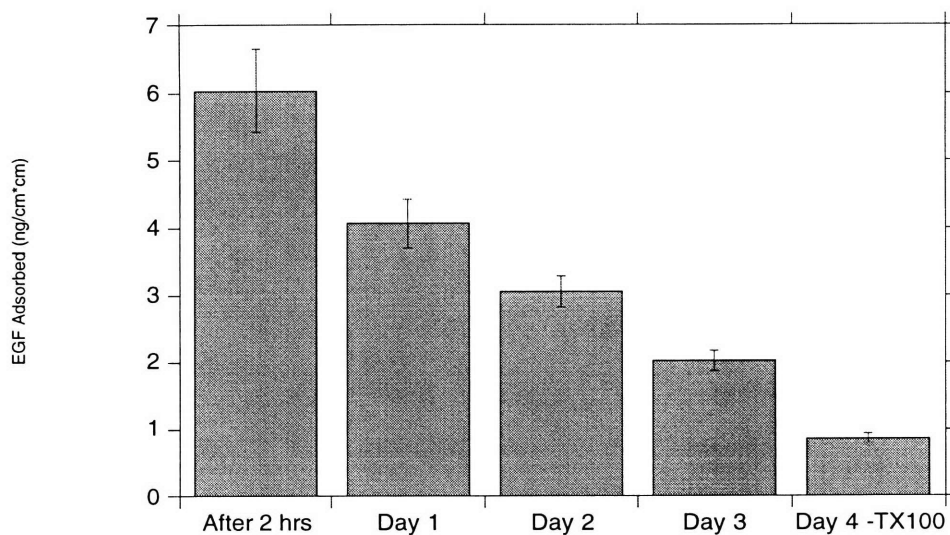


**Figure 2.6** EGF adsorption to and desorption from aminated glass slides. Slides were incubated with 17 ng/ml  $^{125}\text{I}$ -EGF (sp. act. 116  $\mu\text{Ci}/\mu\text{g}$ ) in PBS for two hours, the slides were counted in a gamma counter and soaked repeatedly in aqueous buffer with counting between each solution transfer. After day 3 the slides were transferred to PBS containing 1% Triton X-100.

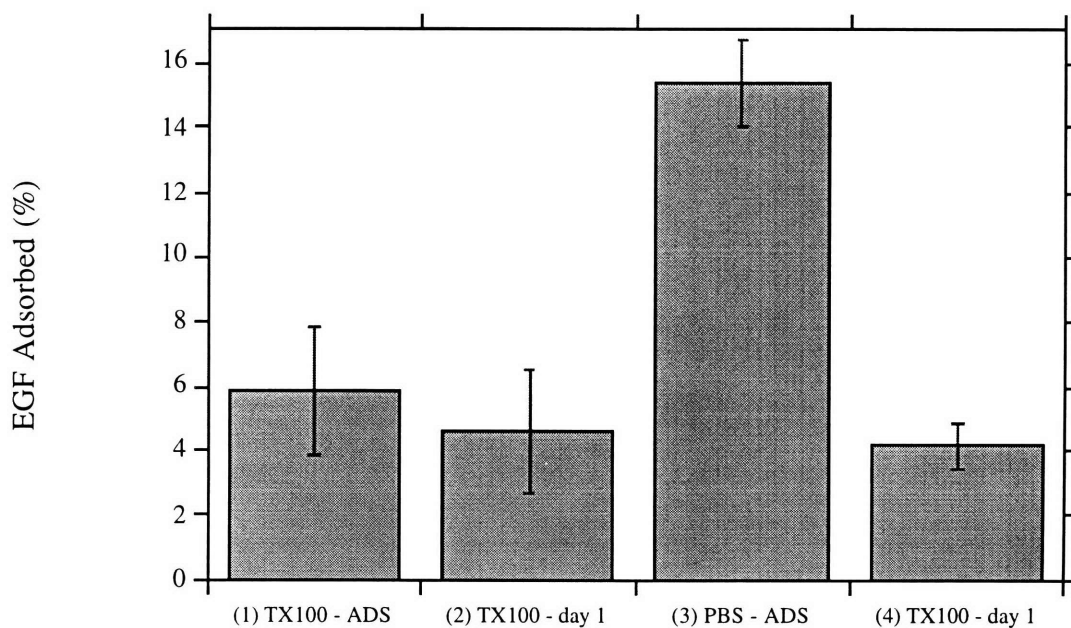


**Figure 2.7** Effect of Triton X-100 on adsorption of EGF to aminated glass slides. Slides were exposed to an average of 2.4 ng/ml  $^{125}$ I-EGF for 24 hours. One group of slides were adsorbed in PBS with 1% Triton X-100 (column 1) and washed in 1% Triton X-100 (column 2), and one was adsorbed in PBS without surfactant (column 3) and washed in 1% Triton X-100 (column 4).

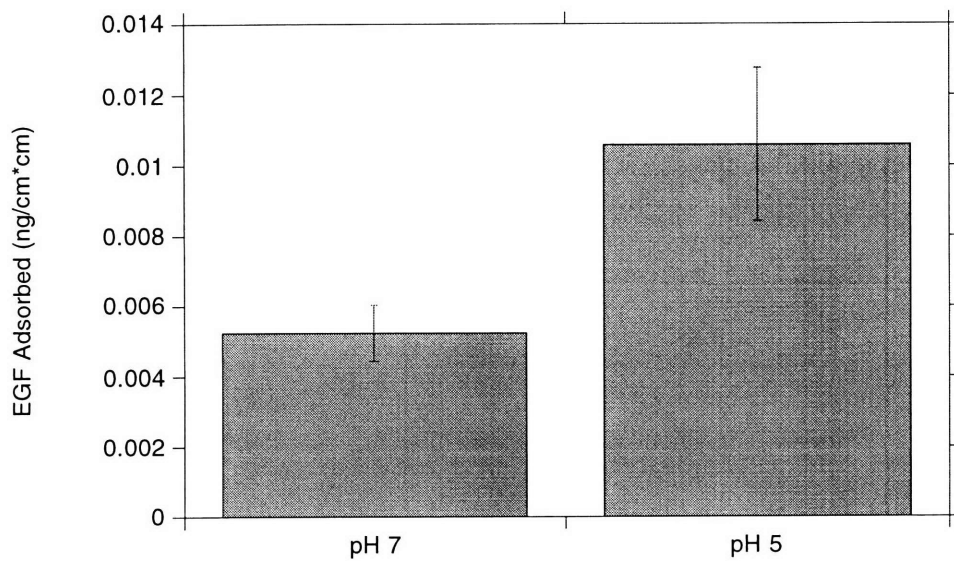


**Figure 2.8** Effect of pH on EGF adsorption to aminated glass slides. Slides were pre-adsorbed in 1% Triton X-100 solutions and incubated in 1.2 ng/ml EGF (with surfactant) overnight at pH 5 and pH 7. Plotted is the amount of EGF adsorbed to the various slides after one wash.

## Chapter 3

# Tethered Growth Factor Surface Preparation and Chemical Characterization

### 3.1 Introduction

Two methods for tethering epidermal growth factor to glass were developed. The surface-first method (Figure 3.1) involves linking the protein to star PEO previously grafted to the surface. The solution-first method (Figure 3.2), which allows greater control over ligand spacing and density, and can be used for polymer substrates, involves synthesis of a protein-polymer conjugate which is then grafted to the surface. Preliminary experiments to validate key portions of the synthesis schemes are described, as well as an attempt to overcome a complication of the surface-first method, direct grafting of EGF to tresyl-activated glass. In addition, binding and internalization data are presented for EGF and EGF-polymer conjugate which are important both for validation of receptor binding in the system chosen and for calculation of binding parameters used in Chapter 5. Finally, important issues for the synthesis of these surfaces including EGF stability and aggregation, and grafting of conjugate after iodination are discussed.

### 3.2 Validation of Coupling Chemistry

#### 3.2.1 Background

Many surface chemistries exist for linking polymers to aminosilanized glass and for coupling biomolecules to polymers. Important selection criteria for these studies include a stable linkage and minimal coupling sites on the protein to minimize its inactivation. Tresyl chloride chemistry meets these criteria for this system. Coupling of primary amine-containing ligands to tresyl-activated PEO (TC-PEO) yields a stable secondary amine



linkage, and since murine EGF has only one primary amine (the N-terminus) and no sulfhydryls, there is only one major coupling site on the protein. To limit the use of expensive reagents, the tethering scheme was validated with BSA and an alternative substrate, tresyl-activated agarose (TC-Ag), a standard substrate for immobilization of biomolecules. Bovine serum albumin (BSA) was grafted to TC-Ag to determine appropriate reaction conditions, and then EGF was successfully grafted to TC-Ag.

### 3.2.2 Methods and Results

Bovine serum albumin was grafted to tresyl chloride-activated agarose (Sigma). Controls for nonspecific adsorption were generated by incubating tresyl chloride-activated beads in 0.2 M tris(hydroxymethyl) aminomethane (Tris base) buffer (pH 8.5) for 12 hours at room temperature to cause complete displacement of TC groups by hydrolysis and reaction with Tris base. Experimental samples and controls were briefly washed in coupling buffer (0.2 M HEPES, pH 7.8) before coupling, which was accomplished by incubating 37 mg beads overnight in 0.01 - 1 mg/ml <sup>14</sup>C-BSA in a volume of 2 ml for a molar excess of tresyl chloride groups over BSA of roughly 100:1 at the lowest concentration and 1:1 at the highest BSA concentration. The amount of protein grafted was determined by subtracting the amount associated with the controls from that associated with the experimental samples. Results are shown in Figure 3.3. At the highest BSA concentration used (1 mg/ml), approximately 17 ng BSA grafted per mg beads.

Epidermal growth factor was grafted to TC-Ag by incubating 3.85 mg beads with <sup>125</sup>I-EGF in 0.2 M HEPES-HCl buffer (pH 7.8) at a concentration of 7 ng/ml in a volume of 1 ml for 15 minutes. The amount of EGF grafted to the beads after washing was 1.2 pg/mg beads, or 0.06% EGF yield. In an attempt to increase the yield of grafted EGF the reaction was carried out in a smaller volume. When 100 µg EGF was contacted with 40 mg beads in a slurry (just enough volume to cover the beads) the yield of EGF increased to

5.8%, or 0.14  $\mu\text{g}$  EGF/mg beads. These results indicated the importance of maximizing reactant concentrations in these bimolecular protein-activated substrate reactions.

### 3.3 EGF Tethering to PEO-Grafted Glass: The Surface First Method

Determination of the amount of EGF covalently grafted and nonspecifically adsorbed to the surfaces was accomplished using  $^{125}\text{I}$ -EGF. This method has the advantage that it permits non-destructive analysis of the surfaces, whereas colorimetric or fluorescent determination of protein requires removal of the protein from the surface. Slides prepared as described in section 2.2.6 were reactivated with tresyl chloride. Slides were first dried in graded ethanol solutions (25%, 50%, 75%, 100% ethanol) and then rinsed in dry acetone and finally in dry methylene chloride. To tresyl activate the grafted star PEO, slides were immersed for 1 hour in 0.06 *M* tresyl chloride, 0.07 *M* triethylamine in methylene chloride at room temperature under a dry nitrogen atmosphere.  $^{125}\text{I}$ -EGF of murine origin was grafted to activated slides in 0.01 *M* phosphate buffer (pH 7.4) (0.01 mg/ml EGF, 8-10 mCi/mg) for 12 hours at room temperature. EGF was grafted to the activated slides within 6 months after activation. The same procedure was followed for control slides which had been mock-activated (tresyl chloride omitted). EGF could not graft to the mock activated slides, only adsorb; these controls are therefore also called the adsorption controls. To remove nonspecifically adsorbed EGF, the slides were washed in PBS, low pH acetate buffer, or 0.01 *M* phosphate buffer (pH 7.4) with or without 0.025% Triton X-100 and with or without 0.1 wt% bovine collagen and 0.003 wt% Cell-Tak cell adhesive (Cell-Tak was added during the final wash only). Collagen was added both as a stabilizer to inhibit disproportionation (see section 3.10), and as an ECM protein to enhance cell attachment to the substrate. Cell-Tak, a formulation of the polyphenolic proteins extracted from *Mytilus edulis*, was added to the final wash to increase cell attachment to substrates. A typical  $^{125}\text{I}$ -EGF desorption profile (out of three experiments) is shown in Figure 3.4. The amount of EGF associated with the various slides after washing is

tabulated in Table 3.1; some EGF remained adsorbed to the slides even after repeated washing. The amount of EGF covalently grafted to the slides was determined by subtracting the amount adsorbed to the adsorption controls from the amount associated with the tresyl-activated slides. Analysis of the slopes of the curves in Figure 3.4 is instructive. If both activated and mock-activated slides have the same amount of adsorbed EGF and the difference in EGF density is due to covalently bound EGF, the amount desorbed per wash should be equivalent for both sets of slides. This would imply that the stepwise slopes of the curves should be the same for each wash. This is in fact the case, as can be seen in Figure 3.4; a student's t-test verified that there was no statistical difference in the desorption rates for the activated and mock-activated slides ( $p=0.6$ ).

**Table 3.1** EGF Grafting and Adsorption Data -mean +/- sd in  $\text{ng}/\text{cm}^2$ .

Polymer Grafted	Activated	Mock Activated	Difference
5% star PEO 3510	8.52 +/- 1.3 (n=3)	5.20 +/- 0.84 (n=3)	3.32 +/- 1.7
1% star PEO 3510	9.59 +/- 2.3 (n=2)	4.20 +/- 0.04 (n=2)	5.39 +/- 2.3
0.1% star PEO 3510	8.25 +/- 0.6 (n=4)	4.63 +/- 0.85 (n=4)	3.62 +/- 0.98
3.6% star BS10.2	5.06 +/- 0.08 (n=2)	1.86 +/- 0.42 (n=2)	3.20 +/- 0.5
<b>Average</b>	<b>7.99 +/- 1.26</b>	<b>4.20 +/- 0.78</b>	<b>3.79 +/- 1.44</b>

### 3.4 Silanol Blocking

In addition to activating the terminal hydroxyls of the PEO star molecules, tresyl chloride activation could theoretically activate residual silanols present on the glass substrate. To test this hypothesis, glass slides without PEO were activated with tresyl chloride or mock activated as described in the previous section, and incubated with 1 ng  $^{125}\text{I}$ -EGF in a 10  $\mu\text{l}$  droplet. After extensive washing, comparison of the experimental and control slides indicated coupling of 4.2 (+/- 1.6)  $\text{ng}/\text{cm}^2$  EGF (n=2). Tresyl chloride

activation of residual silanols on the surface could be reduced by derivatizing them with a nucleophilic compound after aminosilane derivatization and before polymer grafting and re-tresylation. For example, after addition of the aminosilane, the slides could be exposed to tresyl chloride and then to ethylene diamine (EDA). Introduction of additional primary amines onto the surface would be an additional advantage of this method. Figure 3.5 shows the results of one experiment in which this blocking method was attempted and then the surfaces (and unblocked glass controls) were re-tresylated and challenged with  $^{125}\text{I}$ -EGF. Aminated glass slides were immersed for 1 hour in 0.06 M tresyl chloride and 0.07 M triethylamine in methylene chloride at room temperature. These were then incubated in 0.1M EDA, 0.1M triethylamine in methanol overnight to block activated silanols. Slides were re-tresylated (tresyl chloride omitted for controls) and then incubated with EGF (4 ng in a 10  $\mu\text{l}$  droplet). Unblocked aminated glass controls were re-activated or mock activated and incubated with EGF in an identical manner. Slides were rinsed once before counting. Only a small fraction of reactive silanols were eliminated by this procedure. These results imply that some fraction of the ligand grafted via the solution first method was actually grafted directly to the aminated glass. However, it is expected that the activated PEO end groups are more accessible to react with the protein than silanols on the surface, and similarly that EGF tethered via PEO arms would be more available to bind cell surface receptors than EGF directly linked to the surface. It is thus likely that the biological effects observed for cells seeded on tethered EGF grafted by the surface first method (see section 4.3.3) were due to receptor binding by PEO-tethered ligand molecules.

### **3.5 EGF Coupling to PEO in Solution: The Solution First Method**

#### **3.5.1 Motivation**

In section 3.3 EGF linking to surface-grafted PEO was described. This approach is not readily generalized to other substrates, particularly polymers. For example, re-

activation with tresyl chloride is done routinely in methylene chloride, a good solvent for many polymers. A more versatile tethering scheme involves coupling EGF and a bifunctional amine to the star polymer in solution and then linking the macromolecule to amine-derivatized substrates using any number of amine-linkage chemistries. Such a scheme is described in Figure 3.2 (Sofia *et al.* 1997). Greater versatility in EGF clustering (# EGF/star) and EGF surface density, and decreased nonspecific EGF adsorption are also possible using this method.

Although in many respects glass is an ideal substrate for these experiments, it was determined that some activation of residual silanols on the glass did occur during the re-activation step shown in Figure 3.1 and described in section 3.3. This resulted in some coupling of EGF directly to the glass. These silanols are difficult to block (see section 3.4), further motivating efforts to develop an alternative coupling scheme.

The objective of these experiments was to synthesize surfaces with enough tethered EGF to occupy a fraction (10%) to several fold (10-100X) of available EGF receptors. Assuming a projected cell area of  $500 \mu\text{m}^2$ , and knowing rat hepatocytes have approximately  $10^5$  receptors per cell, 10% receptor occupancy implies a tethered EGF density of  $125 \text{ pg/cm}^2$ , or  $25 \text{ pg/slide}$  for this system. With a specific activity of  $25 \mu\text{Ci}/\mu\text{g}$ , a moderate degree of substitution, that surface concentration would correspond to 3000 CPM. This is easily within the sensitivity of available equipment.

### 3.5.2 Validation of EGF-PEO coupling

To verify that EGF could couple to star PEO in solution, murine EGF ( $0.15 \text{ mM}$ ) was reacted with tresyl-activated linear PEO ( $\text{MW}=5,000$ ) in solution at pH 8.5 and the reaction products were separated using SDS-PAGE (16.5%). The results (not shown) indicated significant coupling of EGF to the PEO at a 1:1 molar ratio and significantly greater coupling when a 10-fold molar excess of tresyl-PEO was used. To confirm this result, star PEO 3510 ( $M_a=5,500$  with 70 arms per star) was reacted with  $^{125}\text{I}$ -EGF (1:1

molar ratio star arms:EGF). The reaction products were separated on a 2ml Sephadex G-50 (Pharmacia) gel filtration column equilibrated with 1% linear PEO (MW=5000) in 0.2 M phosphate buffer, pH 7, to inhibit hydrophobic interactions with the column (Figure 3.6).

### 3.5.3 Prevention of PEO gelation during coupling with bifunctional amine

Since EDA is a bifunctional linker using the tresyl chloride chemistry, it was necessary to define conditions which would prevent gelation (via crosslinking) during activation. EDA and 2-aminoethanol (used in place of EGF, from Sigma) were added to 0.2 M phosphate buffer (pH 8.5) and then tresyl-activated star PEO 3510 (in 10 mM sodium acetate) was added. The final concentration of star arms was 0.16 mM. Several molar ratios, chosen to test a wide range of potential activation conditions, were used in the experiments; they are shown in Table 3.2. In all cases the solution remained totally clear and no gel was observed even after 24 hours.

**Table 3.2** PEO gelation experiments. No gel was observed in any of the experiments.

Experiment	Concentration (mM) 2AE:EDA:star arms	Molar Ratio 2AE:EDA:star arms
1	0.16 : 2.3 (10) <sup>-3</sup> : 0.16	70:1:70
2	0 : 1600 : 0.16	0:10 <sup>4</sup> :1
3	0.16 : 0.016 : 0.16	10:1:10
4	0.16 : 0.16 : 0.16	1:1:1
5	1.6 : 0.16 : 0.16	10:1:1

### 3.5.4 Synthesis and purification of EGF-PEO-Amine

Star PEO with only amine-terminated arms (PEO-Amine) and with both Amine- and EGF-terminated arms (EGF-PEO-Amine) were prepared by adapting the conditions described above. Star PEO was activated with tresyl chloride and reacted with ethylene diamine (EDA) in 0.1 M phosphate buffer (pH 7) with 0.1% dimethoxy PEO

(Polysciences, MW=1,000) as a stabilizer (see section 3.10) with or without  $^{125}\text{I}$ -EGF (mouse, 39.2 mCi/mg) overnight at room temperature. Star PEO, EGF, and EDA concentrations were 9.6  $\mu\text{M}$ , 1.6  $\mu\text{M}$  and 16 mM, respectively. To separate EDA from Amine-PEO the sample was dialyzed in a Slide-a-lyzer dialysis cassette (Pierce) for 12 hours. The yield of the reaction was measured by incubating a small sample of the purified Amine-PEO with O-phthaldialdehyde, which produces a fluorescent derivative in the presence of primary amines (see Figure A.3 for standard curves). The EGF-containing reaction mixture was separated on a Bio-Gel P-60 (Bio-Rad) gel filtration column (bed height 11.5 cm) which was packed using 0.1 M phosphate buffer (pH 7). The star PEO fractions were pooled. Amine-PEO-EGF was separated from amine-terminated PEO having no EGF (PEO-Amine) using a Hi-Trap Q anion exchange column from Pharmacia and the buffers listed in Table 3.5 using the following procedure. The sample was loaded onto the column after equilibration with buffer C, the column was washed with five column volumes of buffer C to elute PEO-Amine, and Amine-PEO-EGF was eluted in five column volumes of buffer B. The yield of the reaction was typically approximately 0.1% in terms of EGF (0.1% of the EGF bound to star arms) and roughly 300 ng EGF bound to star polymer was obtained after purification. Scale up of this process was limited by the use of radioactive EGF in the synthesis step. Since the yield of the reaction was so low, protein with high specific activity was required (39 mCi/mg). Nuclear Regulatory Commission regulations limit the amount of radioactive iodine in the laboratory, making significant scale up impossible. An attempt to perform the synthesis with non-radioactive EGF and iodinate the conjugate after the purification is described below.

**Table 3.5** Anion Exchange Buffers for conjugate purification.

Buffer	Constituents
A. Low pH, low salt	10 mM bis tris propane pH 7
B. Low pH, high salt	10 mM bis tris propane, 0.5 M NaCl pH 7
C. High pH, low salt	10 mM piperidine, pH 10.8

### 3.6 Grafting of EGF-PEO-Amine to Agarose

To validate the synthesis of EGF-PEO-Amine and to help determine reaction conditions for grafting to glass slides, the polymer macromolecule was grafted to 4% beaded agarose activated with either tresyl chloride or glutaraldehyde. Comparison of the yields for beads treated with glutaraldehyde or tresyl chloride gave an indication of the loss of coupling capacity due to hydrolysis of the tresyl chloride. Tresyl activated beads were rinsed briefly in coupling buffer or blocked for 3 days in 0.1M Tris (pH 8.5) to displace tresyl groups (adsorption control) and then rinsed briefly in coupling buffer. Three coupling buffers were tested, 0.1M phosphate (pH 7), 0.1M phosphate (pH 8), and 0.1M phosphate (pH 9). Beads were incubated with 0.6 pmole EGF (in the form of EGF-PEO-Amine) for 24 hours at each pH, rinsed with coupling buffer, and counted. The results are indicated in Figure 3.7; grafting was achieved, and the reaction did not appear to be sensitive to pH in the range tested. Glutaraldehyde-treated beads were rinsed briefly in coupling buffer (0.1M phosphate, pH 7) or blocked by incubation overnight in 1M Tris-HCl in the presence of reductant (sodium cyanoborohydride) and then rinsed briefly in coupling buffer. The beads were incubated with 0.4 pmole EGF with reductant for 24 hours before rinsing successively in 1M NaCl, 7M guanidine hydrochloride (GuHCl), and 0.2% sodium dodecyl sulfate (SDS) to remove nonspecifically adsorbed EGF. The counts associated with the quenched and unquenched beads after these washes are shown in



Figure 3.8. The high percentage of activity remaining associated with the quenched beads after the extremely vigorous washing regimen (compare with 5% adsorbed for the TC-Ag beads) suggests that the quenching was not sufficient to remove all of the reactive aldehyde groups, and that grafting to both samples occurred. That grafting was achieved was important because the grafting reaction is quite specific for primary amines; these results therefore strongly suggested that EGF-PEO-Amine had indeed been synthesized.

The difference in yields for the two reactions, 15-18% for the tresyl chloride activated agarose and 80% for glutaraldehyde-substituted beads is also noteworthy. The tresyl chloride grafting method is hindered by the competing hydrolysis reaction; indeed, hydrolysis is the basis for the blocking procedure described above. No such competition occurs for the Schiff's base reaction, which may explain the higher yield obtained.

### **3.7 EGF-PEO-Amine Grafting to Aminated Glass Slides**

Aminated glass slides were chosen as the model system for testing the biological activity of tethered EGF. Numerous cross-linkers are available for amine functional groups. Glutaraldehyde was chosen because it yields a hydrolytically stable secondary amine linkage after reduction with sodium cyanoborohydride, a mild reducing agent, and because of its superior yield compared to tresyl chloride (see previous section).

Aminated glass slides were rinsed in anhydrous methanol and 0.1M phosphate (pH 7) and then incubated with 2.5% glutaraldehyde and 23 mM sodium cyanoborohydride overnight at room temperature. For adsorption controls, glutaraldehyde was omitted. Both control and experimental slides were incubated with EGF-PEO-Amine (37 nM) in 0.1M phosphate buffer with 0.1% dimethoxy PEO (stabilizer used in place of BSA--see section 3.10) and 23 mM sodium cyanoborohydride for two hours to tether EGF. As an additional control for potential biological effects of the tether, PEO-Amine was grafted at the same concentration under the same reaction conditions. The slides were then rinsed in phosphate buffer repeatedly and the amount of radioactivity on the tethered EGF surfaces and on the

adsorption controls was measured using a Molecular Dynamics model 4005 phosphorimager. Two separate syntheses were performed using two distinct batches of conjugate. Good grafting was achieved with minimal adsorption, as shown in Figure 3.9.

### **3.8 EGF-PEO-Amine Iodination and Grafting to Glass**

#### 3.8.1 Methods and Results

The use of  $^{125}\text{I}$ -EGF in the synthesis of EGF-PEO-Amine limits the scale up of this process, as described in section 3.5.4. In an effort to scale up the conjugate synthesis, EGF-PEO-Amine was prepared (see section 3.5.4) with uniodinated EGF. After purification, the conjugate was iodinated using the same protocol as for EGF. The yield of product was significantly increased, to 0.9  $\mu\text{g}$  with specific activity 79 mCi/mg. However, when this conjugate was reacted with glutaraldehyde-treated aminated glass dishes at a concentration of 228 ng/ml, very little grafting was observed (see Figure 3.10). Moreover, significant nonspecific adsorption (1.73 ng/cm<sup>2</sup>) occurred even after extensive washing with PBS. The reason for this high degree of nonspecific adsorption is unknown, but may be due to uncharacterized derivatization of the star arms during the iodination reaction.

#### 3.8.2 Grafting to Primaria-coated plastic

The conjugate prepared as described in the previous section (3.8.1) was reacted with tissue culture plastic having a primary amine functionality (Primaria--Becton Dickinson) which was derivatized with glutaraldehyde in the manner described in section 3.7. Adsorption on these surfaces was also quite high compared to glass (compare Figure 3.11 to Figure 3.9) but significant grafting to the Primaria dishes was achieved. The exact composition of the Primaria surfaces is unknown, and it is not clear why grafting of the conjugate post-iodination to Primaria was achieved but not to aminated glass.

### 3.9 Direct EGF Grafting to Aminated Glass

In an attempt to graft EGF directly to aminosilane-derivatized glass without the use of a polymer tether, slides were incubated at room temperature with a 2.5% solution of glutaraldehyde or buffer without glutaraldehyde (adsorption control) overnight, washed thoroughly and incubated with various concentrations of  $^{125}\text{I}$ -EGF for two hours. Slides were rinsed several times before exposure to phosphor plates, using the same wash protocol as for EGF-PEO-Amine grafting (Figure 3.9). The results are shown in Figure 3.12; little or no EGF grafting was apparent. This may be because nonspecific adsorption of EGF competes with grafting sites on the surface. Alternatively, EGF may couple and adsorb to the same sites on the slides. Additional experiments using chaotropic salts or surfactants may be necessary to elucidate this.

### 3.10 EGF Stability in Solution

Variation in coupling efficiency between experiments provided motivation to investigate the stability of radiolabeled EGF during storage. Commercial preparations of  $^{125}\text{I}$ -EGF normally contain 0.1% BSA and standard iodination protocols call for addition of BSA after iodination of the target protein. Since BSA, or any other nucleophilic compound, competes with EGF for tresyl-activated hydroxyls it was omitted from preparations of EGF used for these experiments. Apparently this protein serves not only to inhibit EGF adsorption during storage but removal of the label from the protein as well. Label removal is presumably due to radiolysis caused by the radioactive decay. Radiolysis of water leads to the formation of free radicals which may go on to attack the labeled protein. The carbon-iodine bond is relatively weak and therefore particularly susceptible to rupture (Knoche 1991). EGF was stored at 4°C and -70°C with different stabilizers. Aliquots were taken at various time points and the amount of protein-associated label was determined by precipitation with phosphotungstic acid or by gel-filtration chromatography.

**Table 3.3** Stability of  $^{125}\text{I}$ -EGF under various storage conditions.

Stabilizer	Temperature	# days	% protein-associated
None	-70	18	34
BSA	-70	6	85
BSA	-70	23	69
PEO	-70	6	81
PEO	-70	18	66
PEO	4	18	56
Mannitol	-70	13	3

As shown in Table 3.3, in the absence of EGF or any other stabilizer, only 34% of the label was associated with the EGF after 18 days. 0.1% BSA limited the loss of label to 69% after 23 days, and importantly, 1% PEO (1000 MW) was also effective. As expected, label removal was hindered by lower temperature, but surprisingly storage in 0.1% mannitol, often used as a free-radical scavenger, caused almost complete removal of the label.

### 3.11. EGF Aggregation

Since EGF is a much smaller molecule than star PEO, a logical method to separate unreacted EGF from EGF-PEO is gel filtration chromatography. When  $^{125}\text{I}$ -EGF alone was applied to a Superdex-75 column (volume 24 ml) and fractions collected a chromatogram such as that shown in Figure 3.13 was reproducibly obtained. It was assumed that the first peak eluting just after the void volume was aggregated EGF. In later experiments EGF was treated with different agents to dissociate the aggregates. The results are shown in Table 3.4. They imply that the mechanism of aggregation is non-covalent but that chaotropic salt or strong detergent is required for dissociation. Aggregation can be a problem in this system because EGF aggregates can co-elute with EGF-PEO-Amine on gel filtration columns.

**Table 3.4** Dissociation of EGF aggregates.

Dissociation Buffer	% EGF Aggregated
50 mM phosphate, pH 7.4	4.5
0.1% Triton X-100, pH 8.5	1.9
0.1% Triton X-100, pH 12	2.9
3.5 M Guanidine HCl	0.27
3.5 M Guanidine HCl + DTT	0.23
0.1% SDS	0

### 3.12 Conclusions

EGF was covalently linked to aminated glass slides via star PEO using two methods. These surfaces were used in subsequent biological activity experiments described in the next chapter (see Table 3.1 and Figure 3.9 for the amounts of EGF tethered to the slides). Nonspecific adsorption was significantly reduced using the solution-first method. This method has the further advantages that it can be used for polymer substrates using standard amine crosslinking chemistries. The problem of activation of the glass substrate by trisyl chloride, which is not ameliorated by blocking with ethylene diamine, is also avoided using this method. The solution-first method was difficult to scale up using iodinated protein, however. An attempt to iodinate the conjugate after purification gave a molecule that adsorbed strongly to glass but did not graft to Primaria-coated plastic. Direct EGF grafting to aminated glass without a PEO tether was unsuccessful.

Iodinated EGF requires the presence of a stabilizer (BSA in most commercial formulations) to reduce the rate of disproportionation of the radiolabel. Dimethoxy PEO substitutes well for BSA when protein stabilizers are undesirable, as in this case. Finally, it was found that EGF oligomerizes in solution by a noncovalent mechanism that can be overcome by chaotropic agents.

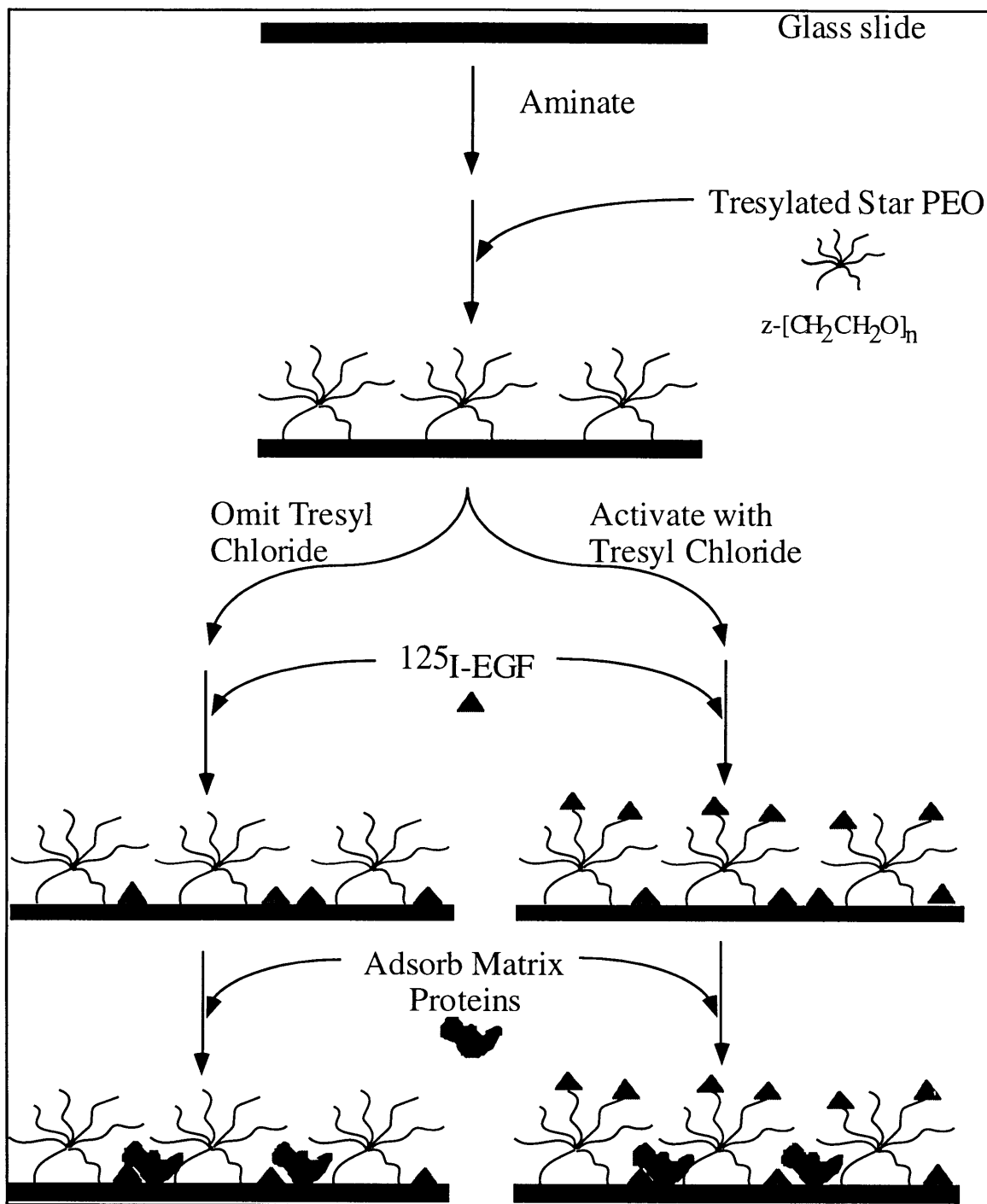


**Figure 3.1** Schematic of EGF surface first tethering protocol to glass-grafted PEO.

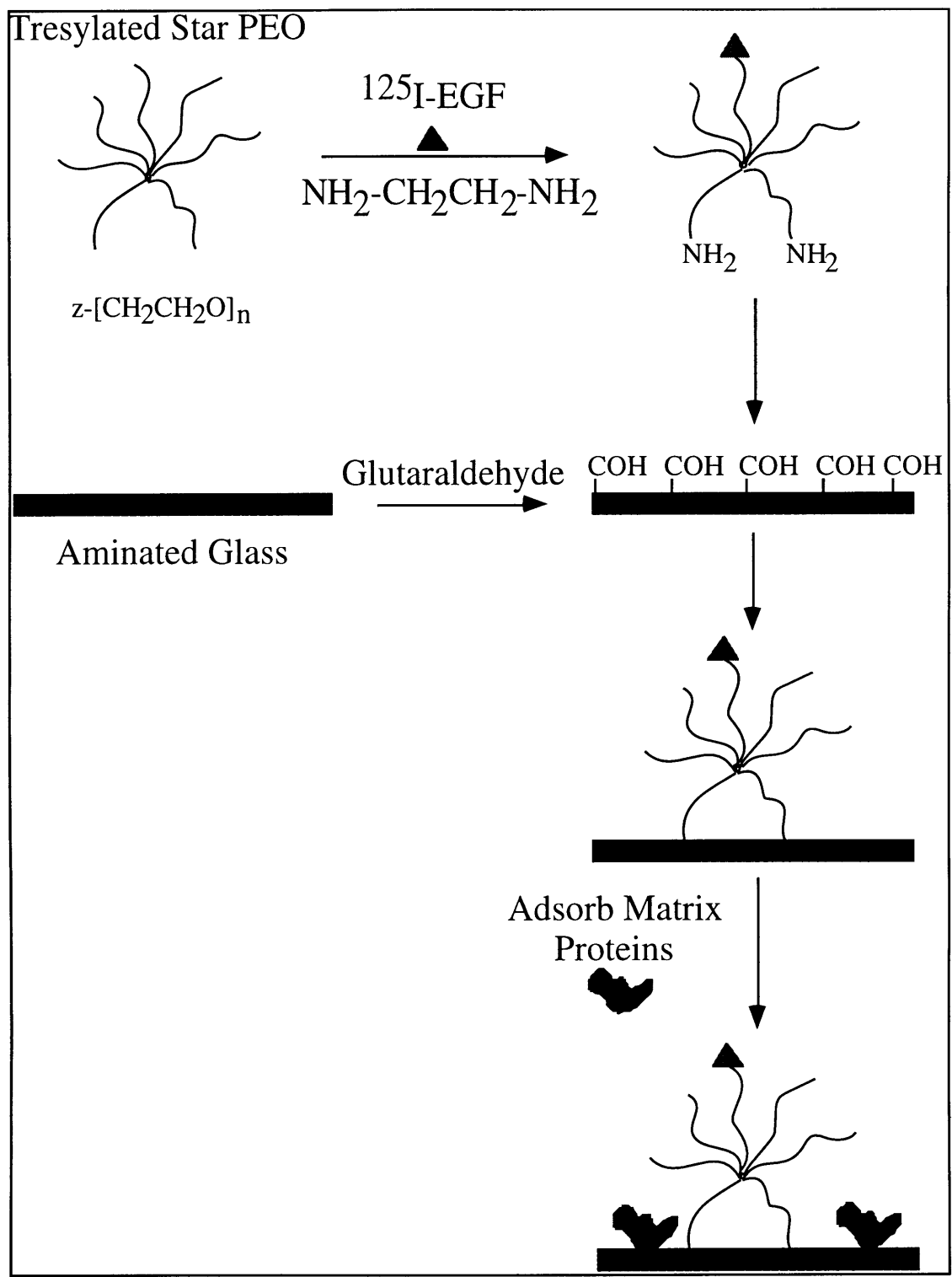


**Figure 3.2** Solution first EGF tethering protocol. EGF and EDA are grafted to tresyl-activated star PEO in solution and then the macromolecule is linked to the surface.

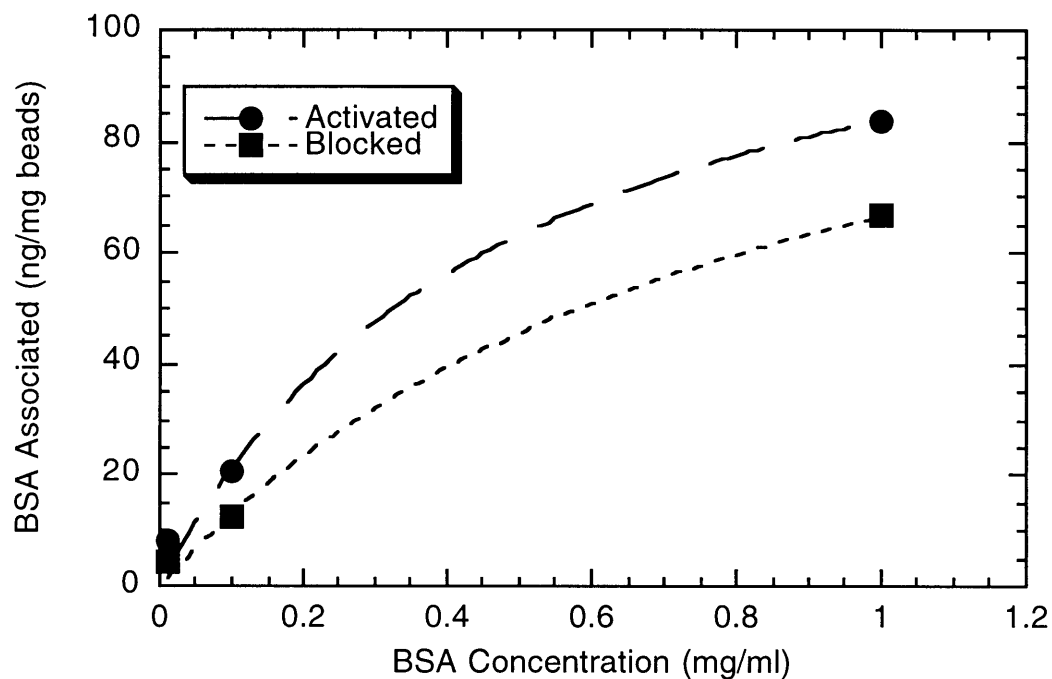


**Figure 3.3** BSA grafting to tresyl chloride activated agarose beads. Control beads were blocked via incubation in 0.2 M Tris buffer (pH 8.5) overnight. Experimental samples (Activated) and controls (Blocked) were briefly washed in coupling buffer (0.2 M HEPES, pH 7.8) before grafting, which was accomplished by incubating 37 mg beads overnight in 0.01 - 1 mg/ml  $^{14}\text{C}$ -BSA in a volume of 2 ml. The amount of protein grafted was determined by subtracting the amount associated with the controls from that associated with the experimental samples.



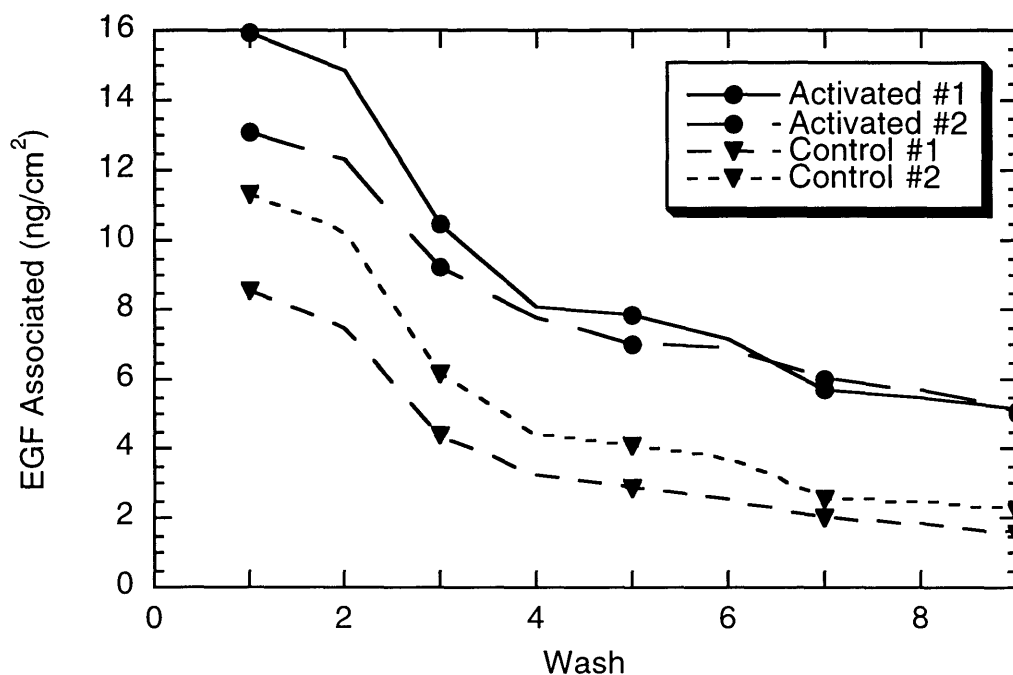


**Figure 3.4** Desorption profile for tethered EGF surfaces and controls during washes. <sup>125</sup>I-EGF of murine origin was grafted to activated slides in PBS (0.01 mg/ml EGF, 8-10 mCi/mg) for 12 hours at room temperature. The same procedure was followed for control slides which had been mock-activated. Slides were washed in 0.1M acetate, 0.5 M NaCl (pH 4) (washes 1-2), PBS (washes 3-6) and 0.01 M phosphate buffer (pH 7.4) with 0.025% Triton X-100 (washes 7-9). Wash 1 was for 2 hours, washes 2-6 for 12 hours, wash 7 for 72 hours, and washes 8 and 9 for 12 hours.

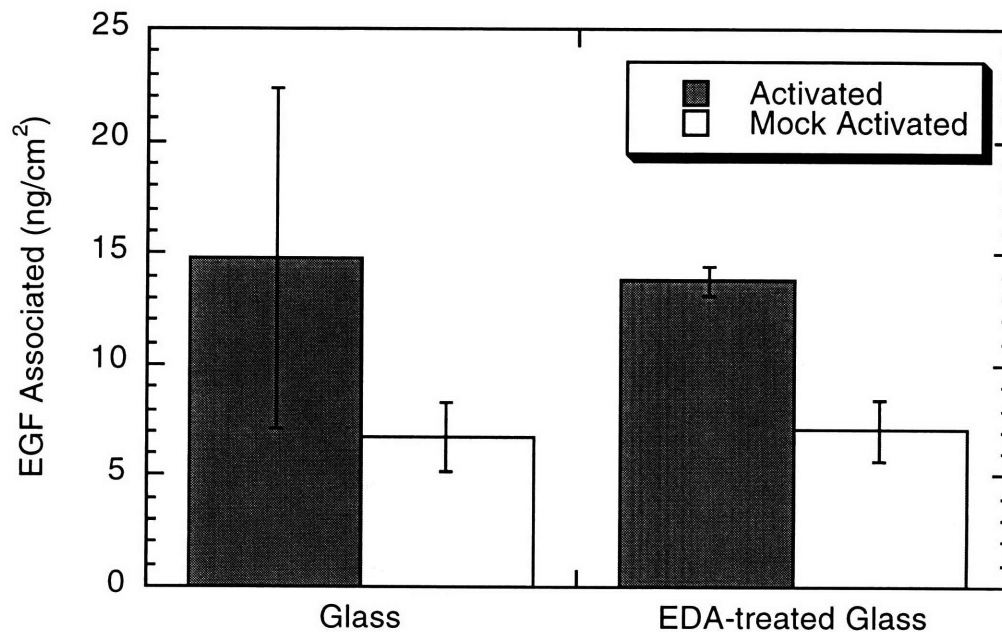


**Figure 3.5** EDA blocking of reactive silanols. Aminated glass slides were immersed for 1 hour in 0.06 *M* tresyl chloride and 0.07 *M* triethylamine in methylene chloride at room temperature. These were then incubated in 0.1*M* EDA, 0.1*M* triethylamine in methanol overnight to block activated silanols. Slides (three for each point) were re-tresylated (tresyl chloride omitted for controls) and then incubated with EGF (4 ng in a 10  $\mu$ l droplet). Unblocked aminated glass controls were re-activated or mock activated and incubated with EGF in an identical manner. Slides were rinsed once before counting.

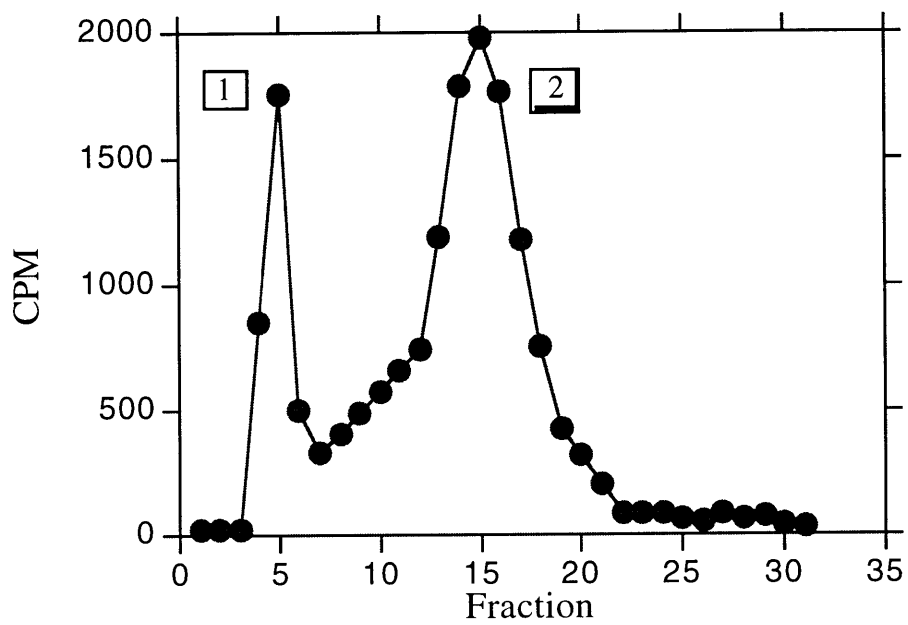


**Figure 3.6** Gel filtration of reaction products after coupling of EGF to star PEO 3510 (1:1 molar ratio EGF:star arms). Peak 1 is EGF-PEO and peak 2 is unreacted EGF.

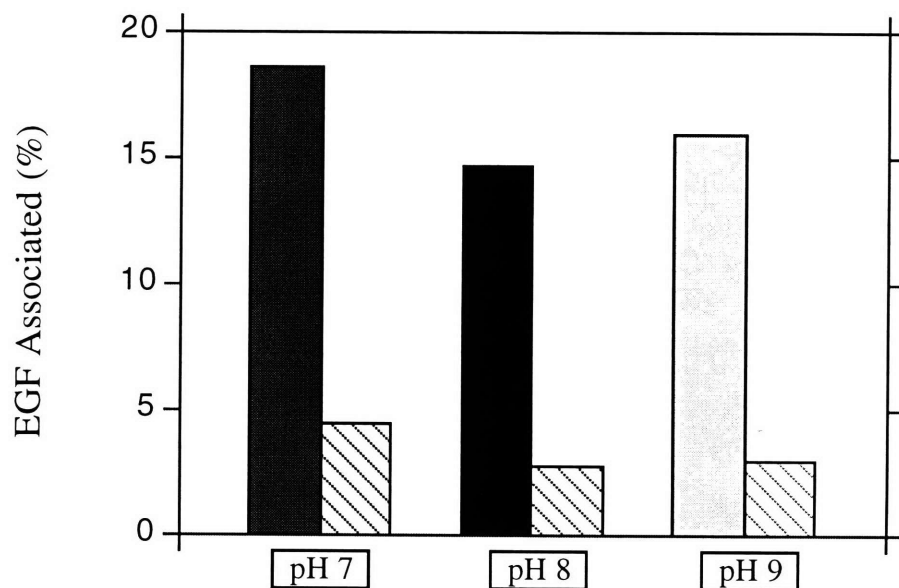


**Figure 3.7** EGF-PEO-EDA grafting to tresyl-agarose. Tresyl activated beads were rinsed briefly in coupling buffer (solid bars) or blocked for 3 days in 0.1M Tris (pH 8.5) to hydrolyze tresyl groups (adsorption control, hashed bars) and then rinsed briefly in coupling buffer. Three coupling buffers were used, 0.1 M phosphate pH 7, 0.1 M phosphate pH 8, and 0.1 M phosphate pH 9. Beads were incubated with 0.6 pmole  $^{125}\text{I}$ -EGF (in the form of EGF-PEO-EDA) for 24 hours at each pH, rinsed with coupling buffer, and counted. Each bar represents a single sample of beads.

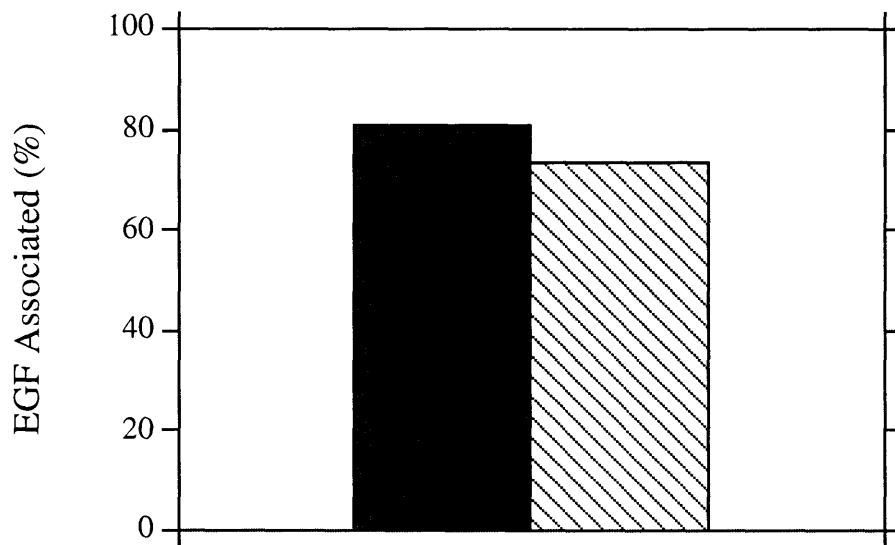


**Figure 3.8** EGF-PEO-EDA grafting to glutaraldehyde-treated agarose. Glutaraldehyde-treated beads were rinsed briefly in coupling buffer (0.1M phosphate, pH 7) (solid bar) or blocked by incubation overnight in 1M Tris-HCl in the presence of reductant (sodium cyanoborohydride) and then rinsed briefly in coupling buffer (hashed bar). The beads were incubated with 0.4 pmole EGF with reductant for 24 hours before rinsing successively in 1M NaCl, 7M GuHCl, and 0.2% SDS and counting. Data for a single sample is shown.

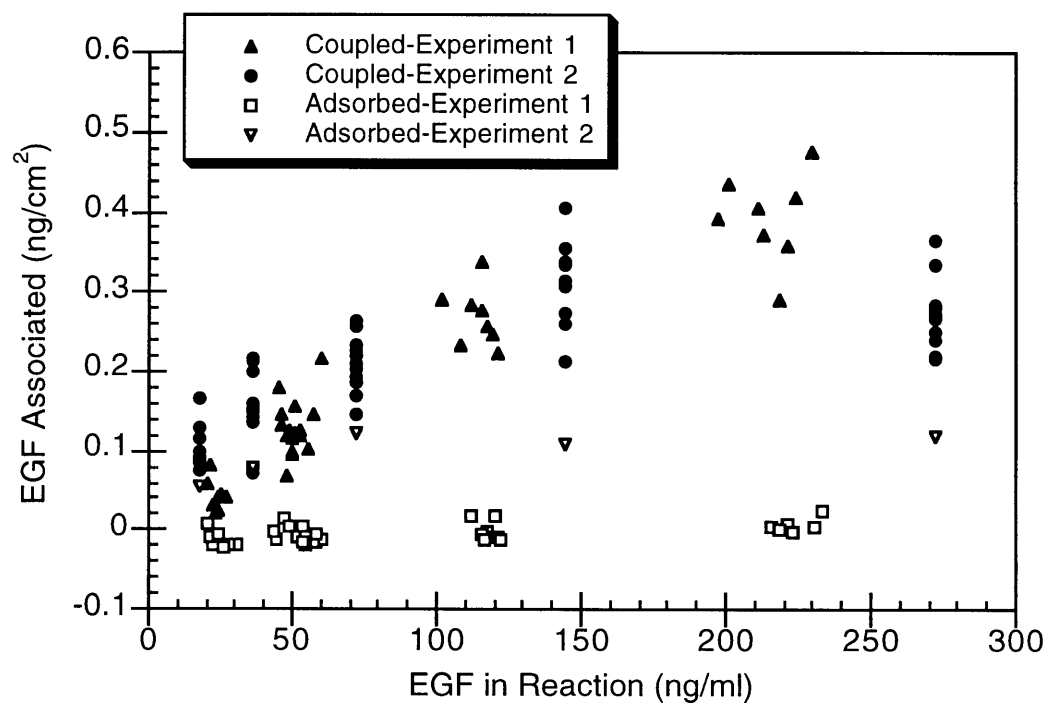
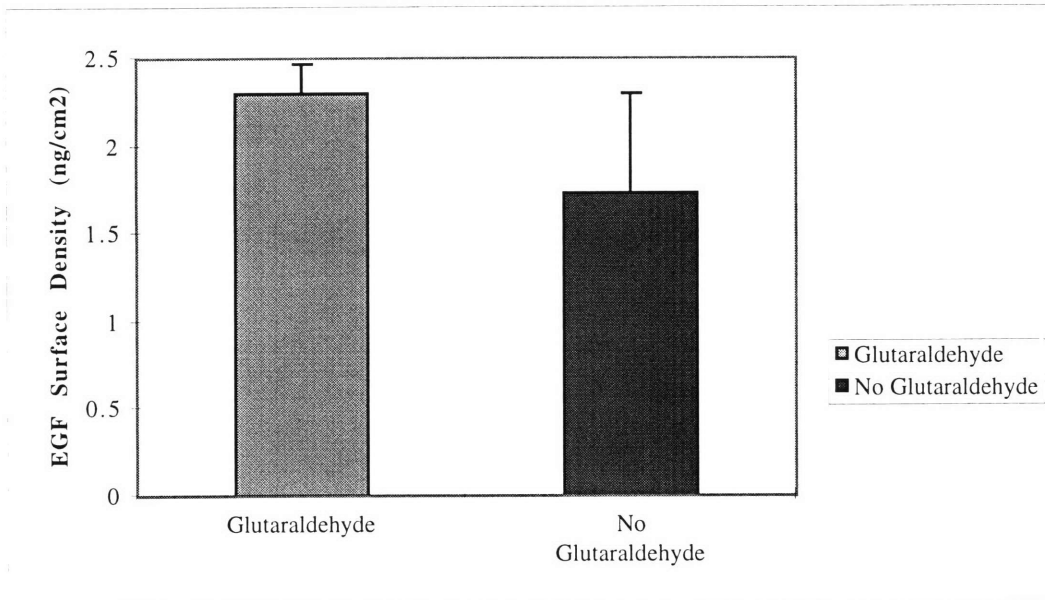
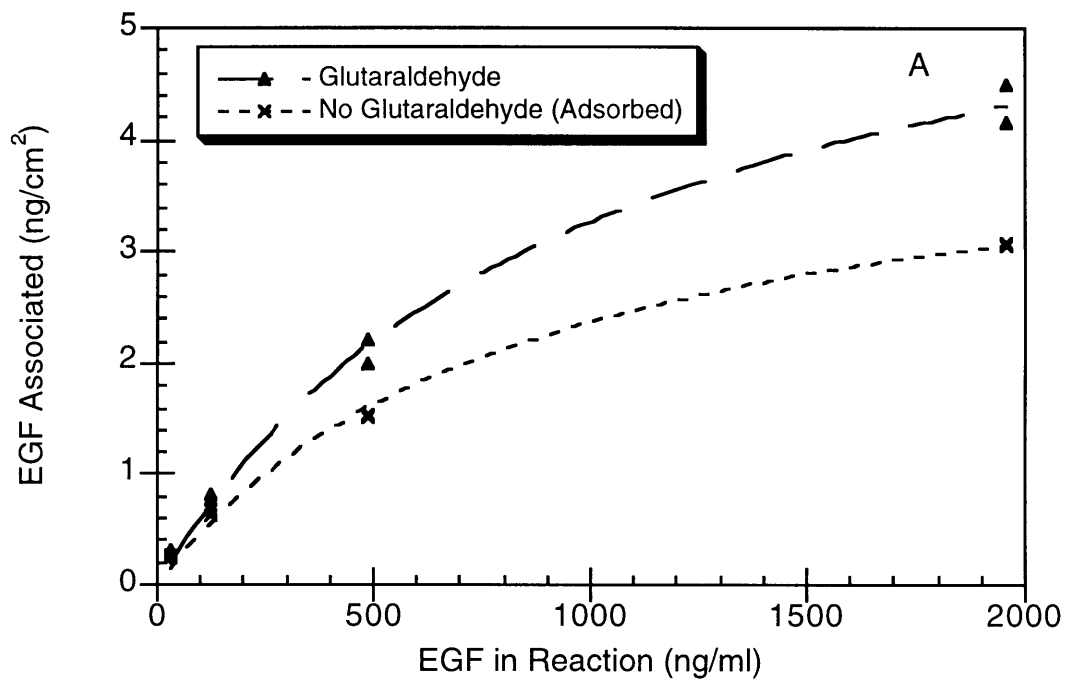


Figure 3.9 EGF-PEO-Amine grafting to aminated glass slides.



**Figure 3.10** EGF-PEO-Amine grafting to aminated glass dishes post iodination.

Conjugate was synthesized with nonradioactive EGF, purified, iodinated and reacted with aminated glass dishes.



**Figure 3.11A** EGF-PEO-Amine grafting to Primaria-coated tissue culture plastic. See next page for legend.



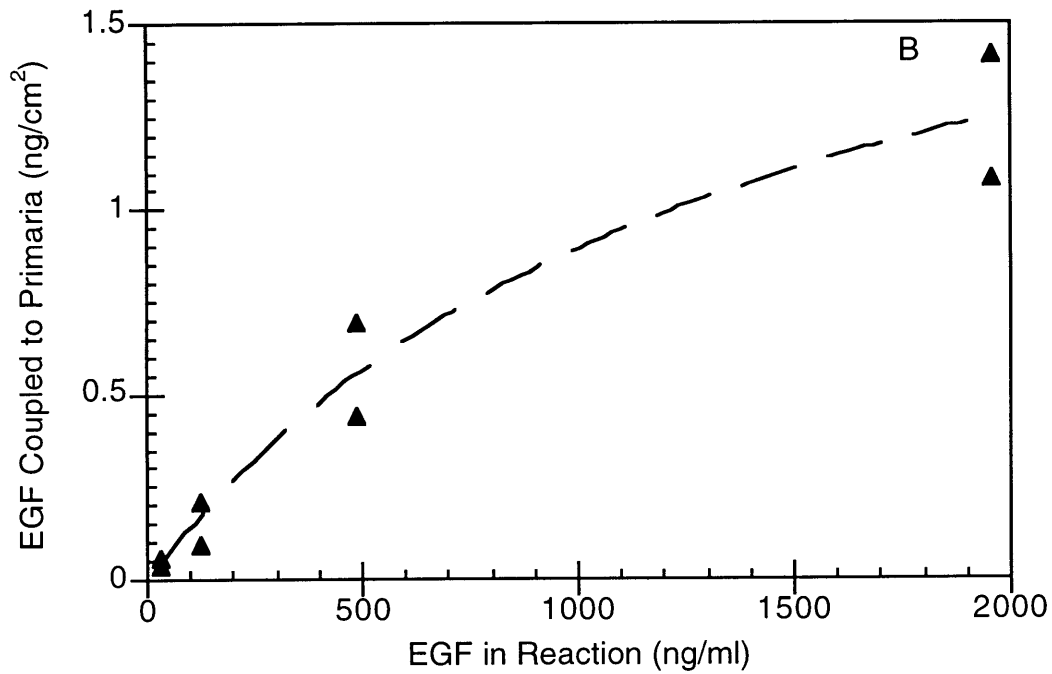


**Figure 3.11B** EGF-PEO-Amine grafting to Primaria-coated tissue culture plastic. A. Grafted + adsorbed EGF ("Glutaraldehyde") and only adsorbed EGF ("No Glutaraldehyde"). Two points are shown for each concentration. B. Amount grafted (nonspecific adsorption subtracted).

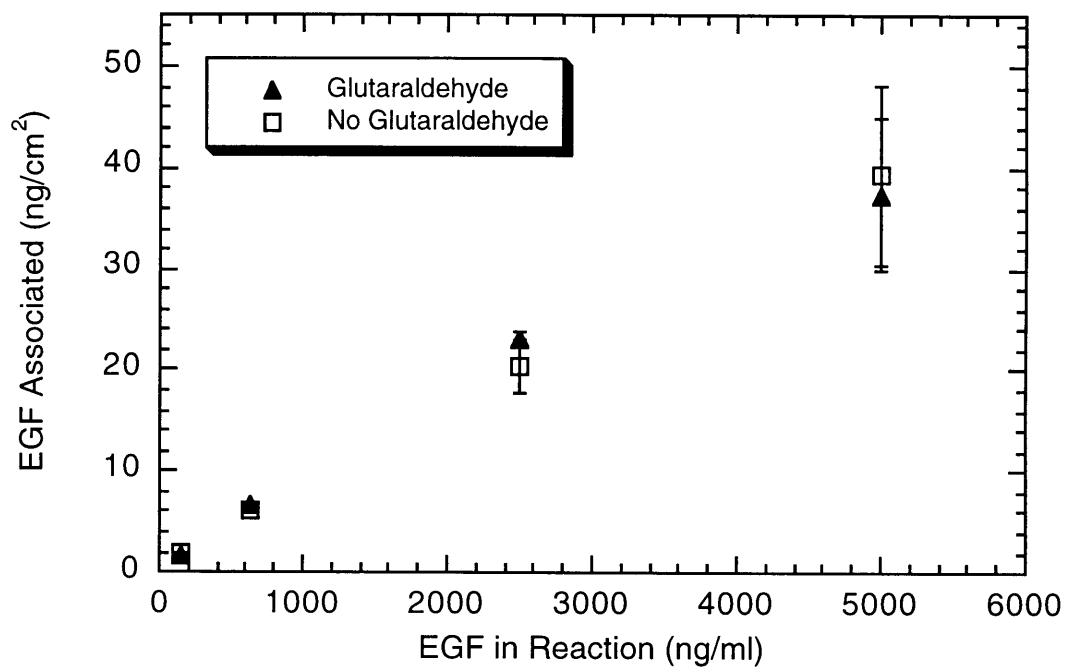


**Figure 3.12** EGF grafting to glutaraldehyde-treated, aminosilane derivatized glass.

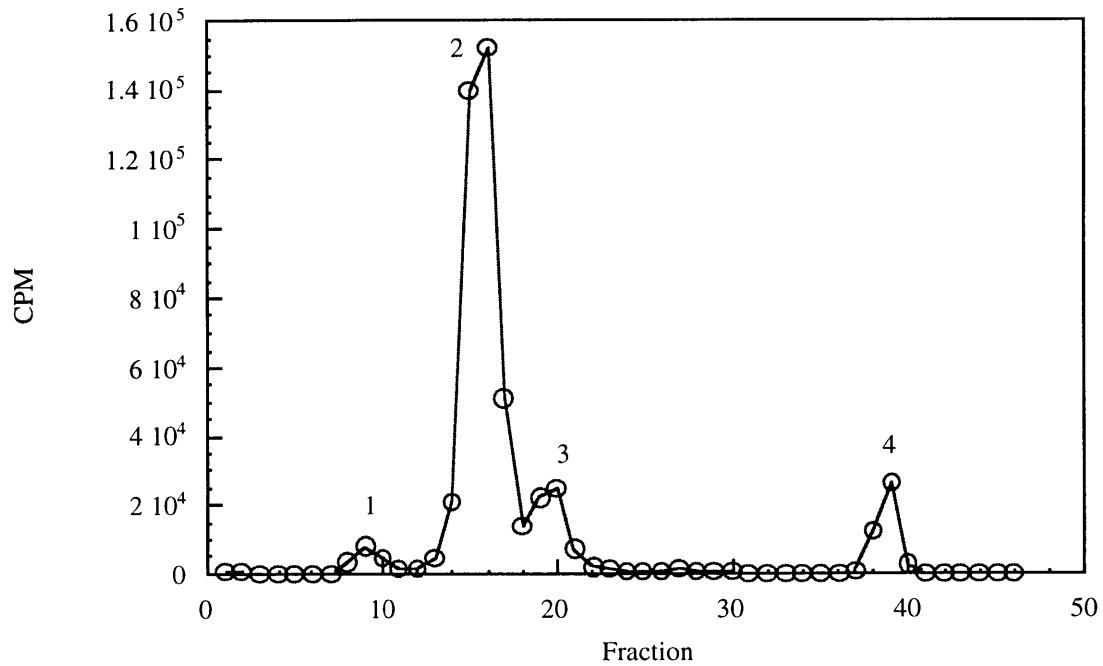


**Figure 3.13** Typical chromatogram of  $^{125}\text{I}$ -EGF. Column buffer was 1 mg/ml BSA in 50 mM phosphate (pH 7).  $^{125}\text{I}$ -EGF was applied to a Superdex-75 column (volume 24 ml) and fractions collected. Peak 2 is presumably the main EGF peak, peak 4 is free label as determined by acid precipitation, and the identity of peak 3 is not known. The first peak eluting just after the void volume is aggregated EGF.

## Chapter 4

# Biological Activity Experiments

### 4.1 Introduction

#### 4.1.1 Overview

In this chapter the response of primary rat hepatocytes to the tethered growth factor surfaces described in the last chapter is discussed. Soluble EGF elicits numerous responses from cells, beginning with receptor autophosphorylation and culminating with such readily observable readouts as proliferation and changes in morphology, as described in the next section. These responses were compared for soluble and tethered growth factor, as well as for growth factor that was nonspecifically adsorbed to glass. In addition, leakage of EGF from the surfaces was characterized, and binding and internalization data were gathered for soluble ligands. These data were important for validation of upstream biological activity and for use in quantitative comparison of soluble and tethered ligand on a per receptor basis, as described in the next chapter.

#### 4.1.2 The EGF Molecule

Epidermal growth factor, or EGF, was the first polypeptide mitogen to be identified (Cohen and Elliott 1963). It is a 53 amino acid polypeptide containing a specific extracellular domain that is common to several factors belonging to the EGF family, including transforming growth factor- $\alpha$  (DeLarco and Todaro 1978), amphiregulin (Shoyab *et al.* 1989), the schwannoma-derived growth factor (Kimura *et al.* 1990), the heparin-binding EGF-like factor (Higashiyama *et al.* 1991), the neu differentiation factors and the heregulins (Holmes *et al.* 1992; Wen *et al.* 1992). This domain is identified by the sequence CX7CX3-5CX10-12CXCX5GXRC (C, cysteine; G, glycine; R, arginine; X,

other amino acids). The six cysteines, one glycine, and one arginine in this sequence are all conserved in EGF-related factors, but not in proteins that contain EGF units with no known growth factor activity. That the six cysteines form three disulfide bonds has been confirmed in EGF by Cooke *et al* (1987), who provided a three dimensional structure of residues 1-48, a derivative which retains biological activity. Komoriya *et al.* (1984) demonstrated that peptides encompassing residues 20-31 of mouse EGF (mEGF) bind to the mouse EGF receptor. These residues form part of the major  $\beta$ -sheet in the structure of human EGF (hEGF) reported by Cooke *et al.* Furthermore, disruption of this  $\beta$ -sheet via cleavage of the 21-22 peptide bond results in loss of EGF activity (Anzano *et al.* 1982).

It has been shown by Simpson *et al* (1985) that rat EGF with up to three of the N-terminal residues missing retains identical activity to the native protein. The N-terminus may exist in a triple-stranded  $\beta$ -sheet arrangement with the major  $\beta$ -sheet described above, but apparently this structure is unstabilized by hydrogen bonds and is present only fleetingly, not affecting EGF activity (Cooke *et al.* 1987). This implies that covalent coupling of a large polymer molecule may not significantly affect the conformation or activity of the growth factor.

#### 4.1.3 Cell Responses to EGF Stimulation

Epidermal growth factor was so named because it was observed to accelerate incisor eruption in newborn mice (Cohen 1964). Since its discovery, however, EGF has been observed to elicit a variety of cellular responses through activation of its cell surface receptor (EGFR). This 170 kDa receptor has a long cytoplasmic region of 543 residues which regulates the intrinsic tyrosine kinase activity of the receptor (Bertics and Gill 1986; Walton *et al.* 1990), including at least five tyrosines which can be autophosphorylated upon ligand stimulation. These phosphotyrosines can associate with the *src* homology-2 (SH2) domains found in numerous second messengers (e.g., PLC- $\gamma$ , Gap, PI-3 kinase) and thus initiate signals along numerous pathways (Carpenter 1992; Lowenstein *et al.* 1992;

Marengere and Pawson 1992; Rotin *et al.* 1992). EGFR activation has been shown to elicit mitogenesis in rat hepatocytes (Blanc *et al.* 1992; Tomomura *et al.* 1987) and cell migration and increased random movement in other cell types (Barrandon and Green 1987; Blay and Brown 1985; Westermark *et al.* 1991).

Activation of the EGF receptor also leads to alterations in cell morphology. Human carcinoma cells A-431 have an unusually high number ( $2-3 \times 10^6$ ) of EGF receptors. These cells undergo rapid and extensive changes in morphology upon exposure to EGF. Within one minute of exposure to EGF, numerous membrane ruffles and filopodia are formed. This effect is transient, peaking at two minutes of treatment, and is followed by a gradual retraction from the substrate at the edges of colonies. Finally, by 12 hours, the cells have completely reorganized from a monolayer into multilayered colonies (Chinkers *et al.* 1979). Ware *et al.* have shown that NR6 cells also undergo marked rounding upon exposure to EGF (Ware, unpublished).

In  $\text{Ca}^{++}$ -free medium the response of A-431 cells to EGF is quite different; under such conditions the cells undergo rapid rounding (See Figure 4.1) (Chinkers *et al.* 1981). These gross morphological changes are accompanied by a redistribution of actin and  $\alpha$ -actinin in these cells (Schlessinger and Geiger 1981), perhaps suggesting that the observed morphological changes are due to changes in the cytoskeleton induced by EGF.

In the present work both DNA synthesis and morphological effects are used as readouts for biological activity of soluble and tethered EGF. Primary rat hepatocytes were chosen for the experiments because they exhibit these biological responses and because of their potential for use in tissue engineering applications.

## 4.2 Receptor Binding and Internalization of Soluble EGF and EGF-PEO Conjugate

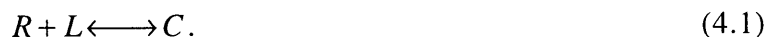
### 4.2.1 Overview

As described in previous sections, growth factors like EGF mediate their effects upon cells by binding to cell surface receptors. The dissociation constant for EGF receptor-ligand binding in rat hepatocytes was determined for comparison of receptor signaling by soluble and tethered EGF as described in Chapter 5. To verify the binding competency of EGF after coupling to star PEO and subsequent purification of the conjugate, the internalization rate constant was measured for EGF-PEO-Amine and compared to that for EGF. The internalization, rather than dissociation constant was measured for the conjugate because the amount of material required for determination of the latter was prohibitively large.

### 4.2.2 Equilibrium receptor binding of soluble EGF by rat hepatocytes

#### 4.2.2.1 Background

Receptor binding by soluble ligands can be calculated from more easily measurable concentrations of ligand in solution through the use of a binding model (Lauffenburger and Linderman 1993). The simplest of these is the two-step binding model,



where  $R$ ,  $L$ , and  $C$  refer to free receptor, ligand and receptor-ligand complex, respectively.

From the principal of mass action kinetics:

$$\frac{d[C]}{dt} = k_f[R][L] - k_r[C] \quad (4.2)$$

where  $[C]$  and  $[R]$  are in units of #/cell,  $[L]$  is expressed as a molar concentration, and  $k_f$  and  $k_r$  have units  $M^{-1}\text{min}^{-1}$  and  $\text{min}^{-1}$ , respectively. Taking into account conservation of receptors:

$$[R] = [R]_T - [C] \quad (4.3)$$

and assuming depletion of ligand from the medium due to receptor binding is negligible ( $[L]=[L]_0$ ) the number of complexes at equilibrium is given by

$$[C]_{eq} = \frac{[R]_T [L]_0}{K_D + [L]_0} \quad (4.4)$$

#### 4.2.2.2 Materials and Methods

Hepatocytes were isolated from 180-250g male Fisher rats (viability 89-90%) by collagenase perfusion as described by Cima *et al* (1991) and suspended in William's Medium E supplemented with 0.55 g/L sodium pyruvate, 0.5 pM dexamethasone, 0.8 mg/ml insulin (bovine), 100 U/ml Penicillin/Streptomycin, and 2 mM L-glutamine. Cells were seeded on 35 mm tissue culture dishes at a concentration of approximately 400,000 cells/dish. The dishes had been incubated with 0.1 wt% bovine collagen for at least 1 hour at 4°C and rinsed in PBS before seeding. After 24 hours in culture at 37°C cells were incubated with 0-3 nM mouse <sup>125</sup>I-EGF (64 μCi/μg) with (adsorption controls) or without 20 ng/ml additional unlabeled EGF at 4°C. After 4 hours the cells were rinsed thoroughly with cold culture medium, solubilized with SDS and cell-associated radioactivity was counted using a gamma counter (Packard). Data for nonspecific adsorption was determined and subtracted to yield specific binding to EGFR.

#### 4.2.2.3 Results

Values for the dissociation constant for soluble EGF ( $K_D$ ) and total receptor number ( $R_T$ ) were measured for rat hepatocytes twenty-four hours after isolation and plating. Equilibrium binding was measured at 4°C after a four hour incubation with 0-3 nM EGF under conditions in which depletion of ligand from the medium is negligible. Nonspecific adsorption of ligand, the amount associated with cells in the presence of excess unlabeled ligand, was subtracted to obtain values for specific binding. Using a nonlinear parameter estimation algorithm (Kaleidagraph; Levenberg-Marquardt algorithm) the equilibrium binding data was fit to equation (4.4) and values of  $K_D=0.56$  nM and



$R_T=175,000 \text{ cell}^{-1}$  were obtained (Figure 4.2). These values are comparable to those obtained previously for this system ( $K_D=0.65 \text{ nM}$  and  $R_T=165,000 \text{ cell}^{-1}$  (Gladhaug and Christoffersen 1987);  $K_D=0.67 \text{ nM}$  and  $R_T=166,000 \text{ cell}^{-1}$  (Dahmane *et al.* 1996)).

#### 4.2.3 Internalization of soluble receptor ligands

##### 4.2.3.1 Motivation

To verify that the conjugate synthesis and purification procedures did not adversely affect EGF receptor binding, the internalization constant for EGF-PEO-Amine was measured and compared to that for EGF. B82 fibroblasts were chosen for these studies to permit comparison with literature values of the internalization rate constant. Conjugates of PEO and various proteins have been synthesized and shown to retain biological activity, as discussed below.

##### 4.2.3.2 Background

Protein-PEO conjugates are of interest to the medical and pharmaceutical communities for several reasons. Covalent attachment of PEO to proteins helps to decrease their immunogenicity and antigenicity (Abuchowski *et al.* 1977), affects transport properties, retards glomerular filtration of the proteins, and inhibits proteolytic degradation (Abuchowski *et al.* 1977). It can also increase water solubility and alter pharmacokinetics of proteins.

PEG-adenosine deaminase has been used for severe combined immunodeficiency disease (Herschfield *et al.* 1987), and PEG-superoxide dismutase and PEG-catalase for limiting tissue damage from ischemia (Beckman *et al.* 1988). Commercially available small drug molecules with attached PEO include penicillin, procaine, and aspirin.

Modification of cytokines and lymphokines with PEO has also been carried out. Tumor necrosis factor (Tsutsumi *et al.* 1994) and interleukin-2 (Katre *et al.* 1987) showed enhanced tumor potency when modified with monomethoxy PEG (MW=5,000), presumably due to decreased rates of plasma clearance. PEG-modification of granulocyte-

macrophage colony stimulating factor (GM-CSF) enhanced neutrophil priming activity in vitro but not colony stimulating activity compared to unmodified GM-CSF (Knusli *et al.* 1992). Wang *et al.* (1993) synthesized a chimeric toxin composed of human transforming growth factor  $\alpha$  fused to a fragment of *Pseudomonas* endotoxin devoid of its cell binding domain. Between the two proteins they inserted a polypeptide with 13 lysine residues and synthesized molecules with various degrees of polymer modification. PEG addition (MW = 6,000-19,000) decreased receptor binding of the conjugate by 74% and cytotoxicity by 85-96%, although mean residence time in the blood was significantly increased. While these reports document the advantages of pegylation of proteins and growth factors, the fate of these altered molecules is not examined. The present work provides the first direct evidence of internalization of a growth factor-polymer conjugate, a finding which has important implications for drug delivery and gene therapy. One idea for future research in this direction is given in Chapter 6.

Measuring the kinetics of receptor mediated internalization involves determining the amount of radioactive ligand on the surface and in the interior of cells as a function of incubation time in the ligand-containing medium. The amount of radioactivity bound to the cell surface can be determined by washing cells in a low-pH medium after incubation in labeled ligand for a suitable time (Haigler *et al.* 1980). Receptor/ligand binding affinity is reduced at low pH, so bound ligand on the cell surface dissociates under such conditions, while internalized ligand remains in the cell and can be measured after solubilization. If recycling of receptors from the cell interior can be neglected, as is the case when the binding experiment for is carried out for short incubation times, an internalization rate constant,  $k_e$ , can be calculated as shown below.

The concentration of internalized ligand,  $[C_i]$ , increases with time according to the following equation:

$$\frac{d[C_i]}{dt} = k_e [C_s] \quad (4.5)$$

Integrating yields:

$$[C_i](t) = [C_i](t=0) + \int_0^t k_e [C_s](t') dt' \quad (4.6)$$

If there are no intracellular complexes at  $t=0$  (i.e., labeled ligand introduced at  $t=0$ ), and if the internalization constant does not change with time:

$$[C_i](t) = k_e \int_0^t [C_s](t') dt' \quad (4.7)$$

Thus, a plot of  $[C_i](t)$  vs. the integral of  $[C_s](t)$  will yield a straight line whose slope is the internalization rate constant (Lauffenburger and Linderman 1993).

The preceding analysis assumes that fluid phase and non-specific uptake of ligand is negligible. If this is not the case, the internalization plot should yield a line with an increased slope compared to unmodified EGF.

#### 4.2.3.3 Materials and Methods

WHIPS buffer is composed of 0.1% polyvinyl pyrrolidone 40,000 MW, 130 mM NaCl, 5mM KCl, 0.5 mM MgCl<sub>2</sub>, 1 mM CaCl<sub>2</sub>, and 20 mM HEPES. Acid strip is 50 mM glycine, 100 mM NaCl, 1 mg/ml PVP-40, and 2 M urea.

B82 fibroblasts, provided by the Lauffenburger laboratory, were cultured in Dulbecco's Modified Eagle's Medium (DMEM) with 3.70 g/L sodium bicarbonate, 10% calf serum, 0.1 M glutamine, penicillin and streptomycin, and methotrexate (MTX). These cells contain a recombinant gene encoding the EGFR which is regulated by an MTX-inducible promoter. The cells were routinely grown in a 5% CO<sub>2</sub> atmosphere in T-flasks and were split twice weekly.

The B82 cells were serum starved in DHB at 37°C in an air atmosphere for three hours before addition of labeled EGF or EGF-PEO-Amine. Parallel cultures were incubated for 1-20 minutes at 37°C in an air atmosphere and then transferred to an ice bath where the medium was removed and the cells washed twice in WHIPS buffer. Surface radioactivity was removed by washing the cells twice in acid strip solution, allowing the cells to incubate for 8 minutes in the acid strip during the first wash and 4 minutes during

the second wash. Internalized ligand was then removed by solubilizing the cells in 1N NaOH.

#### 4.2.3.4 Results and Discussion

Figure 4.3 shows the internalization plot for EGF and EGF-PEO-Amine in a single experiment in which the concentration of both species was 16.4 pM. Table 4.1 gives  $k_e$  values for EGF measured in three separate additional experiments in which the EGF concentration was 16.4 pM (1 ng/ml), 0.164 nM, and 1.64 nM. These values are somewhat smaller than those reported by Starbuck (1991),  $k_e=0.31 \text{ min}^{-1}$ , and Chen (1989)  $k_e=0.2 \text{ min}^{-1}$  (approximately). The cells used in these experiments had been cultured for some time (passage number > 100) so the smaller rate constant for internalization may reflect decreased expression of the transfected EGFR gene.

Interestingly, the  $k_e$  did not vary greatly with EGF concentration. Moreover, the internalization constant for EGF-PEO-Amine was virtually identical to that for EGF. This result is important since it suggests that the coupling of EGF to star PEO and the subsequent purification scheme do not render the protein less able to bind cell surface receptors.

**Table 4.1** Internalization rate constant for EGF at three different EGF concentrations.

<u>EGF Concentration (ng/ml)</u>	<u>Internalization Rate Constant (<math>\text{min}^{-1}</math>)</u>
0.1	0.175
1	0.140
10	0.130

## 4.3 DNA Synthesis in Response to Tethered EGF

### 4.3.1 Overview

In this section, the proliferative responses of primary rat hepatocytes to EGF tethered by the surface first and solution first methods are described (see Chapter 3 for surface synthesis and characterization). Surfaces synthesized by the former method had a significant degree of nonspecific protein adsorption (Table 3.1, see also section 2.3), rendering precise quantitation of lower surface densities of tethered EGF very difficult. Cell response was therefore measured at a relatively high EGF surface density, at least 10-fold greater than the density of cell surface receptors for EGF. Dose response experiments, which required greater control of ligand density, were performed on surfaces with EGF tethered by the solution first method.

### 4.3.2 Materials

<sup>125</sup>I-EGF (murine, in 50mM Kphos. w/0.075% NaCl) was purchased from ICN Radiochemicals; William's Medium E, L-glutamine, insulin (bovine), sodium pyruvate, and penicillin/streptomycin were from Gibco Laboratories, Grand Island, NY. Dexamethasone and bovine serum albumin were from Sigma. Cell-Tak cell and tissue adhesive and murine EGF added to the soluble medium were from Collaborative Biomedical Products/Becton Dickinson, Bedford, MA. Vitrogen 100 (bovine type I collagen) was from Celltrix. All chemicals used in the surface preparation were reagent grade. All water was purified with a 4-cartridge Milli-Q system to 18 megaohm purity.

### 4.3.3 Surface first method

#### 4.3.3.1 Methods

DNA synthesis was measured by incorporation of a non-radioactive DNA precursor, bromodeoxyuridine (BrdU) (see Appendix A2.3). Cells were seeded on glass

slides with EGF tethered by the surface-first method (see Table 3.1, star BS10.2) at a density of approximately 5,000 cells/well (25,000 cells/cm<sup>2</sup>). The slides had been grafted with star PEO BS10.2 ( $f=180$  and  $M_a=10,000$ ) and coupled with EGF as outlined in Figure 3.1. Medium was changed daily. For controls, cells were seeded on tissue culture plastic with adsorbed collagen. BrdU was incorporated between 48-68 hours after cell seeding. An index of DNA synthesis was calculated as the number of stained nuclei divided by the area covered by cells. Assuming that on average cells spread to the same extent on the tethered and non-tethered surfaces, the area measurement gives a measure of the total number of cells in culture. In experiments on surfaces tethered by the solution first method, the total number of nuclei in the culture was determined by counting after fluorescent labeling with Hoescht 33342 (see section 4.3.4)

#### 4.3.3.2 Results and Discussion

The results of the experiment is shown in Figure 4.4. Soluble EGF caused a higher fraction of cells to synthesize DNA than when EGF was omitted from the medium, as has been observed previously (Mitaka *et al.* 1990; Houck and Michalopoulos 1985; Wollenberg *et al.* 1989; Ishigami *et al.* 1993). Figure 4.4 shows that the fraction of cells synthesizing DNA after 48 hours in culture was higher for those seeded on the tethered growth factor surfaces than for those on the controls. In the tethered EGF case, both the EGF<sup>-</sup> and EGF<sup>+</sup> surfaces had  $\sim 2\text{ng/cm}^2$  nonspecifically adsorbed EGF. These adsorbed molecules were immobilized in unknown conformations on the aminated glass surfaces. It is particularly remarkable that the nonspecifically adsorbed EGF did not invoke an observable response because the surface density of adsorbed EGF was at least ten fold greater than the density of EGFR on the cell membrane, even assuming all EGFR distributes to the cell-substrate interface. It is thus likely that the conformation of adsorbed EGF was unsuitable for stimulating DNA synthesis or that receptor mobility was important in the signaling process. Even if all nonspecifically bound EGF desorbed before the first medium change, the resulting concentration would have still been below the threshold value of 1 ng/ml soluble

EGF needed to stimulate DNA synthesis in primary rat hepatocytes (Blanc *et al.* 1992; Tomomura *et al.* 1987).

#### 4.3.4 Solution first method

##### 4.3.4.1 Overview

DNA synthesis by rat hepatocytes in response to stimulation by EGF was measured for various concentrations of soluble and tethered EGF. Dose response data of this kind is useful to compare the maximum rates of proliferation induced by the different modes of delivery. In the next chapter these data are used in conjunction with models for receptor-ligand binding to compare the signaling efficiencies of receptors bound to the soluble and tethered ligands.

##### 4.3.4.2 Materials and Methods

Immediately before cell seeding, slides with tethered EGF (see Figure 3.9 for surface concentrations) were rinsed with PBS and incubated with 0.1wt% bovine collagen for 1-2 hours.

Primary rat hepatocytes were isolated and suspended in medium as described above. The viability of the isolated hepatocytes in three separate experiments was 84-92%. Cells were seeded at a density of 25,000 cells/cm<sup>2</sup> on tethered EGF surfaces in EGF-free medium and on PEO-Amine-grafted surfaces in medium supplemented with 0, 2.5, 5, 10 or 40 ng/ml soluble EGF. Twenty hours and 44 hours after cell seeding half of the culture medium was replaced with fresh medium containing bromodeoxyuridine. Cells were fixed 67 hours after cell seeding and processed for immunocytochemistry. Cells were counterstained with Hoescht 33342 for 72 hours and nuclei were counted using a fluorescence microscope. The percentage of stained nuclei (staining index) was calculated. For each data point 2-3 different surfaces were analyzed and greater than 100 nuclei were counted.

#### 4.3.4.3 Results

Results are shown in Figures 4.5 (A,B,C). For each isolation, maximal mitogenic activity was elicited at growth factor concentrations of 5-10 ng/ml. This agrees with previous results (Blanc *et al.* 1992; Tomomura *et al.* 1987). However, in all cases no more than 25% of the cells entered S phase in response to EGF stimulation, a relatively low number of responsive cells. Other researchers have found optimal staining indices of 75% - 91% (Li *et al.* 1993; Houck and Michalopoulos 1985). Use of alternative medium formulations including one reported to prolong hepatocyte survival in vitro (Block *et al.* 1996) resulted in no significant increase in staining index as observed qualitatively after staining with anti-BrdU antibodies. The low staining index may be due to the age of the donor animals or an unknown factor in the hepatocyte isolation procedure, including preferential isolation of slower growing cells from the perivenous region of the liver acinus. The response to tethered EGF reached the maximum level of DNA synthesis at concentrations of approximately 0.4 ng/cm<sup>2</sup>. As will be shown in the next chapter, the different shapes of the dose response curves can be explained by differences in receptor binding behavior.

### **4.4 DNA Synthesis in Response to Adsorbed EGF**

#### 4.4.1 Background

Protein adsorption to biomaterials has been extensively studied since it is thought that cellular interactions with implanted materials are mediated through the adsorbed protein layer. Proteins adsorb to solid surfaces as a result of enthalpic and entropic driving forces, the former dominant in the case of hydrophilic surfaces and the latter in the case of hydrophobic surfaces. It is generally believed that preliminary contacts between the protein and the surface are followed by partial unfolding of the protein to minimize the free energy of the protein-surface system. Thus, residues that are buried in a globular protein



dissolved in an aqueous buffer may form strong contacts with a hydrophobic surface as the protein unfolds. These interactions may result in proteins with altered biological activity as compared to those in free solution. This phenomenon has been studied for plasma proteins. In the case of fibrinogen, for example, platelets adhere to the adsorbed molecule but not to the free solution analog unless the fibrinogen is first stimulated by adenosine diphosphate (ADP) (Young *et al.* 1982). Lindon *et al* (1986) studied platelet adhesion to polyalkyl methacrylates with adsorbed fibrinogen and found that fibrinogen activity varied greatly with the hydrophobicity of the polymer and was less dependent on the amount of the adsorbed protein. Studies of Hageman factor adsorption to quartz by transmission circular dichroism measurements showed that conformational change was directly related to contact time for periods of up to 10 days (McMillin and Walton 1974). In another study, adsorption of fibronectin and bovine albumin onto hydrophilic quartz were measured by fluorescence and total internal fluorescence reflection (TIRF), respectively. In the former case the fluorescence maximum experienced no change upon adsorption, suggesting little or no conformational change, and in the latter case the fluorescence maximum shifted from 342 nm (1 mg/ml BSA in PBS) to 333 nm upon adsorption (Andrade 1985).

Taken together these results indicate that the conformation of proteins adsorbed on surfaces is protein-dependent, and also varies with the characteristics of the surface and the details of the adsorption conditions (e.g., time and pH).

The biological activity of adsorbed EGF is of critical importance. Complete prevention of EGF adsorption by PEO grafting is very difficult, complicating the measurement of biological response to tethered growth factor. In addition, complete prevention of protein adsorption would necessitate grafting of adhesion proteins or peptides to permit cell adhesion. The biological activity of adsorbed EGF was tested by seeding cells on surfaces with and without adsorbed EGF and measuring DNA synthesis by BrdU incorporation in response to various concentrations of soluble EGF.

#### 4.4.2 Methods

Aminated glass slides were sterilized with 70% ethanol and incubated with iodinated mouse EGF (13  $\mu\text{g/ml}$ , 20  $\mu\text{l}$ ) for 24 hours at room temperature. Slides with adsorbed EGF and sterilized glass slides without adsorbed EGF were rinsed with PBS and incubated with 0.1 wt% bovine collagen at 4°C. Adsorbed EGF slides had 41 $\pm$  23.9  $\text{ng/cm}^2$  (at least 7  $\text{ng/cm}^2$ ) adsorbed EGF at the time of cell seeding. Freshly isolated rat hepatocytes were isolated (viability 85%) and seeded on the slides at a density of 3000  $\text{cells/cm}^2$  in a very small volume of culture medium (see above). Two hours after seeding, medium containing EGF was added so that the final concentration of soluble EGF in the medium was 0, 2.5, 5, 10 or 40  $\text{ng/ml}$ . Twenty-six hours after seeding the medium was partially (50%) replaced with fresh medium containing the same concentration of EGF originally added to the culture dish and bromodeoxyuridine (BrdU). Medium was partially replaced in the same manner at 50 hours. BrdU was incorporated until 68 hours after seeding, when the cells were fixed and processed for immunocytochemical staining. Cells were counterstained with Hoescht 33342 for 72 hours and nuclei were counted using a fluorescence microscope. At least three different surfaces were analyzed and greater than 100 nuclei were counted for each data point.

#### 4.4.3 Results and Discussion

Freshly isolated rat hepatocytes seeded on surfaces with or without adsorbed EGF looked morphologically similar, assuming a normal spread morphology typical for a collagen-coated surface. Soluble EGF stimulated DNA synthesis in these cells in a dose-dependent manner, with maximal stimulation achieved by 10  $\text{ng/ml}$  (Figure 4.6). Adsorbed EGF did not cause any enhancement of DNA synthesis activity, as would be expected if the adsorbed growth factor molecules were competent for signaling.

Epidermal growth factor is a globular protein with an active site made up of residues that are not continuous on the polypeptide chain (see section 4.1.2). This is in

contrast to many of the extracellular matrix (ECM) proteins, which have short, well defined, continuous sequences making up the receptor binding domains. Adsorption of EGF to a substrate followed by partial unfolding, therefore, would presumably result in a more extensive loss of receptor-binding capability as compared to the ECM proteins. Alternatively, the adsorbed EGF could be sterically inhibited from interacting with the EGF receptor. The hydrophilicity of the aminosilane layer suggests that the primary mode of interaction between the protein and the surface is ionic in nature.

## **4.5 Cell morphology experiments**

### 4.5.1 Overview

As described in section 4.1.3, EGF stimulation causes a variety of biological responses in different cell types, including morphological changes. Surfaces grafted with small star PEO molecules, which resist protein adsorption (see section 2.3), would be expected to adsorb less protein than those grafted with large molecules, since the smaller molecules could pack more efficiently. Rat hepatocytes seeded on these minimally adhesive surfaces rounded in response to EGF presented in either the soluble or tethered form.

### 4.5.2 Methods

Freshly isolated rat hepatocytes were suspended in medium as described above and seeded on tethered EGF surfaces grafted by the surface first method (see Table 3.1, star 3510) at a density of approximately 25,000 cells/cm<sup>2</sup>. Cells were observed daily via phase-contrast microscopy until day 3 or 4 when they were fixed in 95% ethanol. Images were acquired using a digital camera and the area per cell was determined and normalized to rounded cells. For each data point, a minimum of two slides and three fields, corresponding to at least 300 cells total, were examined. The viability of the cells was

verified by incubation with 25  $\mu\text{M}$  Syto 16 fluorescent viable cell dye for 2 hours (Molecular Probes).

#### 4.5.3 Results and Discussion

The relatively large stars used in the DNA synthesis experiments described in section 4.3.3 did not inhibit spreading to any significant extent. However, when cells were seeded on surfaces grafted with a smaller tethering molecule, star 3510, which has 70 arms/star of molecular weight 5500 daltons, cell spreading was inhibited. The cell rounding behavior observed was presumably due to more efficient packing of the smaller PEO molecules on the surface and as a result more inhibition of protein adsorption. In the absence of EGF or in the presence of nonspecifically adsorbed EGF cell rounding was inhibited but not completely abolished. This result again suggests that nonspecifically adsorbed EGF is not competent for signaling. Interestingly, the presence of EGF in either the soluble or tethered form enhanced the rounding effect on these surfaces (Figure 4.7) such that the cells were almost completely rounded for the duration of the culture period.

The extent of cell spreading on surfaces with adsorbed EGF or no EGF decreased with increasing surface concentration of PEO. Hepatocytes were seeded on tethered EGF surfaces and adsorption controls grafted with star PEO 3510 at different concentrations. The amount of EGF associated with the various slides is shown in Table 3.1. The extent of spreading depended both on the concentration of PEO in the coupling solution and on the presence or absence of tethered EGF. Figure 4.8 shows cell spreading data as a function of star PEO grafting density for slides with grafted and adsorbed EGF and for slides with adsorbed EGF only. It should be noted that the surface concentration of star PEO could not be measured directly; the concentration of PEO in solution was converted to a grafting density (fractional surface coverage) using ellipsometry measurements from Susan Allgor (Ito *et al.* 1996). For the mock activated slides with only adsorbed EGF, the extent of spreading decreased with increasing PEO grafting density. Interestingly, when

EGF was tethered to the PEO grafted slides, not only was cell spreading severely inhibited, but this effect totally dominated inhibition of spreading due to PEO concentration. These morphological effects were observed during the entire 3-day culture period.

## **4.6 EGF desorption during cell culture**

### 4.6.1 Surface first method

Experiments were performed to determine the extent of desorption of nonspecifically adsorbed EGF during cell culture for both the adsorption controls and tethered EGF surfaces grafted by the surface first method. Slides were prepared as described in the previous sections and coupled or mock coupled with  $^{125}\text{I}$ -EGF at either high or low surface density (15 ng/cm<sup>2</sup> or 2.5 ng/cm<sup>2</sup> tethered EGF, respectively). Rat hepatocytes were isolated and seeded in the same manner as for the biological activity experiments, and medium was changed and counted in the gamma counter each day. Figure 4.9 shows the results of these experiments; in neither case did the amount of desorbed EGF approach the 1 ng/ml concentration needed to stimulate DNA synthesis in rat hepatocytes (Blanc *et al.* 1992; Tomomura *et al.* 1987) and the amount desorbed for both the activated and mock activated slides was virtually identical.

### 4.6.2 Solution-first method

Experiments were performed to determine the extent of desorption of nonspecifically adsorbed EGF during cell culture for both the adsorption controls and tethered EGF surfaces grafted by the solution first method. Slides were prepared as described in the previous sections. Rat hepatocytes were isolated and seeded on the surfaces in the same manner as for the biological activity experiments, and medium was changed and counted in the gamma counter each day. 11% (+/- 0.9%) of the CPMs associated with the slides desorbed from the tethered EGF (after subtraction of mock

activated controls) per day. This amount may include free label (see section 3.10) and monoiodotyrosine in addition to intact EGF, and, as for the surface first method, did not approach the concentration needed to stimulate rat hepatocytes.

#### **4.7 Conclusions**

In the solution-first method, EGF is reacted with star PEO in the presence of EDA. Purification of the conjugate from unreacted starting materials included treatment with 7*M* guanidine hydrochloride. Neither the tethering reaction nor the purification had deleterious effects on the protein however, since both EGF and EGF-PEO-Amine were internalized at the same rate by B82 cells. This result also has important implications for receptor-mediated drug delivery via the EGF receptor, for example.

Tethered EGF grafted to aminated glass by either the solution first or surface first method stimulated the same biological effects in primary rat hepatocytes as those observed for soluble EGF, including cell rounding and increased DNA synthesis activity. This is the first clear demonstration that a growth factor covalently linked to a solid substrate, presumably preventing internalization, stimulates the same biological activities to the same extent as the soluble analog.

As with previous studies, nonspecifically adsorbed EGF could have potentially confounded these results in two ways. The first is through desorption during culture, introducing soluble ligand into the medium, and the second is through direct receptor binding of the adsorbed ligand. Both of these possibilities were ruled out in this study. Since the amount of growth factor tethered in these experiments was so low, even complete removal of the ligand from the surface would have been insufficient to cause cell responses. That complete removal did not, in fact, occur during culture was verified by monitoring the appearance of <sup>125</sup>I in the medium. Ideally, an additional experiment should be performed in which the cells are gently removed from the tethered growth factor surface without disrupting the covalent linkages, and cell-associated radioactivity counted.

Nonspecifically adsorbed EGF was shown to be incompetent for cell signaling as measured by cell rounding and DNA synthesis assays.

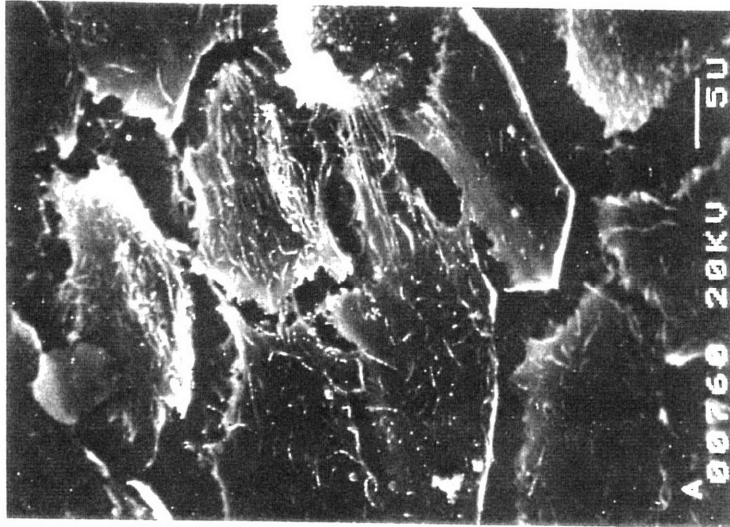
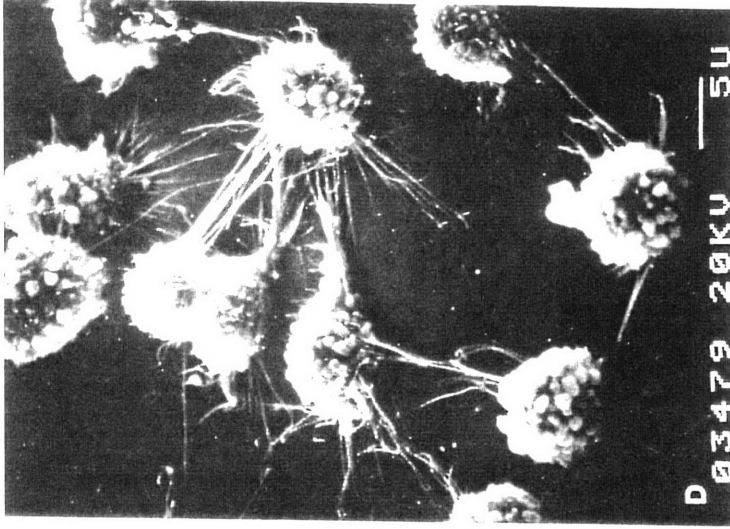




**Figure 4.1** EGF-induced rounding of A-431 cells (from Chinkers, McKanna, and Cohen, J. Cell Biol. (1981) **88**: 422-429). (A) Untreated culture. (D) Incubation for 20 minutes at 25°C in calcium- and magnesium-free medium containing 100 ng/ml EGF. Scanning electron micrographs at x1,400.

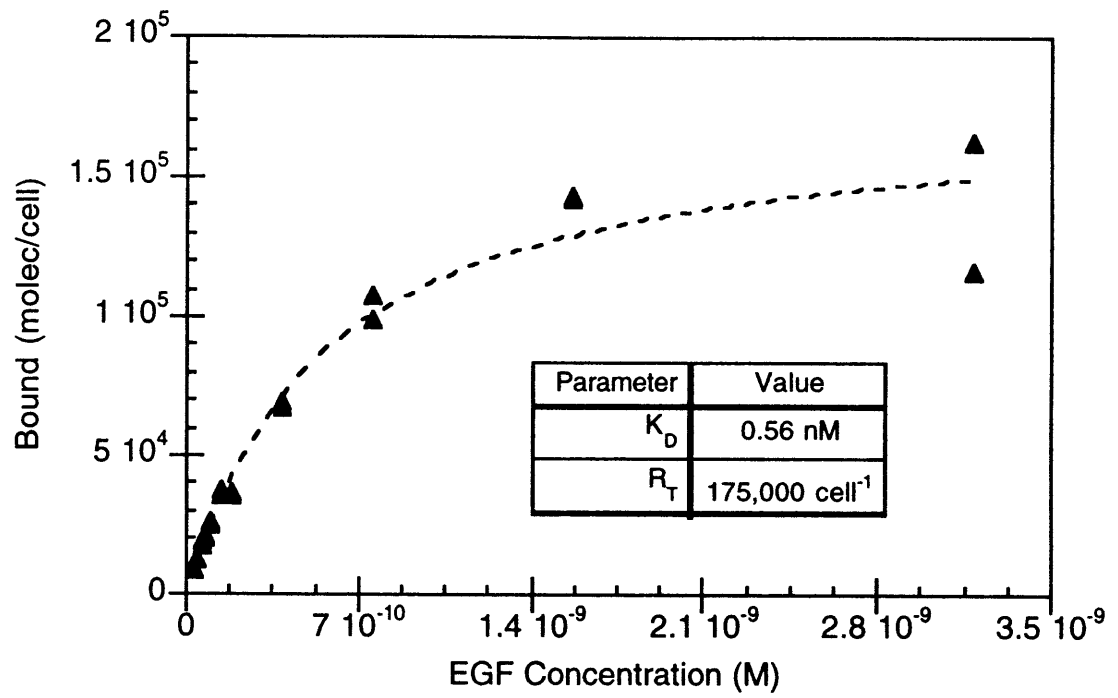


**Figure 4.2** Equilibrium binding data for rat hepatocytes.

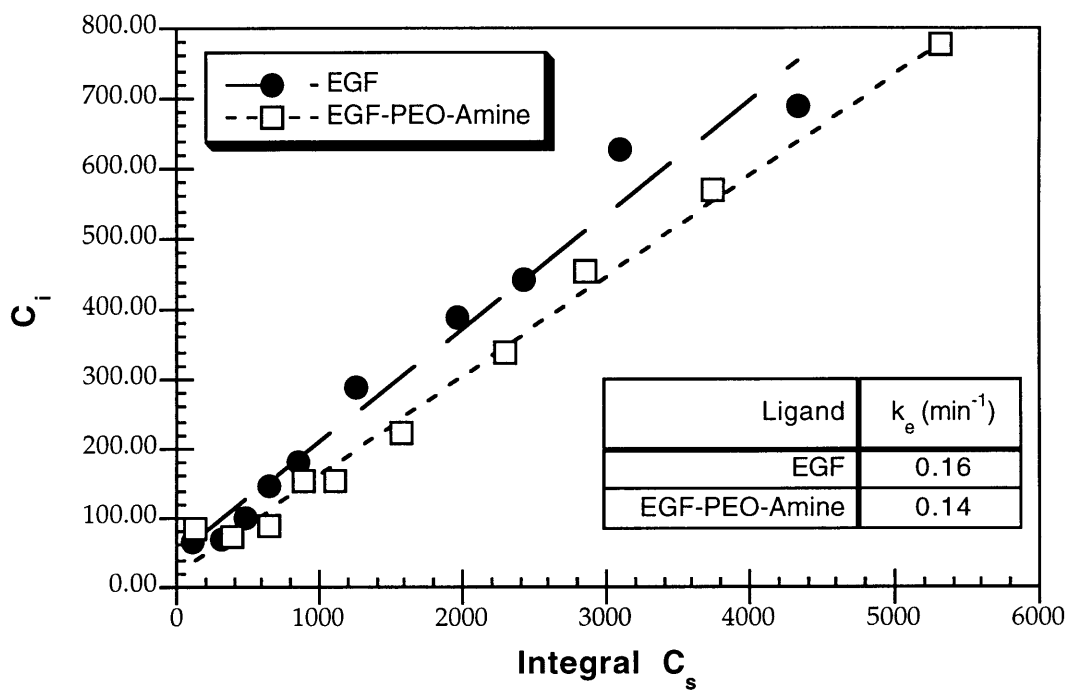


**Figure 4.3** Internalization plot for EGF and EGF-PEO-Amine (both in soluble form).. The concentration of both species was 16.4 pM.

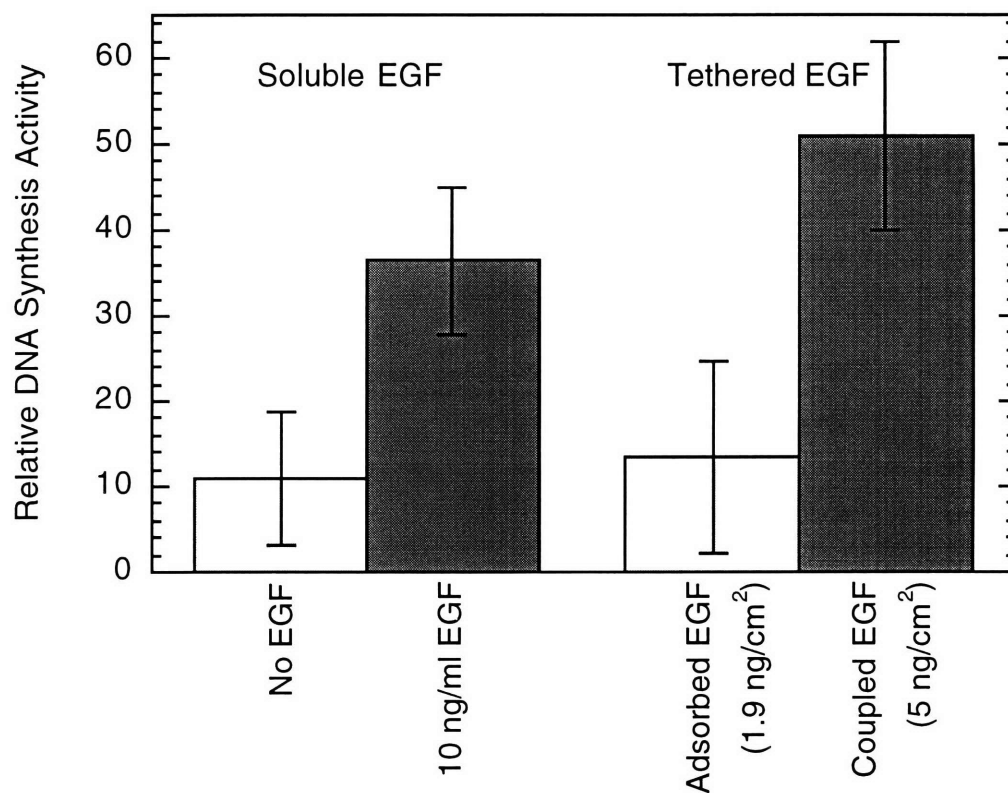


**Figure 4.4** DNA synthesis activity of cells exposed to soluble or tethered EGF. BrdU was incorporated between 48-68 hours after cell seeding. An index of DNA synthesis was calculated as the number of stained nuclei per area surface coverage. Results represent the mean +/- standard deviation for at least 100 stained nuclei.

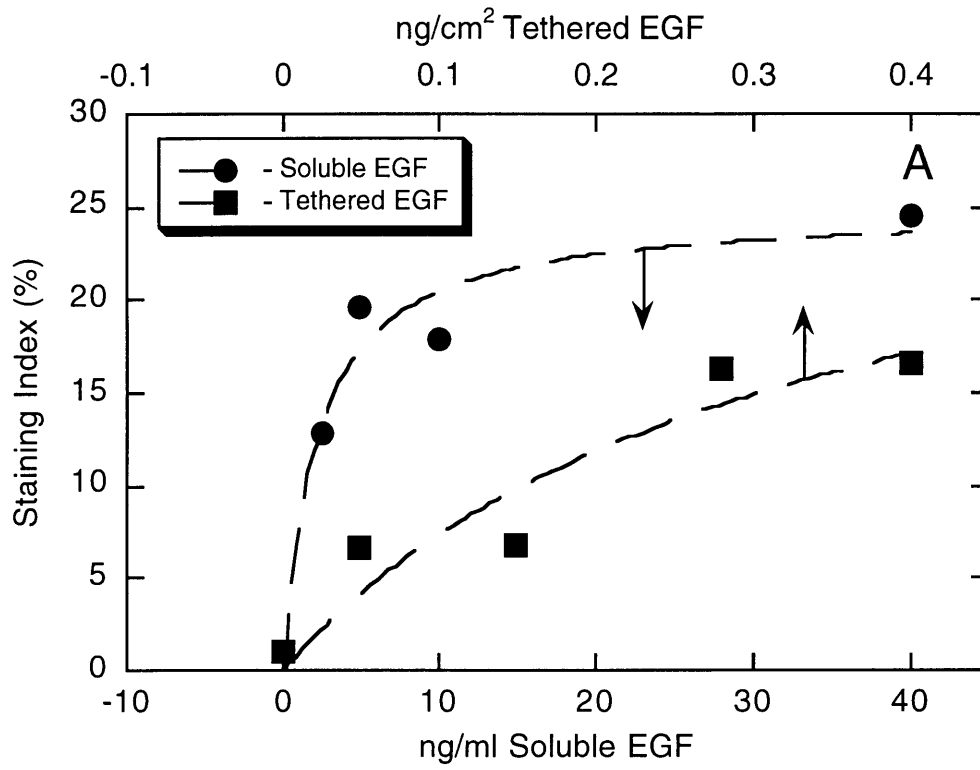


**Figure 4.5A** Soluble and tethered EGF dose response data (isolation 1).

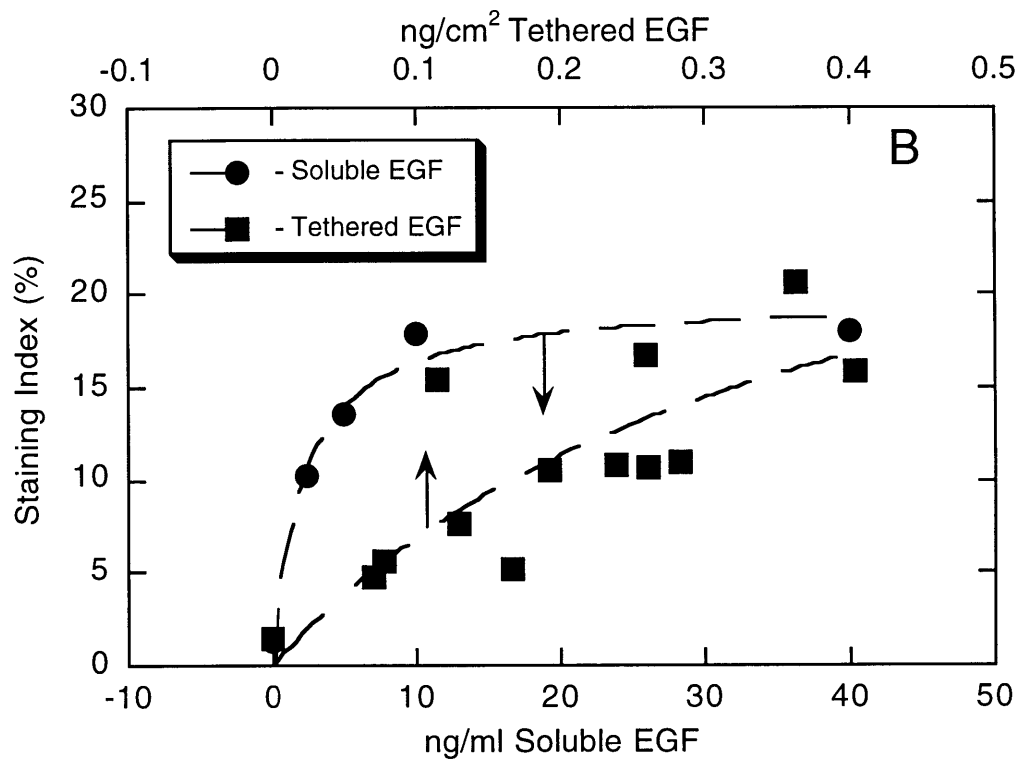


**Figure 4.5B** Soluble and tethered EGF dose response data (isolation 2).

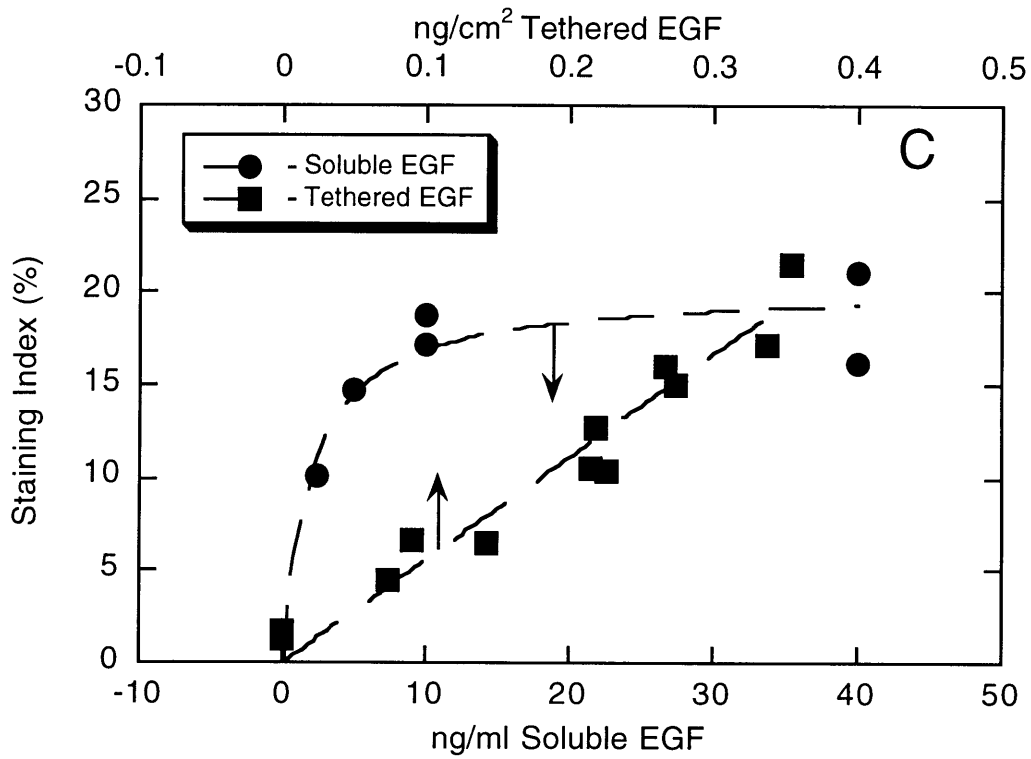


**Figure 4.5C** Soluble and tethered EGF dose response data (isolation 3).

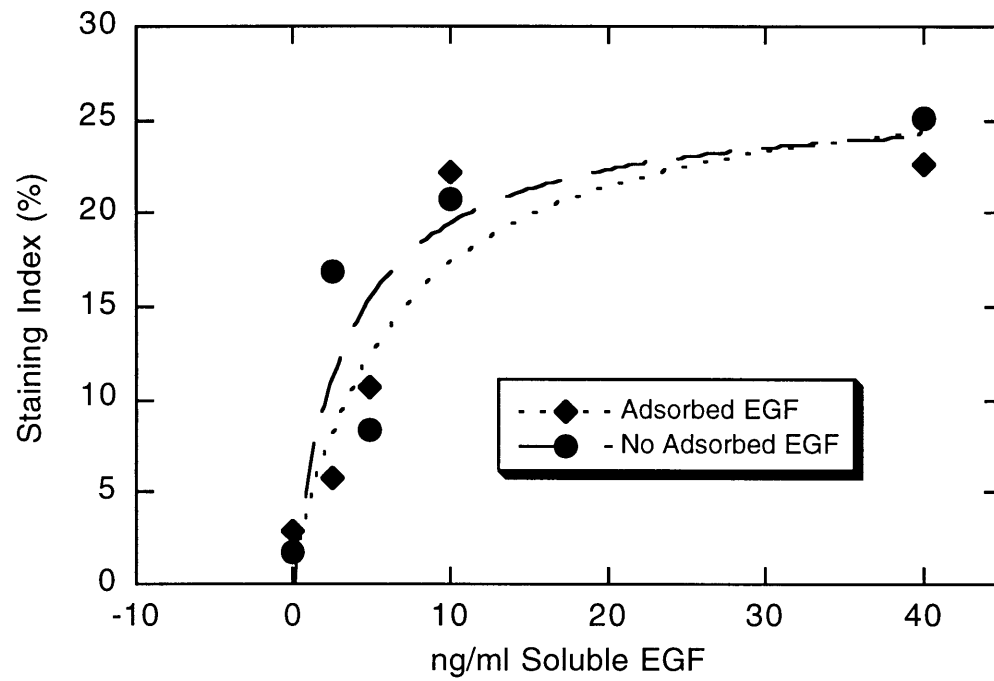


**Figure 4.6** DNA synthesis dose response to soluble EGF by cells seeded on glass with or without adsorbed EGF. Staining index represents the percentage of cells labeled with anti-BrdU antibodies.



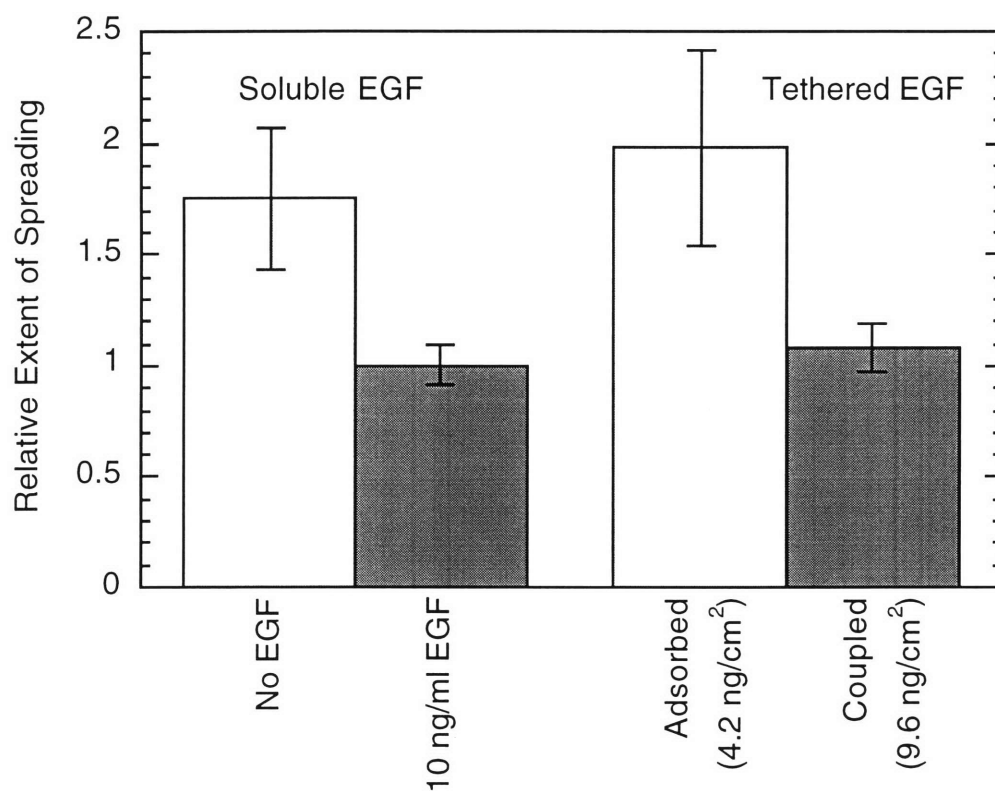


**Figure 4.7** Extent of cell spreading on surfaces grafted with star PEO ( $f=70$ ,  $M_a=5200$ ) from 1% solution and exposed to soluble or tethered EGF. For each data point, a minimum of two slides and three fields, corresponding to at least 300 cells total, were examined. Degree of spreading is normalized to that for completely rounded cells (=1).

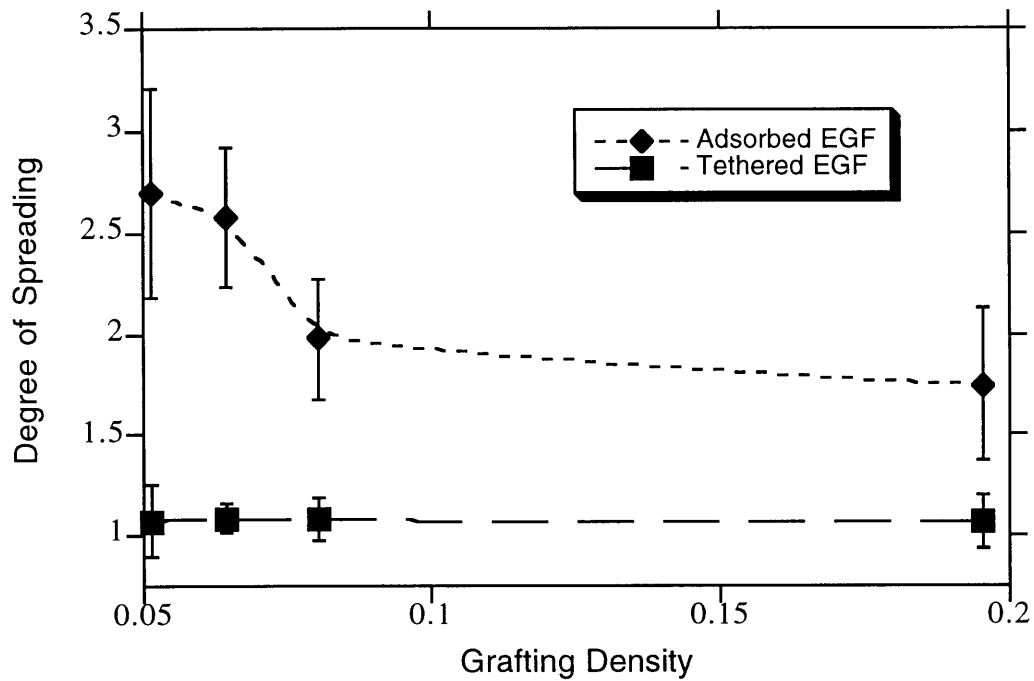


**Figure 4.8** Extent of cell spreading vs. PEO grafting density. Cell spreading was quantified as in Figure 4.7. Data for cells seeded on PEO surfaces in the complete absence of EGF (not shown) was similar to those for nonspecifically adsorbed EGF. Degree of spreading is normalized to that for completely rounded cells (=1). Grafting density is a dimensionless parameter; a grafting density =1 implies the cores are separated by the radius of gyration.

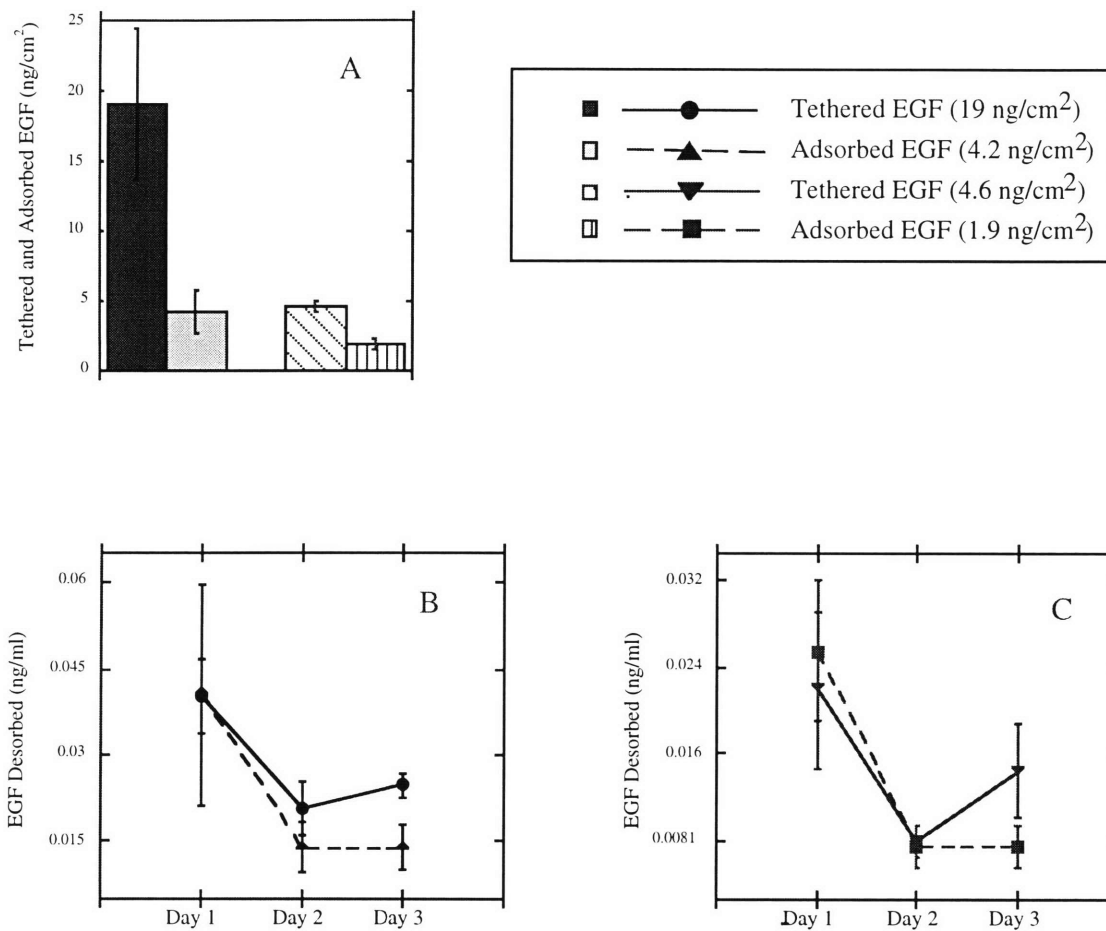


**Figure 4.9** Desorption of EGF from glass slides in culture. Slides were prepared as described in section 3.3 and coupled or mock coupled with either <sup>125</sup>I-EGF at high and low surface density (15 ng/cm<sup>2</sup> and 2.5 ng/cm<sup>2</sup> tethered EGF, respectively). Rat hepatocytes were isolated and seeded in the same manner as for the biological activity assays, and medium was changed and counted in the gamma counter each day. A. Amount of EGF associated with slides. B. and C. Desorption of EGF in culture for slides with high (B) or low (C) density of adsorbed EGF as described in panel A.

## Chapter 5

# Comparison of Soluble and Tethered EGF Signaling Efficiency

## 5.1 Introduction

### 5.1.1 Overview

In the previous chapter, the response of rat hepatocytes to stimulation by EGF in the soluble and tethered forms was examined. This data was presented in terms of EGF concentration in solution or EGF density on the surface, and it was shown that both forms of EGF stimulate DNA synthesis and cell rounding to the same maximum levels (see Figures 4.4, 4.5A-C, 4.7). In this chapter the question of whether receptors bound to tethered EGF signal as efficiently as receptors bound to soluble EGF is addressed. This efficiency was measured in terms of DNA synthesis activity elicited as a function of receptor occupancy. The comparison required the development of models for receptor occupancy as a function of ligand concentration for the tethered case. It was found that soluble and tethered EGF signal with equal efficiencies when the efficiencies were compared as functions of either initial equilibrium or steady state receptor occupancy.

### 5.1.2 Background

EGF binding to its cell surface receptor results in a flurry of intracellular enzyme activity leading to DNA synthesis as well as cell migration and morphological changes in various cell types (Barrandon and Green 1987; Blay and Brown 1985; Westermarck *et al* 1991). The mitogenic signaling cascade, reviewed by Campbell *et al.* (1995), begins with autophosphorylation of the receptor on multiple tyrosine residues. In one of the ensuing signaling cascades (Figure 5.1), Grb2 then binds to the phosphorylated receptor via its SH2 domain and recruits a guanine nucleotide exchange factor, Sos, to the cell membrane.

Sos accelerates nucleotide exchange in the membrane-bound G-protein p21<sup>ras</sup>, which goes on to activate Raf-1, as reviewed by Avruch *et al.* (1994). Raf-1 is an essential link between the receptor tyrosine kinase and the well-studied mitogen-activated protein (MAP) kinase signaling cascade. Raf-1 phosphorylates MEK (or MAP kinase kinase), which goes on to phosphorylate MAP kinase. MAP kinase phosphorylates a variety of intracellular proteins including transcription factors such as Elk-1 and the 40S ribosomal protein S6.

Importantly, the signal cascade just described begins while the receptor is in the membrane, i.e., before internalization. The role of internalization in signal transduction, if any, is unclear. It has been shown that substrate phosphorylation by the activated EGFR can continue in the endosome following internalization (Bevan *et al.* 1996) and that in some cases the greatest fraction of activated receptors is intracellular (Wiley and Cunningham 1981). Further, there have been numerous reports of nuclear translocation of EGF or EGFR (Johnson *et al.* 1980; Rakowicz-Szulczynka *et al.* 1986; Jiang and Schindler 1990; Holt *et al.* 1995), although some of this evidence is controversial (Carpentier *et al.* 1987). In total, the evidence is compelling that some fraction of EGF and/or its receptor remains undegraded and active after internalization and eventually appears associated with the cell nucleus in normal cells. The reports to date do not clearly address, however, what the biochemical role of this phenomena is, and whether it is required for mitogenesis or other downstream effects of growth factor stimulation. EGF binding sites have been reported to be present in the nuclei of rat liver cells (Ichii *et al.* 1988), and several components of the growth-factor induced signal transduction cascades, including phosphoinositide kinases, PLC, and protein kinase C, have been found in the nucleus (Leach *et al.* 1992; Payrastre *et al.* 1991). This raises the possibility that a secondary signal transduction cascade, analogous to that elucidated in the cytoplasm, could take place in the nucleus. Still, the question remains: how would EGF gain access to the interior of the nucleus? Amphiregulin (Johnson *et al.* 1992), Schwannoma-derived growth factor (Kimura 1993), and heregulin (Li *et al.* 1996) are ligands for the EGFR and have been shown to accumulate

in the nucleus following internalization, but these growth factors contain nuclear localization signals (NLS) (Holmes et al. 1992) which allow for their entry through the nuclear pore complexes. Deletion of the nuclear targeting signals from Schwannoma-derived growth factor resulted in the loss of mitogenic activity, even though activation of the early genes *c-fos* and NGFI-A were unimpaired (Kimura 1993). EGF is not known to contain an NLS. However, a putative NLS was found in residues 645-657 of the EGFR (Holt *et al.* 1994).

The demonstration by Wells *et al.* (1990) that an internalization-deficient mutant EGFR (c'973) imparted *greater* ligand sensitivity to transfected NR6 cells than WT receptor showed conclusively that neither EGF/EGFR internalization nor translocation to the nucleus is required for mitogenic stimulation by EGF in NR6 fibroblasts, a transformed cell line. Although a very small level of non-specific (constitutive) internalization of mutant EGFR was detected, and the putative NLS described above was not deleted in the c'973 mutant, if internalization or nuclear transport were in some way required for mitogenic stimulation, cells transfected with c'973 would be expected to grow far more slowly than cells having the WT EGFR. In fact, the opposite was observed.

Likewise, tethering of EGF to a solid substrate presumably restricts the tethered ligand receptor complex to the cell membrane. As illustrated in Figures 4.4, 4.5A-C, and 4.7, tethered and soluble EGF elicited qualitatively similar responses from primary hepatocytes when two different endpoints of the signal transduction cascade, DNA synthesis and cell rounding, were examined. These data further support the observation of Wells *et al.* (1990) that receptor internalization is not required for signal transduction.

Taken together, these data lead to the hypothesis that soluble and tethered EGF signal with the same efficiency when compared on the basis of equivalent numbers of receptor-ligand complexes formed. This chapter describes a model which allows quantitative comparison of the dose-response data for soluble and tethered EGF on the

basis of numbers of receptor-ligand complexes formed, and application of this model to test the hypothesis regarding signaling efficiency.

## 5.2 Model

### 5.2.1 Model Overview

The goal of the experiments was to directly compare the strength of the signal imparted by soluble and tethered EGF in terms of some measurable, clinically relevant cell response, and on a per receptor basis. To do this, an appropriate readout and the relationship of that particular cell response to cell surface receptor occupancy,  $[C]$ , was required. Ideally one would like to have a readout that depends on  $[C]$  through a straightforward (e.g., linear) relationship. It is most likely that such would be the case for an upstream, intracellular cell response such as RTK activation, but for tissue engineering applications the more clinically relevant readouts are downstream; e.g., proliferation or migration. Unfortunately, the quantitative relationship between receptor occupancy and cell proliferation, for example, is not well understood.  $[C]$  is determined by the concentration of ligand and the receptor-ligand binding kinetics ( $k_{on}$  and  $k_{off}$ ), and by down-regulation and de novo synthesis of receptors. It is therefore a complicated function of time, reaching an initial equilibrium which is then modified by the trafficking processes.

Aharonov *et al.* (1978) demonstrated that EGF must be present for several hours before commitment to proliferation is accomplished. During this time, the number of cell surface receptors decreases several fold. Models of EGFR trafficking (Starbuck and Lauffenburger 1992) and experiments with radiolabeled EGF (Wiley *et al.* 1991) indicate that greater than 50% of cell surface EGF receptors are downregulated within 15 minutes of growth factor stimulation, although steady state is not achieved before six hours. The measurable events of the signal cascade described above are completed within two hours of growth factor stimulation: in EGF-starved rat hepatocytes, maximum kinase activity of

ERK2, part of the MAPK cascade, is achieved by fifteen minutes post stimulation, and returns to baseline levels two hours later (Liu *et al.* 1996). The observation that EGF must be present in the medium hours after the initial burst of signaling has subsided indicates that signaling of some type must persist or be generated via another, later pathway to allow proliferation. Perhaps persistence of activated second messengers at some small, finite level above baseline is responsible, and the discrepancy is too small to detect with current assays. In any case, it is not known whether, during the several hours of EGF presence required for mitogenesis, there exists a critical time window in which the *number* of occupied, active receptors (cell surface or otherwise) determines the magnitude of the proliferative response.

The total number of receptor-ligand complexes per cell as a function of time was not measured in these experiments. However, from the known properties of EGFRs it can be inferred that the number of receptor-ligand complexes likely remains approximately constant or increases with time in the case of tethered EGF, where receptor internalization and degradation are presumably inhibited, and decreases in the case of soluble EGF (Gladhaug and Christoffersen 1987). Thus, to compare the soluble and tethered case it is presumed a critical time window does in fact exist. Two extreme bounds are considered-- initial binding and "steady state" binding-- to judge the relative efficiencies of soluble and tethered EGF at eliciting DNA synthesis.

For the comparison based on initial binding, the rate of cell proliferation in response to various doses of soluble EGF was determined and expressed as a function of the number of receptor-ligand complexes ( $[C^s_{PM}]_{eq}$ ) determined from a model for initial binding equilibrium, i.e., before trafficking events play a significant role. For comparison based on steady state binding, the number of complexes for the soluble case, including surface and internalized ( $[C^s_{TOT}]_{ss}$ ), was calculated from a steady-state model (Wiley and Cunningham 1981). These values are approximations of the true value of  $[C^s_{PM}]$  for the soluble case shortly after stimulation (0.4-2 hours) and  $[C^s_{TOT}] = [C^s_{PM}] + [C^s_i]$  after the



steady state value has been reached ( $> 20$  hours). For the tethered case, the amount of tethered ligand available to a cell depends on its contact area, which increases with time in culture as the cell spreads out on the surface. In order to compare soluble and tethered ligand receptor occupancy for the same time period, receptor occupancy for the tethered case was calculated for cells that had attached but not yet spread on the surface (shortly after stimulation,  $[C^t_{PM}]_{eq}$ ) and for cells that had spread on the surface for approximately 20 hours ( $[C^t_{PM}]_{ss}$ ; for comparison with the steady state soluble values).

DNA synthesis peaks in 4-week old rat hepatocytes at 24, 48 and 72 hours after explantation, with the peak at 48 hours approximately two-fold larger than the other two, and at 48 hours in adult hepatocytes when EGF is added at 2 hours (Tomomura *et al.* 1987). In this work, young adult rat hepatocytes (approximately 12 weeks) were used and DNA synthesis was measured from 20-67 hours after seeding to capture the first major round of DNA synthesis in response to EGF stimulation.

A functional relationship between  $[C]$  and cell proliferation was also required. It has been shown previously that there is a linear relationship between maximum proliferative response and receptor complex number in human foreskin fibroblasts and secondary mouse embryo fibroblasts. This linear relationship holds whether internalized receptor complexes are included (Knauer *et al.* 1984) or excluded (Starbuck and Lauffenburger 1992) based on the number of complexes at a single time point, steady state. It was assumed that such a linear relationship held for the current system as well; this assumption was confirmed experimentally.

### 5.2.2 Linear model for cell response vs. initial equilibrium receptor occupancy

In the ensuing analysis a model for cell response as a function of receptor occupancy is introduced (either initial equilibrium or steady state, the general case denoted by  $[C]$ ) and a hypothesis based upon parameters described in the model is formulated. The observable concentrations of soluble and tethered ligand are then related to receptor

occupancy using literature values for the soluble affinity constant,  $K_D^s$ , and an approximation for the tethered affinity constant,  $K_D^t$ . These relationships allow direct testing of the hypothesis.

The linear model of cell response as a function of receptor-ligand complex number can be expressed as follows:

$$(\% \text{ max response}) = m^s [C^s] \quad (5.1)$$

where the superscript s refers to soluble ligand. With the assumption that response is linearly proportional to complex number for the tethered case; i.e.,

$$(\% \text{ max response}) = m^t [C^t], \quad (5.2)$$

the hypothesis that soluble and tethered ligand signal with equal effectiveness requires

$$m^s = m^t. \quad (5.3)$$

To obtain values of  $m^s$  and  $m^t$ , dose response data in terms of receptor occupancy are required. Values of  $[C^s]$  and  $[C^t]$  are not directly measurable but can be derived from other experimentally accessible parameters. For both the soluble and tethered case, the total number of receptors present on the cell initially is fixed at the same value,  $[R]_{T,0}$ . The number of receptor-ligand complexes in each case can be varied systematically by varying the total concentration of ligand present initially,  $[L^s]_0$  or  $[L^t]_0$  (for soluble and tethered case, respectively).

### 5.2.3 Calculation of initial equilibrium complex number (soluble case), $[C_{PM}^s]_{eq}$

For the soluble case the concentration of soluble EGF can be converted to values of  $[C_{PM}^s]_{eq}$ , the receptor-ligand complex number after initial binding equilibrium has been reached but before trafficking events have played a significant role, according to:

$$[C_{PM}^s]_{eq} = \frac{[R]_{T,0} [L^s]_0}{K_D^s + [L^s]_0}, \quad (5.4)$$

which arises from a one-step model of receptor-ligand binding; a univalent ligand binding to a univalent receptor with no accessory molecules (see Section 4.2.2.1). Studies of

receptor-ligand binding have suggested the presence of two types of receptors on the cell surface, one with a high affinity and one with a lower affinity. The high affinity receptors make up a small fraction of the total receptor population (5,000-9,000 per cell compared to 165,000-166,000 low affinity receptors per cell). (Gladhaug and Christoffersen 1987; Dahmane *et al.* 1996). It has been proposed that the higher apparent affinity is not due to a second class of receptors, but to coupling factors which bind to receptors in the membrane (Mayo *et al.* 1989). A simplified model for both soluble and tethered ligand receptor binding was used in this study both to minimize the introduction of adjustable parameters and because doing so introduces a relatively small error. This error is at maximum approximately 5% (9,000/165,000).

#### 5.2.4 Calculation of steady state complex number (soluble case), $[C^s_{TOT}]_{ss}$ .

The relationship between steady state EGF concentration and receptor occupancy was derived by Wiley and Cunningham (1981). For conditions in which ligand depletion can be neglected (as in these experiments):

$$[C^s_{PM}]_{ss} = \left( \frac{K_{ss}[L^s]_0}{1 + K_{ss}[L^s]_0} \right) \frac{V_s}{k_{ec}}, \quad (5.5)$$

and

$$[C^s_i]_{ss} = \frac{k_e}{k_h} [C^s_{PM}]_{ss} \quad (5.6)$$

where

$$K_{ss} = \frac{k_{ec}k_f}{k_{eR}(k_r + k_{ec})}, \quad (5.7)$$

and the total number of undegraded soluble EGF-EGFR complexes is given by

$$[C^s_{TOT}]_{ss} = [C^s_{PM}]_{ss} + [C^s_i]_{ss}. \quad (5.8)$$

$V_s$  refers to the rate of insertion of receptors into the cell membrane,  $k_{ec}$  is the first order rate constant for internalization of receptor-ligand complexes,  $k_h$  is the rate constant for

degradation of complexes,  $[C_i^s]_{ss}$  is the number of intracellular complexes at steady state, and  $K_{ss}$  is the steady state constant.

The values of the parameters for EGF stimulation of freshly isolated rat hepatocytes in suspension culture, determined by Yanai *et al.* (1991), are given in Table 5.1. Dahmane *et al.* (1996) determined the internalization rate constant for rat hepatocytes in suspension culture as well; they obtained  $k_{eC}=0.41 \text{ min}^{-1}$ , indicating some variability in the value of this parameter for different cell isolations.

**Table 5.1** Steady state model parameter values for EGF-hepatocyte system. All parameters determined by Yanai *et al.* (1991) except for  $R_{T,0}$ , which is from Gladhaug and Christoffersen (1987).

Parameter	Symbol	Value
Forward (association) rate constant	$k_f$	$1.1(10)^9 \text{ min}^{-1} M^{-1}$
Reverse (dissociation) rate constant	$k_r$	$1.6 \text{ min}^{-1}$
Internalization constant (complexes)	$k_{eC}$	$0.11 \text{ min}^{-1}$
Internalization constant (empty receptors)	$k_{eR}$	$0.013 \text{ min}^{-1}$
Degradation rate constant	$k_h$	$0.086 \text{ min}^{-1}$
Rate of turnover of unoccupied receptors	$k_t$	$0.013 \text{ min}^{-1}$
Rate of new receptor synthesis (using $R_{T,0}=165,000 \text{ cell}^{-1}$ )	$V_s=k_t R_T$	$2145 \text{ min}^{-1} \text{ cell}^{-1}$

### 5.2.5 Tethered ligand-receptor binding model.

Tethered ligands are, by definition, covalently bound to a solid substrate. This makes determination of  $[C]$  very difficult in this case, since free and bound fractions cannot be determined by the standard techniques. This quantity could theoretically be determined by competition binding experiments with soluble ligand, but these require preparation of significantly more material than is currently feasible. With a reasonable estimate of the

dissociation constant for the tethered system, however,  $[C^t_{PM}]_{eq}$  and  $[C^t_{PM}]_{ss}$  can be calculated.

The one step binding model for tethered ligand is



where the superscript refers to tethered species. The concentration of tethered ligand,  $[L^t]_0$ , in units of #/cell, was determined from the average surface density ( $\langle L^t \rangle$ , mol/ $\mu\text{m}^2$ ) according to the equation:

$$[L^t]_0 = A_{cell} N_{AV} \langle L^t \rangle, \quad (5.10)$$

where  $A_{cell}$  is the average cell area,  $N_{AV}$  is Avagadro's number, and the subscript zero refers to the initial concentration of tethered ligand free to bind receptors. The bound and unbound receptor concentrations,  $[C^t_{PM}]$  and  $[R]$ , respectively, are also in units of #/cell. Cell area was an important parameter in these studies. Mooney *et al.* (1995) reported that hepatocytes seeded on high density of laminin (1000 ng/cm<sup>2</sup>) attached but remained round for the first half-hour following cell adhesion. This lag time was longer at lower ECM densities. Spreading proceeded at a relatively rapid rate for 4-6 hours after seeding at all ECM densities and then slowed. For comparison of the *initial* burst of signaling activity from soluble and tethered EGF receptors, a cell area of 490  $\mu\text{m}^2$  was used, the approximate area of a hepatocyte shortly after seeding and before spreading has occurred (Lopina, 1995). For comparison with steady state receptor occupancy in the soluble case, the cell area was measured at approximately 20 hours after seeding, after cell spreading is nearly complete. Thus, for less than saturating amounts of EGF, receptor occupancy *increases* with time for the tethered case, while it decreases with time for the soluble case.

Equation (5.10) also contains the assumption that the tethered growth factor molecules are distributed such that on average the number of molecules in a unit area does not vary greatly with the location of that area on the slide.

The rate of formation of receptor ligand complexes is given by:

$$\frac{d[C'_{PM}]}{dt} = k'_f [R][L'] - k'_r [C'_{PM}], \quad (5.11)$$

where  $k_f$  and  $k_r$  have units of cell/#/min and 1/min, respectively. The conservation law for receptors is

$$[R] = [R]_T - [C'_{PM}], \quad (5.12)$$

and, taking into account depletion of tethered ligand by receptor binding yields the following expression for  $[L']$ :

$$[L']_0 = [L'] + [C'_{PM}]. \quad (5.13)$$

At equilibrium the expression for the tethered complex concentration is given by the implicit equation:

$$\frac{[C'_{PM}]_{eq}}{[R]_T} = \frac{A_{cell} \langle [L'] \rangle - [C'_{PM}]_{eq}}{K'_D + A_{cell} \langle [L'] \rangle - [C'_{PM}]_{eq}} \quad (5.14)$$

where  $K_D^t$  is the tethered ligand receptor binding constant, with units of #/cell. This equation also holds for steady state.

### 5.2.6 Estimation of receptor binding for tethered EGF

The local concentration of EGF at the basal cell surface is extremely high in the tethered case, since diffusion of the protein into the bulk is restricted by the tether. For example, using a moderate tethering density of 50 pg/cm<sup>2</sup> (approximately 5(10)<sup>9</sup> molecules/cm<sup>2</sup>), and a diameter per star of 25 nm, the concentration of EGF in a unit volume of area 490 μm<sup>2</sup> (=A<sub>cell</sub>) and depth 25 nm (see Figure 5.2) is approximately 3 μM. It is therefore reasonable to assume that each tethered ligand molecule within the contact area of the cell will bind a receptor until all receptors are occupied, or

$$\begin{aligned} [C'_{PM}]_{eq} &= [L']_0 \quad \text{for } [L']_0 < [R]_{T,0} \\ [C'_{PM}]_{eq} &= [R]_{T,0} \quad \text{for } [L']_0 \geq [R]_{T,0} \end{aligned} \quad (5.15)$$

The effects of relaxing this requirement is examined in subsequent sections.

### 5.3 Results

In the previous chapter the dose response of primary rat hepatocytes to soluble and tethered EGF for three separate isolations was presented in terms of ligand concentration (Figures 4.5A-C). To compare the signaling capability of soluble and tethered ligand on a per receptor basis, receptor occupancies at these ligand concentrations were calculated at two extremes: initial burst and steady state. For comparison of the initial burst of signaling activity after EGF stimulation, ligand concentrations were converted to receptor occupancies using equation (5.4) for soluble EGF and (5.14) for tethered EGF and expressed as a fraction of total receptors occupied.

The combined dose response data for soluble EGF for the three separate isolations in terms of percentage of maximum response are shown in Figure 5.3. The data were reasonably linear, in agreement with previous results for human fibroblasts (Knauer *et al.* 1984). The slope of the line ( $m_{eq}^s = 95.7$ ) provides a measure of the efficiency of these EGFRs bound to soluble ligand at eliciting a mitogenic response. It is noteworthy that maximal DNA synthesis in rat hepatocytes required approximately 90% initial receptor occupancy. Figure 5.4 shows the dose response data for tethered EGF plotted as a percentage of the maximum staining index versus fraction of total receptors occupied (analogous to Figure 5.3 for soluble EGF). Importantly, the slopes of the curves ( $\langle m_{eq}^t \rangle = 81.6$ ) are comparable to that obtained for soluble EGF ( $m_{eq}^s = 95.7$ ), indicating that the data are consistent with the hypothesis that soluble and tethered EGF signal with equal effectiveness when initial receptor occupancy is compared.

A key assumption in the preceding analysis is that, within the cell's contact area, all tethered ligand binds to cell surface receptors (equations 5.15). This hypothesis was tested assuming a nonzero dissociation constant in order to determine the sensitivity of the results to variations in this parameter. Using  $K_D^t$  values up to  $82,500 \text{ cell}^{-1}$ , receptor occupancy was calculated using equation (5.14) and the tethered EGF dose response data were fit as

before to obtain  $m_{eq}^t$ . Table 5.2 shows the results of this analysis. With  $K_D^t=82,500 \text{ cell}^{-1}$ , half of the receptors are occupied by tethered ligand when  $[L^t]_0 = [R]_{T,0} = 165,000 \text{ cell}^{-1}$ . For comparison, with  $[L^s]_0 = 3 \mu M$  (e.g., in the vicinity of the basal surface cells exposed to  $25 \text{ pg/cm}^2$  tethered EGF), half of the receptors are occupied by soluble ligand according to equation (5.4) if  $K_D^s=3 \mu M$ . Importantly, an increase in the value of  $K_D^t$  implied that fewer occupied receptors are needed to stimulate DNA synthesis; i.e., the tethered growth factor is more effective. In a sense, then,  $\langle m_{eq}^t \rangle = 81.6$  is a lower bound for the initial tethered EGFR signaling efficiency, particularly since it is unknown if all the tethered EGF is truly accessible to bind receptors. Nevertheless, even at the highest value of  $K_D^t$  the value of  $m_{eq}^t$  remained within a factor of 2 of that obtained for the limiting case of zero dissociation. As shown in Figure 5.5, values of  $K_D^t$  significantly greater than zero caused the model to overpredict the maximum response of the cells; this value was established for this hepatocyte isolation using soluble EGF (Figure 4.5A).

The sensitivity of the results to variations in  $[R]_{T,0}$  was also measured, since the total number of EGF receptors may vary between isolations and with time in culture. For example, Gladhaug and Christoffersen (1987) found 165,000 receptors per cell and Dahmane *et al* (1996) found 166,000 receptors per cell. The results, shown in Table 5.3, indicate that variations in this parameter over physiological expectations do not significantly affect the model predictions.



**Table 5.2** Effect of tethered ligand dissociation constant on  $m_{eq}^t$  values. Receptor occupancy by tethered EGF was calculated using equation (5.14) (with  $A_{cell} = 490 \mu m^2$ ) and the dose response data from isolation #3 was fit to a linear model as in Figure 5.4 using  $[R]_{T,0}=165,000$ .

$K_D^t$ (#/cell)	$m_{eq}^t$
0	82.5
33,000	124
82,500	160

**Table 5.3** Effect of  $[R]_{T,0}$  on  $m_{eq}^s$  and  $m_{eq}^t$ . Receptor occupancy was calculated as in Figure 5.3 (soluble case) and Figure 5.4 (tethered case) with  $K_D^t=0$  #/cell,  $A_{cell} = 490 \mu m^2$ , and  $K_D=0.65$  nM.

$[R]_{T,0}$	$m_{eq}^s$	$m_{eq}^t$	$m_{eq}^s/m_{eq}^t$
130,000	95.7	71.5	1.34
165,000	95.7	82.5	1.16
250,000	95.7	124	0.77

The signaling efficiency of EGFRs bound to soluble EGF (both cell surface and internalized, undegraded complexes) at steady state and to tethered EGF after cell spreading were also compared. Table 5.1 gives values of the kinetic rate constants for the EGF-rat hepatocyte system as determined by Yanai *et al.* (1991). Using these values, the steady state total receptor-ligand complex number (equation 5.8) was calculated and plotted as a function of initial ligand concentration (Figure 5.6). The analysis assumes negligible depletion of ligand from the medium occurs, an assumption that is justified in the experimental protocols since large volumes of medium were used. As shown in Figure

5.6, the number of steady state complexes exceeds the initial number of cell surface receptors determined for this system by Gladhaug *et al.* (1987) (165,000 cell<sup>-1</sup>), Dahmane *et al.* (1996) (166,000 cell<sup>-1</sup>), and the value we determined experimentally (175,000 cell<sup>-1</sup>, Figure 4.2). This is due to new receptor synthesis ( $V_s=2145 \text{ min}^{-1}\text{cell}^{-1}$ ) and a low rate of ligand degradation in these cells ( $k_h=0.086 \text{ min}^{-1}$ ).

To compare the dose responses of rat hepatocytes to soluble and tethered EGF based on steady state receptor occupancy, ligand concentrations were converted to receptor occupancies using equations (5.5-5.8) for soluble EGF and (5.14) for tethered EGF and normalized by the initial number of receptors present on the surface of the cell. The soluble case will be treated first. Figure 5.7 shows the combined dose response data for soluble EGF for the three isolations in terms of percentage of maximum response as a function of total receptor occupancy, including internalized and cell surface complexes (equation 5.8). These data are reasonably fit by linear models (equation 5.1) assuming a nonzero threshold receptor occupancy below which no mitogenic signaling takes place (fit 2,  $m^{s_{ss}}=86.8$ ) and assuming no such threshold (fit 1,  $m^{s_{ss}}=52$ ). For comparison, threshold fractional receptor occupancies of 0.091 and 0.092 have been observed for a human fibroblast cell line (Knauer *et al.* 1984) and for NR6 cells Wells *et al.* (1990), respectively. It is likely, therefore, that the high threshold value obtained by fit 1 for rat hepatocytes ( $=0.53$ ) is an overestimation and therefore  $m^{s_{ss}}=87$  is an upper bound for this parameter. This slope was also determined assuming the proliferative response is a function of cell surface complexes only ( $[C^{s_{PM}}]_{ss}$ ). Cell surface complexes represent a small fraction of the total at steady state; in this system, the ratio of cell surface to internalized complexes is approximately 13 based on the parameters in Table 5.1. As a result, the calculated efficiency of receptors bound to soluble EGF is significantly higher when only cell surface complexes are included ( $m^{s_{ss}}=715$ ).

Signaling efficiencies were determined for the tethered case and compared to the soluble steady-state signaling efficiencies calculated above. Equation (5.14) was used to

convert tethered EGF surface density to receptor occupancy. The area of rat hepatocytes seeded on tethered EGF surfaces was measured approximately 20 hours after seeding. The average area of the hepatocytes was  $1300 \mu\text{m}^2$  with a standard deviation of  $300 \mu\text{m}^2$ . The increased cell area implies that a greater number of EGFRs have access to tethered ligand at a given surface density (if the amount of tethered ligand is limiting). The converted dose response data for isolation 3 (with  $A_{\text{cell}}=1300 \mu\text{m}^2$  and  $K_D^t=150,000 \text{ cell}^{-1}$ ) are shown in Figure 5.8. One isolation is shown to simplify interpretation of the results. As shown above,  $m^t$  increases with increasing  $K_D^t$ . Using values of the tethered ligand dissociation constant of  $10,000\text{-}200,000 \text{ cell}^{-1}$ , a range of values of  $m_{ss}^t$  were determined ( $68 < m_{ss}^t < 123$ ). This range is comparable to that obtained for  $m_{ss}^s$  based on the total number of complexes ( $52 < m_{ss}^s < 87$ ), but is significantly smaller than that obtained assuming only surface complexes are important ( $m_{ss}^s=715$ ) (see Table 5.4).

**Table 5.4** Signaling efficiencies of receptors bound to soluble and tethered EGF.

Case	Symbol	Value
Initial equilibrium, soluble	$m_{eq}^s$	96
Initial equilibrium, tethered	$\langle m_{eq}^t \rangle$	81.6
Steady-state soluble, all complexes	$m_{ss}^s$	52-87
Steady-state soluble, surface complexes only	$m_{ss}^s$	715
Steady state, tethered	$m_{ss}^t$	68-123

## 5.4 Discussion

### 5.4.1 Discussion Overview

In attempting the first direct comparison between soluble ligand that is free to be internalized and ligand that is covalently linked to a solid substrate, cell proliferation as a function of *initial* receptor occupancy and *steady state* receptor occupancy was compared for the two systems. The same conclusion was reached by both analyses; i.e., that tethered and soluble EGF signal with comparable efficiencies. It is important to bear in mind that it is not known during which time period, if any, the number of signaling receptors truly drives the proliferative signal. In fact, efforts to quantify the relationship between EGF receptor occupancy and cell proliferation have been rendered difficult by the considerable lag time (8-12 hours) between stimulation by EGF and onset of DNA synthesis (Carpenter and Cohen 1976). For many years it has been known that the mitogenic stimulus must be present for several hours before commitment to enter M phase is achieved (Aharonov *et al.* 1978). For example, removal of the stimulus after 1 hour of exposure totally prevents DNA synthesis (Carpenter and Cohen 1979). During this time the majority of the EGF receptors are internalized and some are degraded in lysosomes, a process termed downregulation (Carpenter and Cohen 1976; Haigler *et al.* 1979). The number of receptor-ligand complexes on the cell surface and intracellularly is therefore a function of time, and the question remains how this function dictates the rate of cell proliferation.

Insight may be gained from studies of intracellular signaling. The signaling events of the MAP kinase cascade (see Section 5.1.2) are remarkably rapid. Maximal MAP kinase activity in rat hepatocytes is achieved by fifteen minutes post stimulation, and returns to baseline levels two hours later (Liu *et al.* 1996), although small deviations from baseline levels may be undetectable by commonly used assays. The onset of DNA synthesis requires the activation of protein synthesis during G0 (Brooks 1977). This activation coincides with phosphorylation of ribosomal protein S6 (Thomas *et al.* 1980). S6

ribosomal protein activation is essentially complete within two hours after EGF stimulation. Interestingly, withdrawal of serum from serum-stimulated 3T3 cells after one hour results in a net dephosphorylation of S6 (Hershko *et al.* 1971) and an inhibition of protein synthesis (Thomas *et al.* 1980). Moreover, the rapid phosphorylation of S6 in response to EGF stimulation occurs in a dose-responsive manner and correlates with the extent of DNA synthesis (Thomas *et al.* 1982). These results imply that, although the continued presence of EGF is required at some level for commitment to M phase, information regarding the rate of proliferation is imparted within minutes of initial stimulation. Therefore the relevant comparison appears to be between *initial* soluble and tethered ligand receptor binding.

Initial receptor occupancy for the soluble case was calculated using a two-step model (Equation (5.4)). When replotted in terms of fractional receptor occupancy the data were reasonably fit by a linear model (Figure 5.3). The slope ( $m^{s_{eq}}$ ) gives a measure of the proliferative signal of the soluble EGF. The tethered EGF dose response data were replotted in terms of receptor-ligand complex number assuming all ligand binds receptors within the cells' contact area ( $490 \mu\text{m}^2$ ) until all receptors were occupied (Equations (5.15), see Figure 5.4). The contact area chosen is that of an attached cell before it has completely spread on the surface, and allowed direct comparison with initial binding equilibrium in the soluble case. Importantly, the slopes of the lines fit to the data were comparable to those obtained for soluble EGF, implying that soluble and tethered EGF signal with equal effectiveness. This conclusion is also reached if steady state receptor occupancy is used to calculate the signaling efficiencies. Steady state receptor occupancy was calculated using a model developed by Wiley (1981) (equations 5.5-5.8). Comparisons were made for the soluble case including both cell surface and internalized, undegraded complexes, and surface complexes only. For the former comparison, it was assumed that internalized, undegraded complexes and complexes residing in the plasma membrane are equivalent in terms of signaling, an assumption which awaits experimental verification. Two values of  $m^{s_{ss}}$  were obtained for total receptor occupancy (Figure 5.7), one assuming a threshold

receptor occupancy below which signaling does not occur, and one assuming no such threshold; these provide an upper and lower bound for this parameter ( $52 < m_{ss}^s < 87$ ). Since surface complexes make up a small fraction of the total for this system ( $[C_{i}^s]_{ss}/[C_{PM}^s]_{ss}=13$ ), the signaling efficiency becomes much larger for the soluble case when only surface complexes are included in the calculation ( $m_{ss}^s=715$ ). For the tethered case, steady state receptor occupancy was calculated using equation (5.14) with a cell area measured twenty-two hours after seeding (i.e., after the bulk of cell spreading has taken place,  $A_{cell}=1300 \mu\text{m}^2/\text{cell}$ ). Using a range of  $K_D^t$  values ( $10,000\text{-}200,000 \text{ cell}^{-1}$ ), a range of values of  $m_{ss}^t$  were determined ( $68 < m_{ss}^t < 123$ ). This range is comparable to that obtained for  $m_{ss}^s$  calculated based on total complexes, but is significantly lower than that based on surface complexes only (see Table 5.4). Internalized complexes have been shown to continue signaling in the endosome (reviewed in Bevan *et al* 1996; Baass 1995), implying that calculation of the signaling efficiency based on total complexes is more appropriate.

The diffusion of tethered ligand molecules is physically restricted by definition, as is that of the receptor once it has bound a tethered ligand. The question of signaling efficiency of tethered EGF-EGFR complexes relative to the freely-diffusing analog becomes whether this physical restriction is likely to cause a change in the dissociation constant of the complex, or in subsequent substrate phosphorylation. It is assumed herein that the intrinsic rate constants for ligand-receptor binding,  $k_{on}$  and  $k_{off}$ , are unaffected by tethering. The forward and reverse rate constants for the reaction between receptor and ligand is actually a composite of these intrinsic on and off rate constants and a rate constant for diffusion. The latter is likely to be affected by tethering, since diffusion of receptors in the membrane would likely be limiting in the tethered case. However, cell proliferation in response to initial *equilibrium* receptor occupancy is compared in this study, so kinetic effects (e.g., diffusion effects) will not be dealt with further in this section. The remaining

question is whether tethered EGFR will be physically restricted from interacting with its usual substrates and thereby signal less efficiently.

Since the focus of this work is on engineering cell-substrate interactions, it is tempting to adopt an oversimplified view of the cell interior and assume that EGFR kinase substrates are either freely diffusible in the cell membrane or exist homogeneously distributed in the cytosol. This view has been cast into doubt by recent experiments demonstrating that the cytoskeleton plays an important role in orienting some protein tyrosine kinase substrates (reviewed in (Carraway and Carraway 1995)). Phosphatidylinositol kinase, phosphatidyl-4-phosphate kinase, diacylglycerol kinase, and phospholipase C are all associated with cytoskeletal elements (Payraastre *et al.* 1991; Grondin *et al.* 1991; Vaziri and Downes 1992; Yang *et al.* 1994). Moreover, EGFR itself is an actin-binding protein (den Hartigh *et al.* 1992) and recruitment of the receptor to the cytoskeleton causes a potentiation of the receptor kinase. Cytoskeleton-associated receptors are able to phosphorylate their substrates more efficiently than receptors not associated with the cytoskeleton (Gronowski and Bertics 1993). Cytoskeletal microfilaments and stress fibers are clearly not homogeneously distributed throughout the cell, and their points of intersection with the cell membrane are discrete, not continuous. Furthermore, the classes of proteins present in these localized areas, some of which are EGFR substrates, vary with position. On the basal surface, where in traditional cell culture the cell is in contact with adhesion proteins on a solid substrate and where cells would contact tethered growth factor molecules, focal adhesion complexes are present. The apical surface presents a second membrane environment. In the following sections the current literature on EGFR substrates in both of these membrane environments is reviewed, and the potential effects of restricting activated EGFRs to discrete points on the basal surface are considered.

## 5.4.2 Membrane Localization

### 5.4.2.1 EGFR Distribution in Hepatocytes in Vivo

The hepatocyte is a polarized epithelial cell with three plasma membrane domains: sinusoidal, lateral, and bile canalicular (reviewed in (Evans 1980)). The sinusoidal, or basal domain, possesses numerous microvilli and is specialized for exchange of metabolites with the blood. The lateral domain is in contact with adjacent hepatocytes and possesses junctional elements for cell-cell adhesion and communication. Membrane components of the bile canalicular or apical domain are restricted from the other domains by tight junctions. EGFR have been localized in vivo to the sinusoidal and lateral domains of rat hepatocytes before treatment with EGF, and are absent from the apical region. 2-4 minutes after EGF treatment, complexes can be found in coated vesicles, larger vesicles, and tubules near the cell periphery. By 15 minutes after stimulation EGFR can be found in multivesicular endosomes near the apical surface (Dunn *et al.* 1986; Bartles and Hubbard 1986). These results imply that presentation of EGF solely on the basal surface of cells in vitro (i.e., the tethered case) should not inhibit receptor binding or access to the usual RTK substrates.

### 5.4.2.2 Focal Adhesion Contacts (FACs) and hemidesmosomes

The discovery of at least one type of growth factor receptor, a high affinity FGF receptor, *flg* (Plopper *et al.* 1995) within the focal adhesion complex has generated much interest. The FGF receptor has been shown to phosphorylate a critical protein involved in FAC formation, p125<sup>FAK</sup> (Hatai *et al.* 1994), and bradykinin phosphorylates both FAK and paxillin, a FAK-binding protein and another player in FAC formation. Information on the role of EGFR in FAC formation or signaling is scarce. EGFR does not phosphorylate FAK or paxillin, nor has it been shown to associate with FACs.

While EGFR stimulation has been shown to cause phosphorylation of at least one integrin ( $\alpha 6\beta 4$ ) in hemidesmosomes (Mainiero *et al.* 1996), there is no evidence that EGFR acts directly on the integrin molecule. Nevertheless, integrins and growth factor



receptors including EGF cooperate to stimulate the MAP kinase pathway, but only if both are aggregated and occupied by ligand (Miyamoto *et al.* 1996). This brings up the intriguing question of whether co-clustering of integrin and growth factor receptors would enhance or inhibit mitogenic stimulation. This question could be addressed by presentation of both ligands in pre-clustered form on a biomaterial surface.

#### 5.4.2.3 Membrane Localization Summary

There does not appear to be any evidence that localization of active EGFR exclusively to the basal surface of cells will inhibit or enhance interactions with kinase substrates important for mitogenic activity of EGF. The apical cell surface of hepatocytes does not appear to possess EGFR *in vivo*, and although the basal surface presents a unique signal transduction environment due to the presence of FACs, EGFR has not been localized to FACs.

### **5.5 Conclusions**

The signaling efficiencies of soluble and tethered EGF were measured in this chapter as a function of initial equilibrium receptor occupancy and assuming that all tethered EGF binds cell surface receptors. The latter assumption is justified by the extremely high local concentration of EGF near the basal surface of the cell in the tethered case. The signaling efficiencies were also measured as a function of steady state receptor occupancy. It was found that tethered and soluble EGF stimulate mitogenesis in rat hepatocytes with comparable efficiencies by both analyses. Although it is not clear during which time period the number of receptor-ligand complexes determines the rate of cell proliferation, the bulk of the evidence implies that early events are most likely to be important. In any event, it can be concluded that soluble and tethered EGF signal with equal efficiencies, confirming that internalization of EGF is not required for biological activity. This is the first such demonstration in a primary cell type. This result has important implications for the

quantitative study of cell responses to growth factor stimulation, as described in the final chapter.

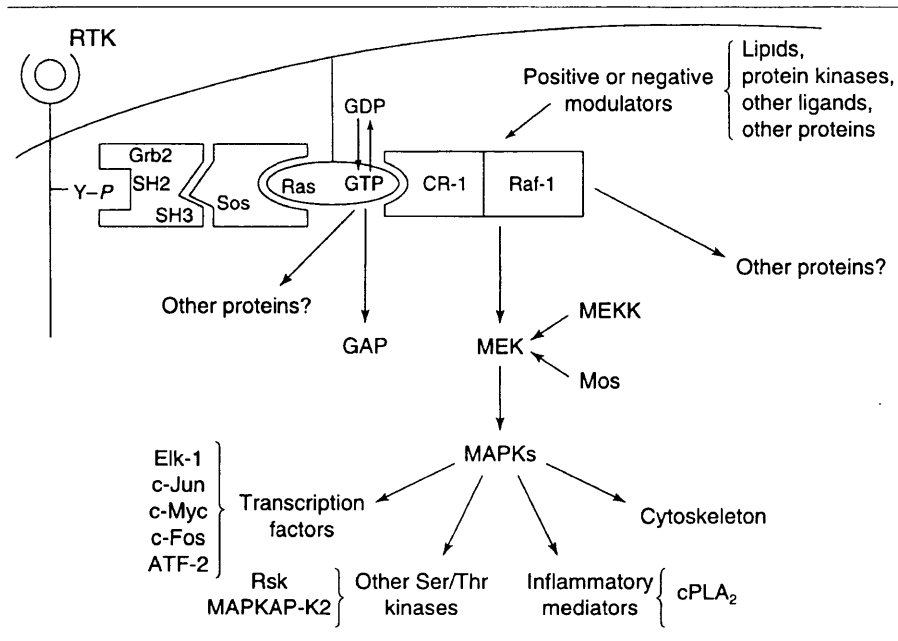


**Figure 5.1** Model for RTK signal transduction through the Ras-activated protein kinase cascade. From Avruch *et al.* (1994).

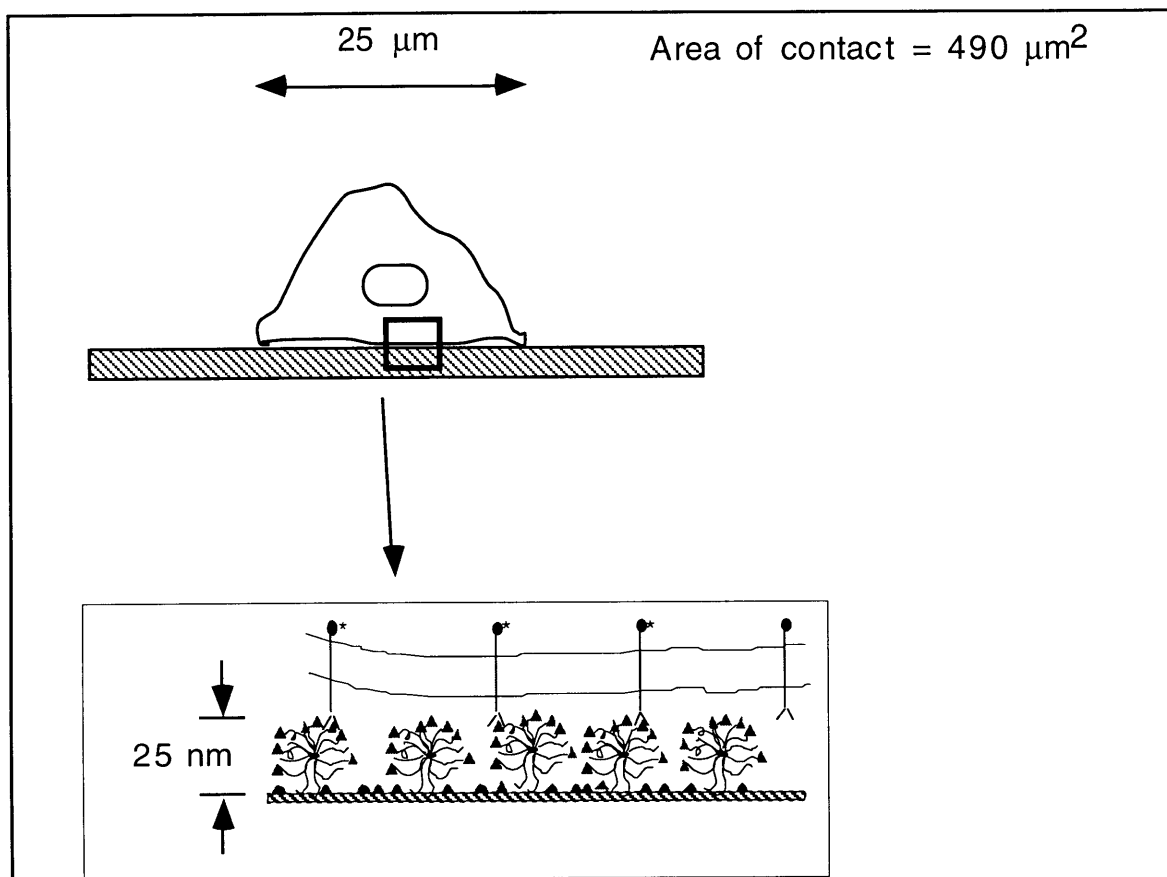


**Figure 5.2** Size scales for determination of local EGF concentration in the tethered case.

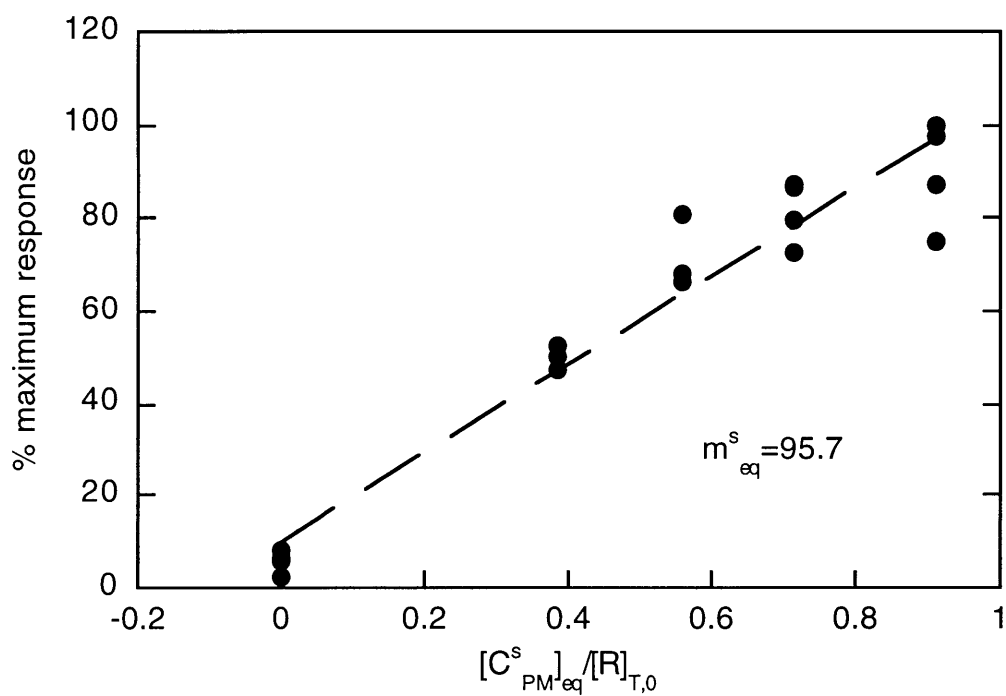


**Figure 5.3** Dose response data for soluble EGF in terms of fraction of total receptors occupied at initial binding equilibrium. Data from three separate isolations (see Figures 4.5A-C) were replotted using equation (5.4) with  $K_D^s=0.65$  nM and  $[R]_{T,0}=165,000$ . Abscissa is the percentage of the maximum staining index.

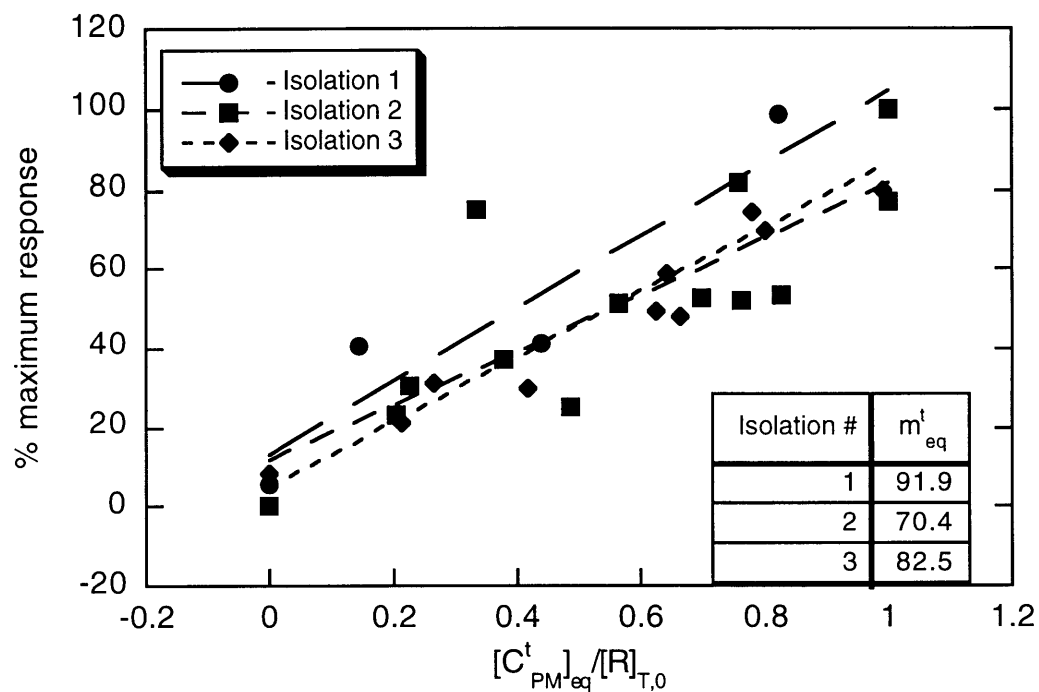


**Figure 5.4** Dose response data for tethered EGF in terms of fraction of total receptors occupied after cells have attached to the surface but before significant spreading. Data from three separate isolations (see Figures 4.5A-C) were replotted using equations (5.14) with the following parameter values:  $[R]_{T,0}=165,000$ ,  $K_D^t=0$  #/cell, and  $A_{cell} = 490 \mu\text{m}^2$ . Abscissa is the percentage of maximum staining index.

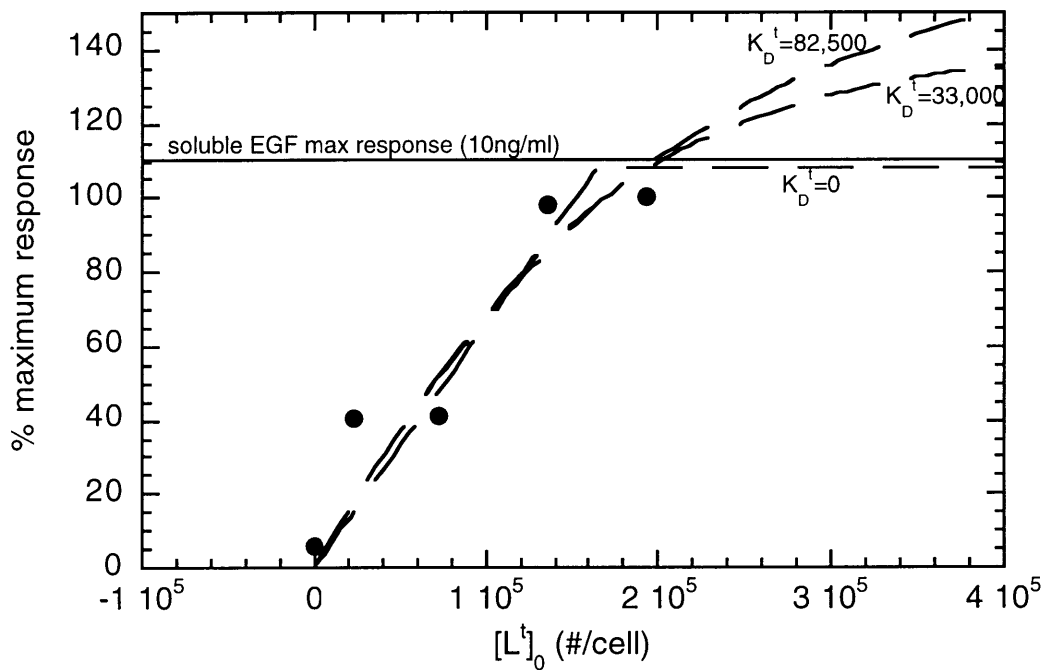


**Figure 5.5** Curve fits to tethered EGF dose response data (isolation 1) with various values of  $K_D^t$ . Data (see Figure 4.5A) were replotted in terms of ligand density per cell using equation (5.10). These data were fit using equation (5.2) and (5.14) with the indicated values of  $K_D^t$ .

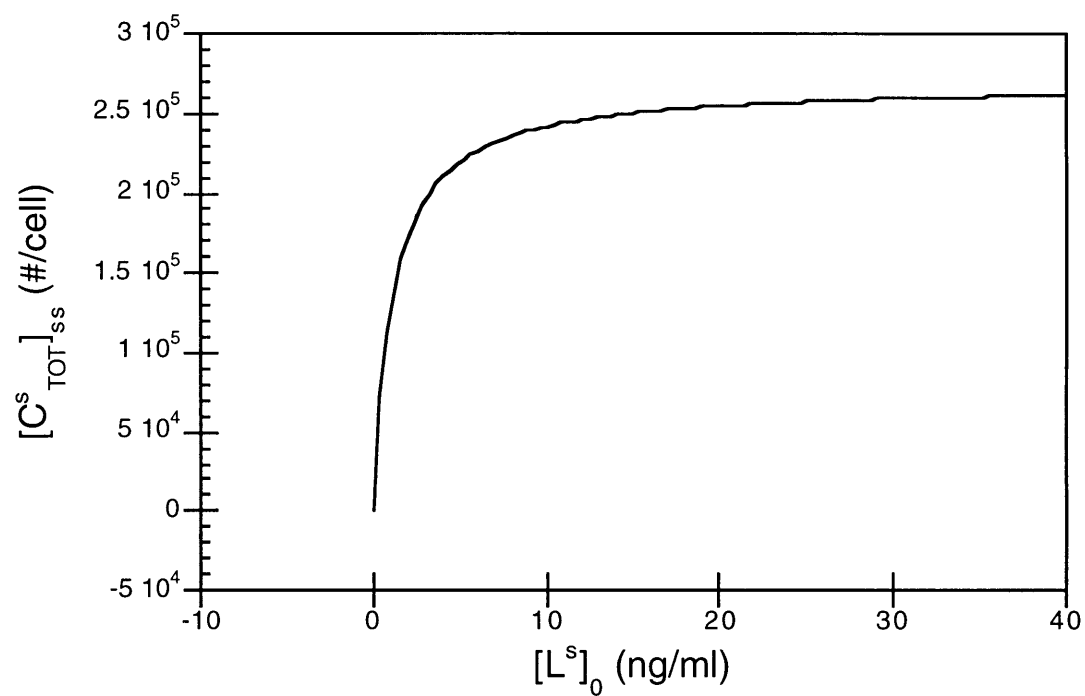


**Figure 5.6** Cell surface and internalized receptor-ligand complex number at steady state as a function of ligand concentration rat hepatocytes stimulated by EGF. Complex number was calculated using equations (5.5-5.8) with the parameters given in Table 5.1.



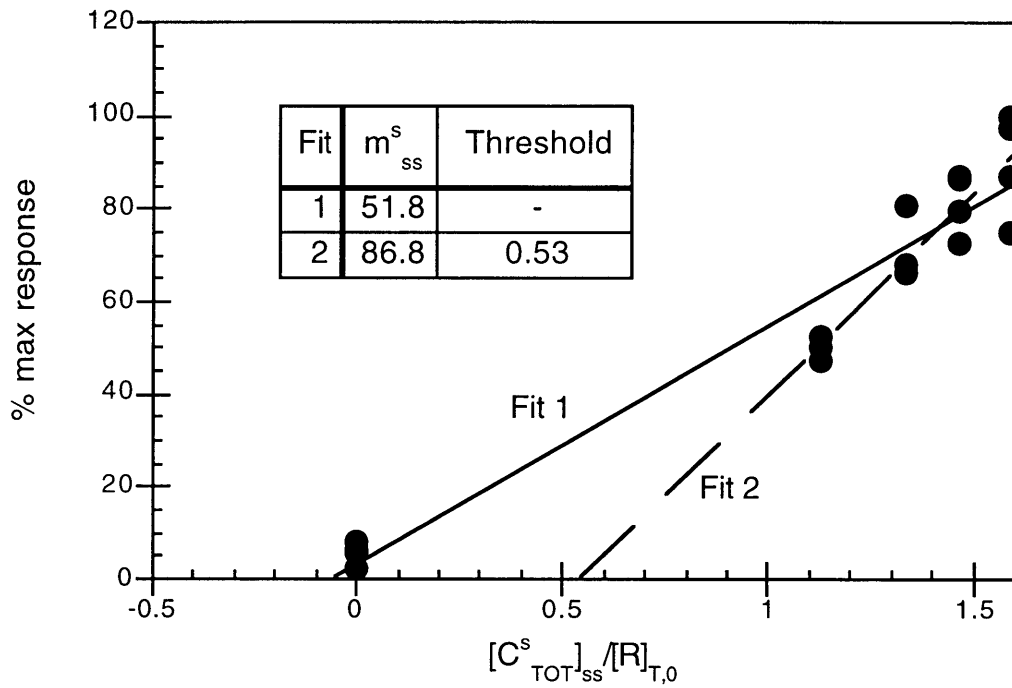


**Figure 5.7** Dose response data for soluble EGF stimulation of primary rat hepatocytes as a function of steady state surface and internalized, undegraded receptor-ligand complexes. Data are fit to least-squares linear models assuming a nonzero threshold value below which no proliferative signal is generated (fit 2) and assuming no threshold value (fit 1).

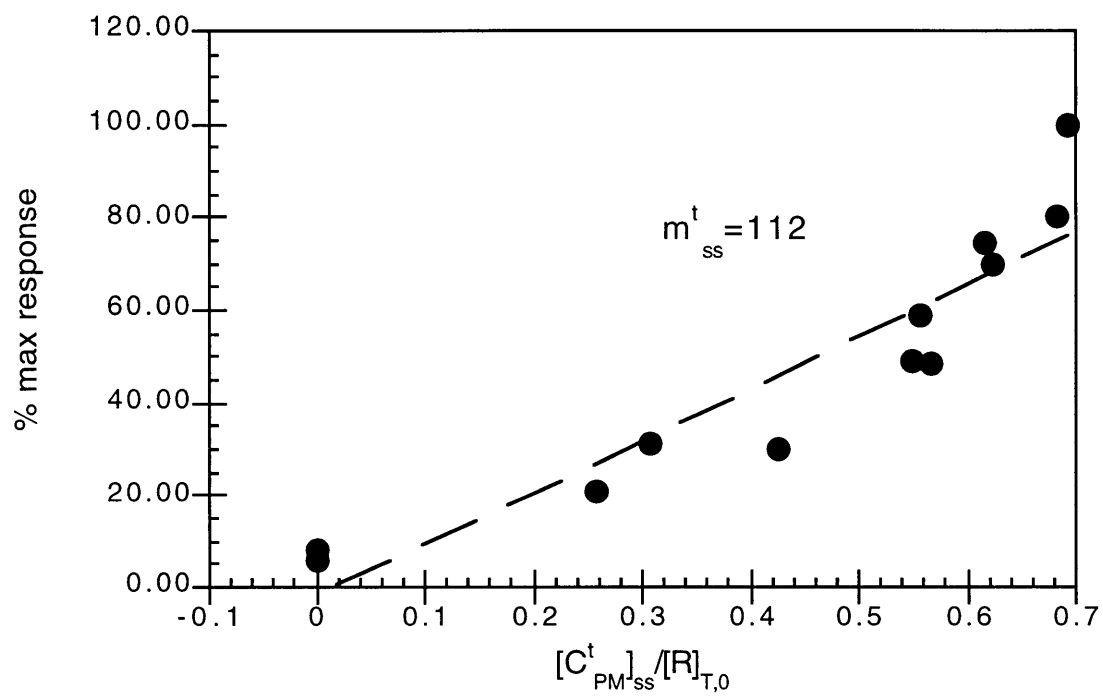


**Figure 5.8** Dose response data for tethered EGF (isolation 3) in terms of fraction of total receptors occupied twenty hours after seeding. Data were replotted using equation (5.14) with  $A_{\text{cell}}=1300 \mu\text{m}^2$  and  $K_D^t=150,000 \text{ cell}^{-1}$  to convert ligand concentrations to values of  $[C^t_{PM}]_{ss}$ .

## Chapter 6

### Future Directions

#### 6.1 Overview

In the preceding chapters it was demonstrated that cell behavior could be influenced by receptor ligands incorporated into a biomaterial surface. In addition to being of use in tissue engineering, engineered biomaterials such as these can be used to answer fundamental questions of receptor biology. The protein-polymer conjugate synthesized for grafting to surfaces has intriguing applications in the untethered form, as well. In the following sections research directions spawned from the experiments described earlier in this work are put forth.

#### 6.2 Membrane domain considerations in biomaterials

Traditional in vitro cell culture methods employ solid impermeable substrates upon which cells attach and spread; typically the surface is the bottom of a culture dish, with medium present on top of the cells. This environment bears little resemblance to the situation in vivo, in which cells (particularly epithelial cells) perceive distinct signals from their basal, lateral, and apical surfaces. For example, epithelial tissues may typically receive signals from integrins and hemidesmosomes on their basal surfaces, desmosomes on their lateral surfaces, and some growth factor and nutrient receptors on their apical surfaces. It is not clear what the effect of restricting certain signals (e.g., growth signals) to a particular membrane surface (e.g., the basal surface) has on the biological response to the signal. Yet for a working understanding of cell responses to engineered biomaterials which mimic the normal biological environment (for example, the sandwich culture system developed for liver cells) it is important to be able to predict how *where* a signal is delivered will impact *what* cellular response is obtained.

The roles of growth factor receptors in different membrane domains are just now being elucidated. Desmosomes are localized areas of intercellular contacts that join cells together in epithelial tissues. In the E-cadherin-linked desmosomal complex,  $\beta$ -catenin mediates the interaction between E-cadherin and  $\alpha$ -cadherin; the latter is an actin-binding protein and thereby serves as a link to the cytoskeleton. EGFR is important in this context because it phosphorylates  $\beta$ -catenin, causing the entire complex to dissociate from the cytoskeleton (Hoschuetzky *et al.* 1994). In this particular system, then, activated EGFR serves a role in substrate phosphorylation at the cell-cell junction. If the EGF signal were present but the activated receptor restricted to an area removed from the desmosome, would the normal cellular responses to EGF be observed? Is EGFR kinase activity necessary for dissociation of the E-cadherin complex? Investigators have reported localization of EGFR to membrane ruffles in A431 cells along with signal transduction molecules (Diakovna *et al.* 1995). This has led to intriguing speculation by the same investigators that these ruffles are in some way special sites for signal transduction. Using non-internalized forms of the ligand, this hypothesis can be tested without altering the cellular machinery.

### **6.3 Polymer-enhanced drug delivery**

Delivery of therapeutic agents by cell transplantation holds great promise for treating diseases resulting from tissue or organ loss. The potential is even greater if gene therapy using the donor tissue is also considered. It would be helpful in many of these applications to be able to control the diffusion of these cellular products in order, for example, to retard their disappearance from the local environment or their clearance from the body through the kidneys. Poly(ethylene oxide) has been used to modify pharmacokinetics of numerous drugs and to retard glomerular filtration. The PEO is covalently attached to the target drug, effectively increasing its hydrodynamic radius, often without affecting the activity of the drug. If a system could be designed in which

modification of cell-synthesized therapeutic proteins with highly branched PEO could be accomplished before its secretion into the extracellular space, an additional level of control of the diffusion of the agent could be achieved. Such a system would require delivery of the polymer to secretion vesicles in the cell interior, which could be accomplished by ligand (mannose-6-phosphate, EGF) coupling to a branch of the polymer (via a labile linker), and coupling of the polymer to the engineered protein. This latter step could be accomplished theoretically by covalently attaching an antibody for the therapeutic to another arm of the branched polymer. Such an antibody would have to be of high affinity and not interfere with the active site of the therapeutic protein.

The use of Sertoli cell products in cell transplantation applications is one situation where this technology would be useful. Sertoli cells serve a vital function in testis; they secrete immunosuppressive factors that are needed to protect sperm, which are immunogenic. Tissue engineers have recently been intrigued by the possibility of using these cells in combination with allografts or xenografts of cells transplanted to deliver therapeutic proteins (e.g., islets of Langerhans). In this case it would be helpful to retard diffusion of the factor away from the implant to avoid unwanted immunosuppression in the host tissue. Using a high molecular weight PEO molecule with a slowly hydrolyzable linkage to the factor would accomplish this goal and permit later clearance of the factor from the body.

#### **6.4 Receptor-ligand binding to engineered biomaterials**

Within seconds of implantation, biomaterials typically become coated with a layer of adsorbed protein. This adsorbed protein layer forms the interface between the tissue and the material, and therefore cells experience the biomaterial only indirectly through these proteins. The viability of the concept of the engineered biomaterial depends upon being able to control this phenomenon. The studies described herein were performed *in vitro*, and therefore were not exposed to blood proteins and did not experience the trauma of the

initial inflammatory response which an implant would have to endure. It will be important to study receptor-tethered ligand binding in a more typical implant environment. Questions that should be addressed include: To what extent do adsorbed proteins interfere with receptor binding of tethered ligands? Can this phenomenon be mitigated by increasing the tether length? What is the effect of different polymer tethers and different substrates? These studies will be useful in determining design parameters for engineered biomaterials incorporating ligand moieties.

## **6.5 Compartmentalized Signal Transduction**

Tethering a growth factor to a solid substrate provides a new and versatile way to deliver the cytokine. However, the utility of such a system includes not only clinical application, but the investigation of fundamental cellular processes as well. Specifically, the system developed herein can be used to uncover the role of internalization of growth factors and receptors in signal transduction and subsequent downstream processes. Traditional molecular biology approaches to this question are limited by the use of transformed cells lines, typically with mutant receptors. The approach outlined below can be applied to clinically relevant systems.

It is commonly believed that receptor tyrosine kinase activation by ligand results in receptor phosphorylation by either an autocatalytic mechanism or by cross-phosphorylation of neighboring receptors, followed by recruitment of tyrosine kinase substrates (such as Grb-2 and mSos in the case of EGFR) to the plasma membrane, where signal transduction is initiated. Subsequent internalization events are thought to serve chiefly to attenuate the signal. However, there is evidence that internalized receptors continue to signal within endosomes, and moreover, that this phenomena could be important for downstream effects of signaling (Baass *et al.* 1995). For example, EGFR kinase is highly tyrosine phosphorylated in rat liver endosomes (DiGuglielmo *et al.* 1994), and tyrosine-phosphorylated SHC was found mainly in the endosome. Furthermore, a complex of

EGFR, tyrosine-phosphorylated SHC and Grb2-mSOS was found in the endosomal membrane. This is proposed to play a role in augmenting ras phosphorylation, augmenting that performed by membrane-bound EGFR. In this model internalization plays a role in the magnitude of signal rather than influencing its specificity.

In contrast to the EGF receptor, the insulin receptor (I-R) undergoes a decrease in its degree of phosphorylation in the endosome, while its kinase activity actually increases compared to plasma membrane levels. This altered pattern of phosphorylation may indicate that different substrates are phosphorylated by the I-R in the endosome (Baass *et al.* 1995).

Insulin-like growth factor is a third example of a system in which compartmentalized signal transduction has been proposed. IGF-1 receptor and I-R are similar in structure, but mediate different biological functions. The latter is involved in induction of a long-term growth response, whereas the former serves mainly metabolic functions. It has been proposed that this is due to differences in rates of internalization, ligand degradation and ligand-receptor dissociation (Zapf *et al.* 1994).

By comparing the phosphorylation of intracellular substrates following stimulation by internalized and non-internalized receptor ligands it will be possible to decipher the biological role of internalization of these factors. Receptor systems having different downstream phosphorylation substrates will be chosen. This insight will not only provide a greater understanding of receptor biology, but provide an opportunity for engineering the cell response to stimulation by receptor ligands. By selectively activating one of several signal transduction pathways, desired cell responses (e.g., proliferation, migration) may be elicited.

## Appendix

### A1 Analysis of Desorption Controls in Immobilized IL-2 System

Horwitz *et al.* (1993) immobilized 0.6 - 28 ng/cm<sup>2</sup> IL-2 on activated polystyrene membranes, and made desorption controls by plating cells on top of microporous filter paper placed on top of the immobilized growth factor membranes. Adsorption of IL-2 to the filter paper would invalidate the control since it would prevent desorbing IL-2 from reaching the cells, while no such barrier would exist for the experimental samples. The amount of IL-2 that would have to desorb before the filter paper would be saturated and diffusion through it could occur can be roughly estimated as follows. As an upper bound, a monolayer of adsorbed protein corresponds to approximately 1 µg/cm<sup>2</sup>, and in the experiments described in Chapter 2, approximately 1 ng/cm<sup>2</sup> EGF adsorbs when non-porous, hydrophilic glass slides are exposed to approximately 10 ng/ml EGF for 2 hours. Desorption of nonspecifically adsorbed protein from the immobilized IL-2 membranes (1.8 cm<sup>2</sup>) was found to be approximately 0.25% of immobilized protein per day both in the presence and absence of cells. For membranes with 30 ng immobilized protein, this corresponds to 77 pg desorbed per day, more than enough to maintain cell viability in a 1 ml culture, but very possibly not enough to passivate the filter paper (i.e., at that rate it would take more than 10 days to passivate a 1 cm<sup>2</sup> area of filter paper if the maximum amount of protein that could adsorb was only 1 ng/cm<sup>2</sup>).

### A2 Protein Assays

#### A2.1 Background

Three protein assays with different sensitivities were studied and are discussed below for comparative purposes: reaction with Folin reagent, fluorescamine, and O-



phthaldialdehyde (OPA). The Bio-Rad DC protein assay is based on the reaction of protein with an alkaline copper tartrate solution and Folin reagent. Two steps lead to color development: the reaction between copper and protein in alkaline medium and the subsequent reduction of Folin reagent by the copper-treated protein. Tyrosine and tryptophan residues are mainly responsible for color development, but cystine, cysteine, and histidine also contribute. Folin reagent is reduced by loss of 1, 2, or 3 oxygen atoms in the presence of proteins, producing one or more of several possible reduced species which have a characteristic blue color with maximum absorbance at 750 nm and minimum absorbance at 405 nm (Lowry *et al.* 1951; Peterson 1979). Fluorescamine reacts with  $\alpha$ -amino groups of proteins and with the  $\epsilon$ -amino groups of lysine residues. Fluorescamine labeling permits detection of as little as 5  $\mu$ g of protein; its excitation maximum is 390 nm and the emission maximum is 475 nm.

### A2.2 Protein Assay Experiments

Standard curves were generated using the Bio-Rad assay and a bovine serum albumin (BSA) standard. A typical standard curve is shown in Figure A.1. The curve appears to reach a plateau at higher concentrations.

Detection of fluorescent compounds in a fluorimeter is typically three orders of magnitude more sensitive than colorimetric assays. A fluorescamine assay was tested to determine its sensitivity in terms of cell number. A typical standard curve is shown in Figure A.2; these were typically more linear than those obtained for the Bio-Rad assay. Using this assay it is possible to detect as few as 100 cells, a 1000-fold increase in sensitivity over the Bio-Rad assay.

An additional requirement of this work was the detection of nanomole quantities of primary amine-containing compounds; this which was accomplished using OPA. This assay method is also applicable to protein determination, and so it is included here. A standard curve was generated using amine-terminated poly(ethylene oxide) is shown in

Figure A.3. Comparison of Figures A.2 and A.3 indicates that the two fluorescent methods are approximately equivalent in terms of sensitivity.

### **A3 DNA Synthesis**

#### A3.1 Background

Incubation of cells in medium containing  $^3\text{H}$ -thymidine or BrdU permits measurement of DNA synthesis, as cells incorporate the DNA precursors during S-phase. For rapidly dividing cells, incubation for as little as 1/2 hour may be sufficient. For higher density cultures or slow growing cells, 24 hours or longer may be needed. BrdU is a thymidine analog. It is detected using monoclonal antibodies to an epitope on the precursor; the monoclonals are in turn detected by an enzyme-linked polyclonal secondary antibody.

#### A3.2 Thymidine Experiments

The Bio-Rad assay was tested in conjunction with  $^3\text{H}$ -thymidine to determine the specific DNA synthesis rate of hepatocytes. Primary rat hepatocytes were seeded in 24 well plates and measurements of total protein using the Bio-Rad assay, cell number using a hemacytometer, and DNA synthesis (1 hour incubation) were made. The assay results are shown in Table A.1 for two experiments (n=2 for each). As a check for accuracy of the total protein data, the total protein per cell was calculated; this quantity was found to be 0.9 ng/cell, which is close to the normally used rule-of-thumb value of 1 ng/cell. These experiments provided some useful information during the early assay development phase of the project. It is apparent that in order to use the Bio-Rad assay on the order of  $10^5$  cells would be required per run; this number is important because it determines how large of a surface is needed for the tethered EGF experiments. Also, calculation of the specific

proliferation rate for the two runs indicated that significant variation from sample to sample could be expected.

### A3.3 DNA synthesis as a function of time using the BrdU assay

An experiment was performed to determine the time of optimal DNA synthesis for hepatocytes after isolation and seeding. Rat hepatocytes were isolated and cultured on tissue culture polystyrene with adsorbed collagen with or without 10 ng/ml soluble EGF; other conditions were as described in section 4.3.2. BrdU was added at various times after seeding for 21 hours before fixing and incubation with antibodies. Figure A.4 shows that DNA synthesis activity reaches a peak for cells incubated in the presence of 10 ng/ml EGF approximately 48 hours after seeding, in agreement with previous observations (Blanc *et al.* 1992).

**Table A.1** Cell proliferation Assay Results.

Experiment	Protein Conc. (mg/ml)	Cell Number (x 10 <sup>4</sup> )	Specific Proliferation Rate (DPM/h-mg protein) (x 10 <sup>6</sup> )
1	0.247	26.5	1.53
2	0.250	25.0	5.43

## **A4 Quantitative Cell Spreading Assay**

### A4.1 Introduction

Quantitative determination of the extent of cell spreading (e.g., see Figure 4.7) is a tedious task when performed manually. The usual parameters to be measured are the

number of cells per field and the area covered by those cells. Division of the latter by the former yields a spreading index. Image analysis software provides the opportunity to automate data collection, but these methods rely on the unambiguous determination of cell borders. Usually a digital image is acquired and converted to a binary image (an image having only black or white pixels) where the computer must be able to accurately assign one pixel value to cellular material and the other to background. To fully accomplish this task, the operator is very often required to assist by adjusting the threshold value (all pixels darker than the threshold value are converted to black). This operation is subjective and difficult to perform reproducibly. Naturally, as the contrast in the original image is improved, less uncertainty and irreproducibility is introduced. Several techniques were investigated to minimize error in the collection of cell spreading data including phase contrast microscopy, colored histological stains, and fluorescent probes. A protocol was developed using fluorescent probes to accurately determine cell area. An additional data collection problem involves accurate determination of the number of cells per field. Some cell types, including primary rat hepatocytes, aggregate in culture and thus the borders between adjacent cells are difficult to ascertain. By staining nuclei the number of cells in an image could more accurately be determined, since these do not overlap as often as the cell bodies. Phase contrast microscopy, colored histological stains, and fluorescent probes were used. Fluorescent probes again proved to be the most effective, and so a protocol was developed using two fluorescent dyes to measure cell area and number of nuclei to accurately determine the spreading index.

#### A4.2 Materials

Maeyer's hematoxylin and eosin-phloxin stains were a gift from Philip Seifert (Elazar Edelman lab). CMFDA (5-chloromethylfluorescein diacetate), DAF (5-(N-dodecanoyl)aminofluorescein), and Hoechst 33342 were from Molecular Probes. Chinese Hamster Ovary (CHO) cell line was a gift of the Lauffenburger lab. Hepatocyte isolation

and culture was performed as described in sections 4.2.2.2. Dulbecco's Modified Eagle's Medium (DMEM) was from Gibco. Fetal bovine serum (FBS), L-glutamine, sodium pyruvate, and penicillin-streptomycin were from Sigma.

### A4.3 Methods

#### A4.3.1 Microscopy

Cells were observed on a Zeiss fluorescent microscope equipped with a Nikon 10X objective and a Sony 3CCD camera.

#### A4.3.2 Colored Histological Stains

CHO cells were grown in 35 mm petri dishes with DMEM supplemented with 10% FBS, 2 mM L-glutamine, 1 mM sodium pyruvate, and penicillin/streptomycin. Hepatocytes were isolated and seeded on 35 mm petri dishes coated with 0.1 wt% bovine collagen. Cells were fixed in 100% ethanol for 5 minutes, then rehydrated with 2 minute incubations in 70% ethanol and distilled water. Hematoxylin was applied for 10 minutes, followed by several 15 minute washes in water. The cells were then counterstained with eosin for 2 minutes and mounted.

#### A4.3.3 Fluorescence Experiments

Medium was removed from cells and replaced with medium containing 10  $\mu$ M CMFDA, 50  $\mu$ M DAF with 0.1% BSA, or 10  $\mu$ M Hoescht and incubated for 15 minutes (Hoescht) or 30 minutes (DAF and CMFDA). The probe-containing medium was then removed and replaced with 1 ml fresh medium and cells were incubated for 15-30 minutes. Some cultures were then probed again with 10  $\mu$ M Hoescht for 15 minutes. Cells were observed after 15-30 minutes using appropriate filters.

### A4.4 Results

Phase contrast microscopy gave clear images of unstained cells, but these did not translate into accurate binary images largely due to uneven lighting effects. Cells appeared more uniform with greater contrast when stained with hematoxylin and eosin (see Figure

A5) , but thresholding and dilating was required to get an accurate binary image. The nuclei of the cells studied did not stain significantly.

In order to achieve an accurate binary image without thresholding and the accompanying inaccuracies it is helpful to begin with an image with low background. This is possible with fluorescent staining, as can be seen in Figure A6, which shows CHO cells and hepatocytes stained with CMFDA, a cytoplasmic fluorescent stain. These images could be directly converted into binary images which reflected the true cell area without thresholding. DAF membrane staining also gave promising results; representative images are shown in Figure A7.

For high density cultures it is often difficult, time consuming and inaccurate to count cells manually. It would be convenient to have a nuclear stain that could be used in conjunction with a cytoplasmic or membrane stain. The former could be used to count nuclei (for mononuclear cell lines this would be equivalent to cell number) while the latter could be used to quantify total cell area. The staining index is arrived at simply by dividing the total cell area by the number of nuclei. The Hoescht 33342 dye is a nuclear probe that gives good nuclear staining with hepatocytes and CHO cells (Figure A8).

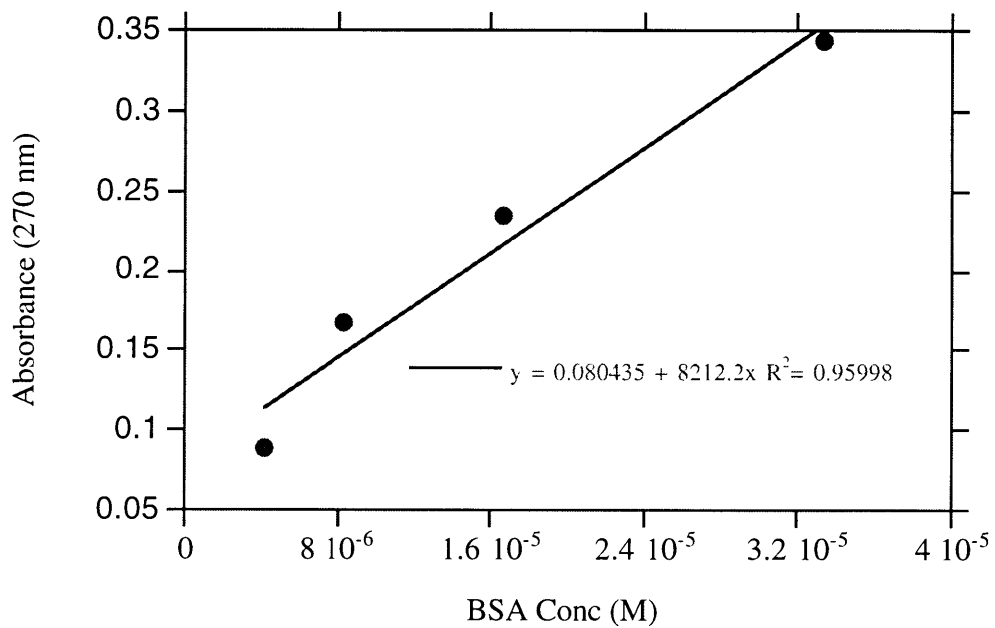


**Figure A.1** Typical standard curve for the Bio-Rad DC Protein Assay.

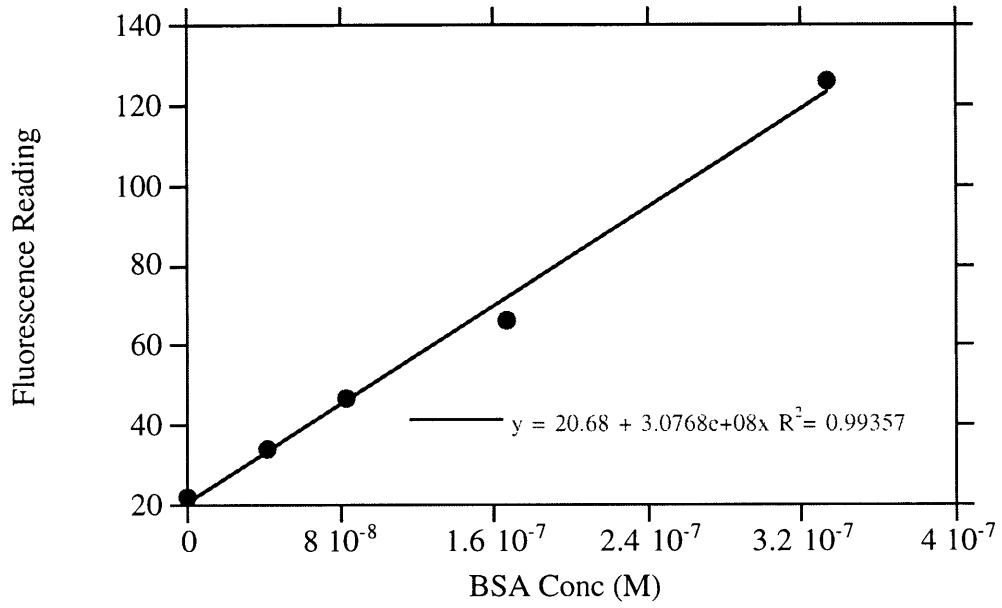


**Figure A.2** Typical Standard Curve for Flourescamine Assay.



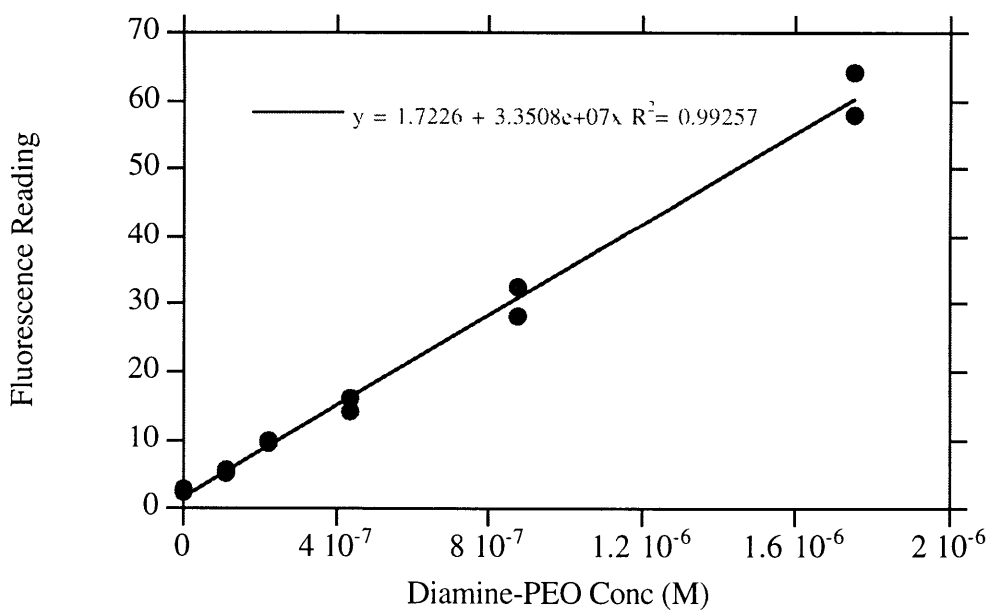
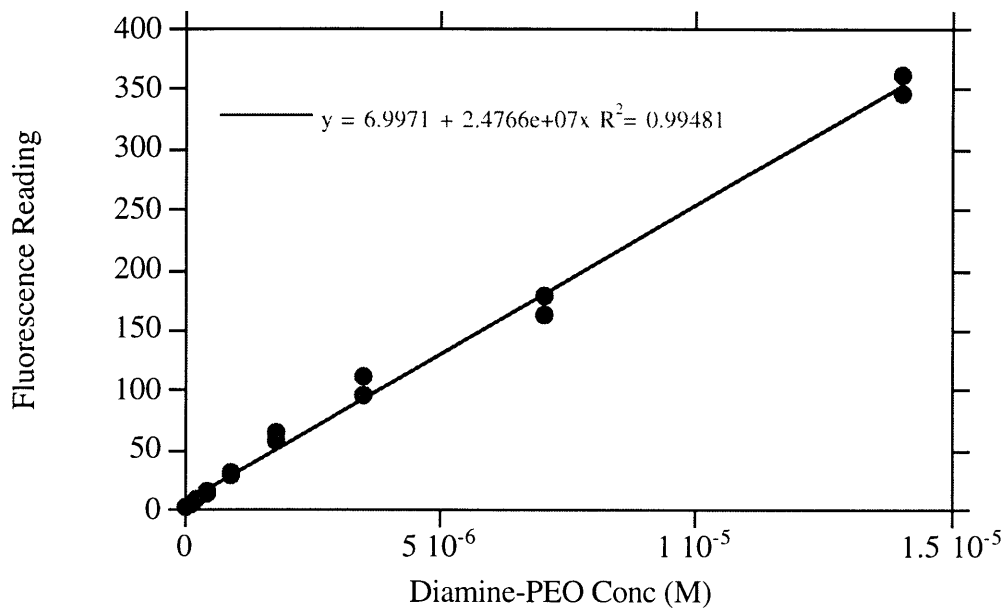


**Figure A.3** Standard curves for OPA assay.

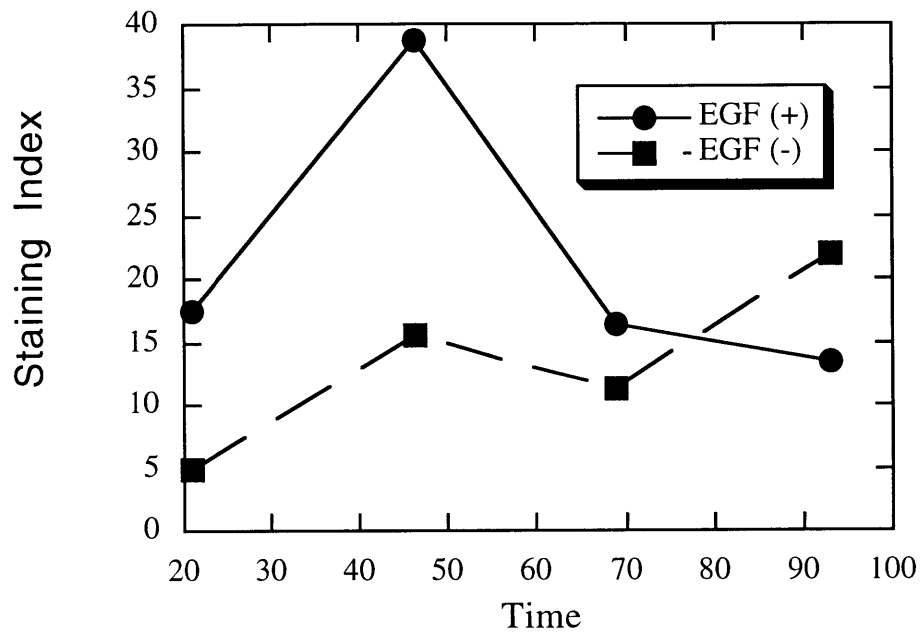


**Figure A.4** DNA synthesis activity in rat hepatocytes as a function of time after seeding. Rat hepatocytes were isolated and cultured on tissue culture polystyrene with adsorbed collagen with or without 10 ng/ml soluble EGF; other conditions were as described in section 4.3.2. BrdU was added at various times after seeding for 21 hours before fixing and incubation with antibodies.

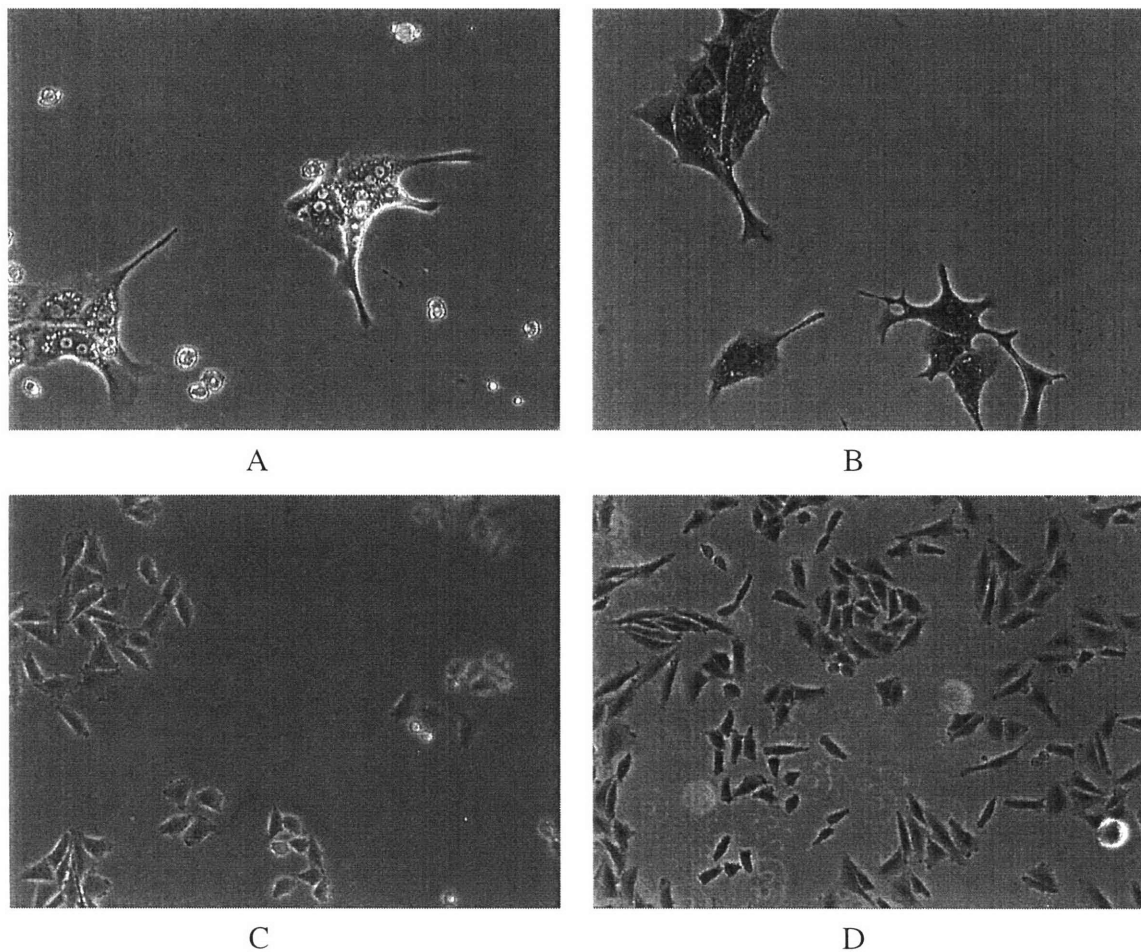


**Figure A.5** Phase contrast images of unstained cells and cells stained with hematoxylin+eosin. A. Hepatocytes (no stain). B. Hepatocytes (hematoxylin+eosin). CHO (no stain). C. CHO (hematoxylin+eosin). Cells were grown as described in the text and fixed in 100% ethanol. These images can be converted to binary images, but thresholding is required for acceptable accuracy.

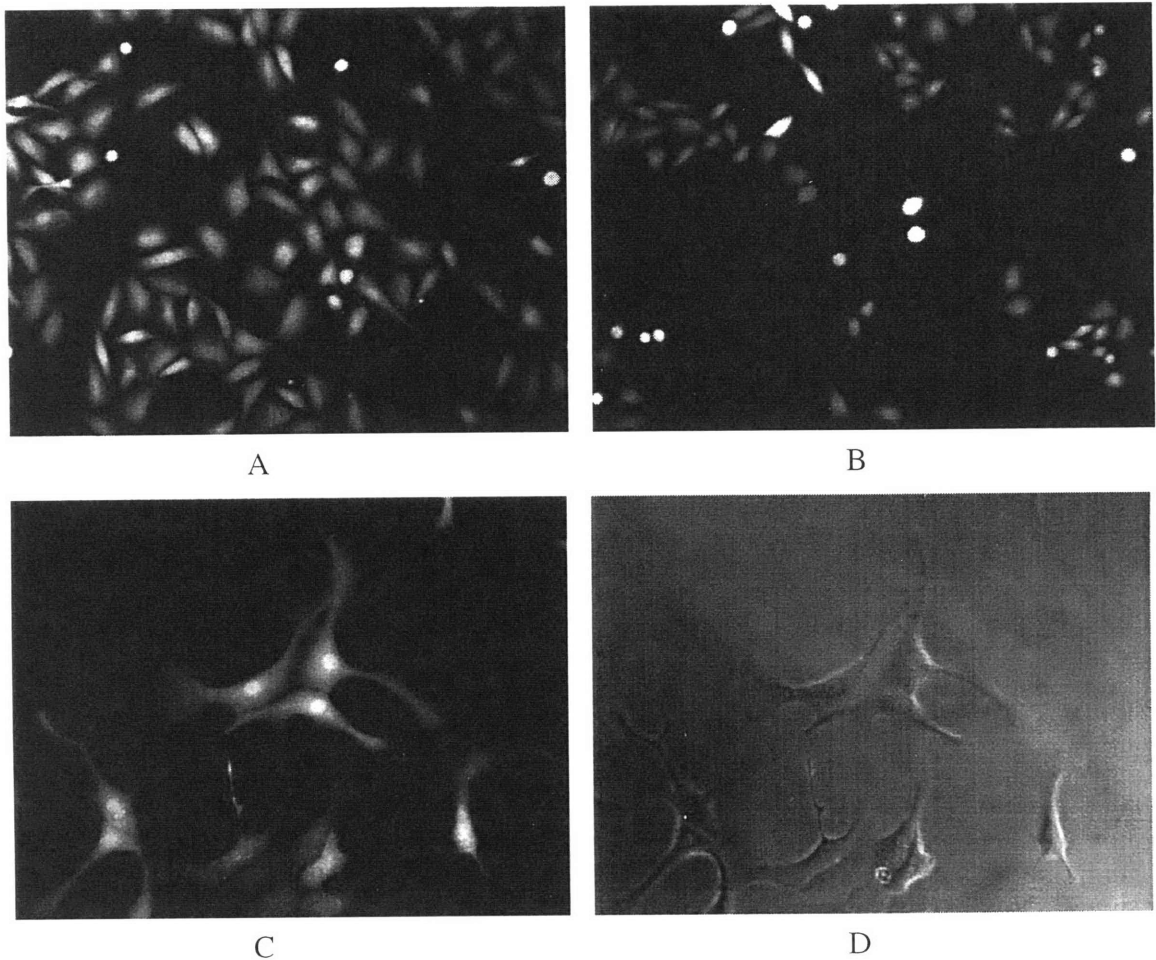


**Figure A.6** Fluorescence and phase contrast images of cells stained with CMFDA at the indicated concentrations. These cells were grown as described in the text and were not fixed prior to staining. A. CHO (25 $\mu$ M CMFDA). B. CHO (10 $\mu$ M CMFDA). C. Hepatocytes (10 $\mu$ M CMFDA). D. Hepatocytes (10 $\mu$ M CMFDA, phase contrast, same field as C). The fluorescent images could be converted directly into binary images for quantitation of cell area.

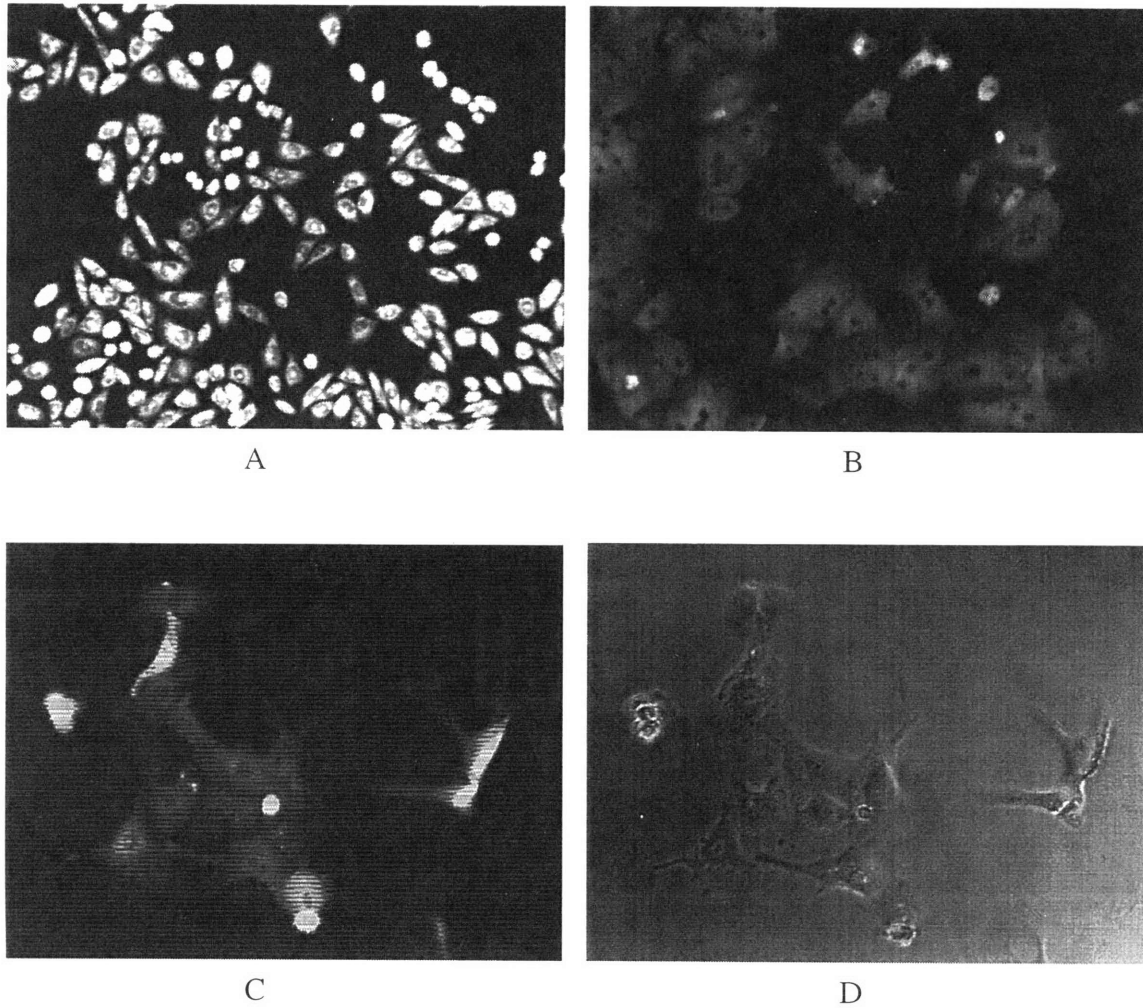


**Figure A.7** Fluorescence and phase contrast images of cells stained with 50 $\mu$ M DAF. These cells were grown as described in the text and were not fixed prior to staining. A. CHO. B., C., Hepatocytes. D. Hepatocytes (phase contrast, same field as C.)

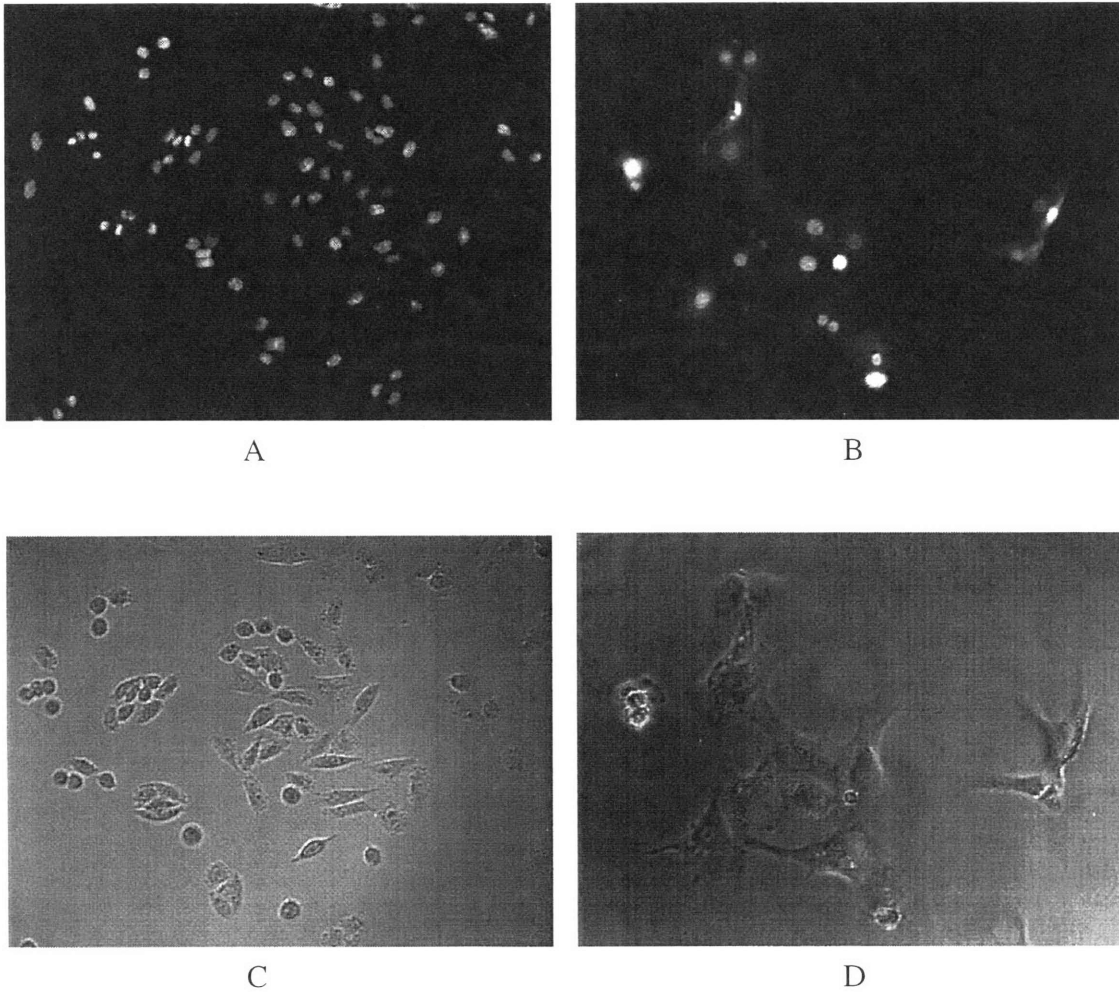


**Figure A.8** Fluorescence and phase contrast images of cells stained with 10 $\mu$ M Hoechst. These cells were grown as described in the text and were not fixed prior to staining. The fluorescent images could be used to determine a cell count allowing the determination of a specific cell spreading index when used in combination with cell area data. A. CHO. B. Hepatocytes. C. CHO (phase contrast, same field as A). D. Hepatocytes (phase contrast, same field as B).

## References

- Abuchowski, A., McCoy, J. R., Palczuk, N. C., van Es, T. and Davis, F. F. (1977). "Effect of covalent attachment of poly(ethylene glycol) on immunogenicity and circulating life of bovine liver catalase." *J. Biol. Chem.* **252**: 3582-3586.
- Abuchowski, A., van Es, T., Palczuk, N. and Davis, F. (1977). "Alteration of immunological properties of bovine serum albumin by covalent attachment of polyethylene glycol." *J. Biol. Chem.* **252**(10): 3578-3581.
- Aharonov, A., Pruss, R. M. and Herschman, H. R. (1978). "Epidermal growth factor: relationship between receptor regulation and mitogenesis in 3T3 cells." *J. Biol. Chem.* **253**: 3970-3977.
- Allgor, S. (1995). personal communication.
- Amiji, M. and Park, K. (1992). "Prevention of protein adsorption and platelet adhesion on surfaces by PEO/PPO/PEO triblock copolymers." *Biomaterials* **13**(10): 682-92.
- Andrade, J. D. (1985). Principles of Protein Adsorption. *Protein Adsorption*. J. D. Andrade. New York, Plenum Press. **2**: 1-75.
- Anzano, M. A., Roberts, A. B., Meyers, C. A., Komoriya, A., Lamb, L. C., Smith, J. M. and Sporn, M. B. (1982). "Synergistic interaction of two classes of transforming growth factors from murine sarcoma cells." *Cancer Res.* **42**: 4776-4778.
- Avruch, J., Zhang, X. and Kyriakis, J. M. (1994). "Raf meets Ras: completing the framework of a signal transduction pathway." *TIBS* **19**(7): 279-283.
- Baass, P. C., DiGuglielmo, G. M., Authier, F., Posner, B. I. and Bergeron, J. J. M. (1995). "Compartmentalized signal transduction by receptor tyrosine kinases." *TIBS* **5**(12): 465-470.
- Bar-Sagi, D., Suhan, J., McCormick, F. and Feramisco, J. R. (1988). "Localization of phospholipase A2 in normal and ras-transformed cells." *J. Cell Biol.* **106**: 1649-1658.
- Barrandon, Y. and Green, H. (1987). "Cell migration is essential for sustained growth of keratinocyte colonies: the roles of transforming growth factor-alpha and epidermal growth factor." *Cell* **50**: 1131-1137.
- Bartles, J. R. and Hubbard, A. L. (1986). "Preservation of hepatocyte plasma membrane domains during division in situ in regenerating rat liver." *J. Cell Biol.* **118**: 286-295.
- Beckman, J. S., Minor, R. L., White, C. W., Repine, J. E., Rosen, G. M. and Freeman, B. A. (1988). "Superoxide dismutase and catalase conjugated to polyethylene glycol increases endothelial enzyme activity and oxidant resistance." *J. Biol. Chem.* **263**(14): 6884-6892.

- Bertics, P. J. and Gill, G. N. (1986). "Self-phosphorylation enhances the protein-tyrosine kinase activity of the epidermal growth factor receptors on plasma membrane preparations." EMBO J. **5**: 247-250.
- Bevan, A. P., Drake, P. G., Bergeron, J. J. M. and Posner, B. I. (1996). "Intracellular signal transduction: the role of endosomes." Trends Endocrin. Metab. **7**(1): 13-21.
- Blanc, P., Etienne, H., *et al.* (1992). "Mitotic responsiveness of cultured adult human hepatocytes to epidermal growth factor, transforming growth factor  $\alpha$ , and human serum." Gastroenterology **102**: 1340-1350.
- Blay, J. and Brown, K. D. (1985). "Epidermal growth factor promotes the chemotactic migration of cultured rat intestinal epithelial cells." J. Cell. Physiol. **124**: 107-112.
- Block, G., Locker, J., Bowen, W. C., Petersen, B. E., Katayl, S., Strom, S. C., Riley, T., Howard, T. A. and Michalopoulos, G. K. (1996). "Population expansion, clonal growth, and specific differentiation patterns in primary cultures of hepatocytes induced by HGF/SF, EGF and TGF $\alpha$  in a chemically defined (HGM) medium." J. Cell Biol. **132**(6): 1133-1149.
- Brooks, R. F. (1977). "Continuous protein synthesis is required to maintain the probability of entry into S phase." Cell **12**: 311-317.
- Buckley, A., Davidson, J. M., Kamerath, C. D., Wolt, T. B. and Woodward, S. C. (1985). "Sustained release of epidermal growth factor accelerates wound repair." PNAS **82**: 7340-7344.
- Campbell, J. S., Seger, R., Graves, J. D., Graves, L. M., Jensen, A. M. and Krebs, E. G. (1995). "The MAP kinase cascade." Rec. Prog. in Hormone Res. **50**: 131-159.
- Carpenter, G. (1992). "Receptor tyrosine kinase substrates: src homology domains and signal transduction." FASEB J. **6**: 3283-3289.
- Carpenter, G. and Cohen, S. (1976). "Human epidermal growth factor and the proliferation of human fibroblasts." J. Cell. Physiol. **88**: 227-237.
- Carpenter, G. and Cohen, S. (1979). "Epidermal growth factor." Ann. Rev. Biochem. **48**: 193-216.
- Carpentier, J.-L., White, M. F., Orci, L. and Kahn, R. C. (1987). "Direct visualization of the phosphorylated epidermal growth factor receptor during its internalization in A-431 cells." J. Cell Biol. **105**(6, Pt.1): 2751-2762.
- Carraway, K. L. and Carraway, C. A. C. (1995). "Signaling, mitogenesis and the cytoskeleton: where the action is." BioEssays **17**(2): 171-175.
- Chen, W. S., Lazar, C. S., *et al.* (1989). "Functional independence of the epidermal growth factor receptor from a domain required for ligand-induced internalization and calcium regulation." Cell **59**: 33-43.
- Chinkers, M., McKanna, J. A. and Cohen, S. (1979). "Rapid induction of morphological changes in human carcinoma cells A-431 by epidermal growth factor." J. Cell Biol. **83**: 260-265.



- Chinkers, M., McKanna, J. A. and Cohen, S. (1981). "Rapid rounding of human epidermoid carcinoma cells A-431 induced by epidermal growth factor." J. Cell Biol. **88**: 422-429.
- Cima, L. G., Ingber, D. E., Vacanti, J. P. and Langer, R. (1991). "Hepatocyte culture on biodegradable polymeric substrates." Biotech. Bioeng. **38**: 145-158.
- Cohen, S. (1964). Isolation and biological effects of an epidermal growth-stimulating protein. Metabolic Control Mechanisms in Animal Cells. National Cancer Institute Monograph 13. W. J. Rutter: 13-27.
- Cohen, S. and Elliott, G. A. (1963). J. Invest. Dermatol. **40**: 1-5.
- Cooke, R. M., Wilkinson, A. J., Baron, M., Pastore, A., Tappin, M. J., Campbell, I. D., Gregroy, H. and Sheard, B. (1987). "The solution structure of human epidermal growth factor." Nature **327**: 339-341.
- Cuatrecasas, P. (1969). "Interaction of insulin with the cell membrane: the primary action of insulin." PNAS **63**: 450-457.
- Dahmane, A., Gil, S., Brehier, A., Davy, J. and Feger, J. (1996). "Kinetic analysis of epidermal growth factor endocytosis in rat hepatocytes. Effects of diabetes." Eur. J. Cell Biol. **69**: 335-342.
- DeLarco, J. E. and Todaro, G. J. (1978). "Growth factors from murine sarcoma virus-transformed cells." PNAS **75**: 4001-5.
- den Hartigh, J. C., van Bergen en Henegouwen, P. M. P., Verkleij, A. J. and Boonstra, J. (1992). "The EGF receptor is an actin-binding protein." J. Cell. Biol. **119**(2): 349-355.
- Desai, N. P. and Hubbell, J. A. (1991). "Biological responses to polyethylene oxide modified polyethylene terephthalate surfaces." J. Biomed. Mat. Res. **25**: 829-843.
- Diakovna, M., Payraastre, B., van Velzen, A., Hage, W. J., van Bergen en Henegouwen, P. M., Boonstra, J., Cremers, F. F. and Humbel, B. M. (1995). "Epidermal growth factor induces rapid and transient association of phospholipase C- $\gamma$ 1 with EGF-receptor and filamentous actin at membrane ruffles of A431 cells." J. Cell Sci. **108**: 2499-2509.
- DiGuglielmo, G. M., Baass, P. C., Ou, W. J., Posner, B. I. and Bergeron, J. J. (1994). "Compartmentalization of SHC, Grb2, and mSos, and hyperphosphorylation of Raf-1 by EGF but not insulin in liver parenchyma." EMBO J. **13**(18): 4629-4277.
- Dunn, W. A., Connolly, T. P. and Hubbard, A. L. (1986). "Receptor-mediated endocytosis of epidermal growth factor by rat hepatocytes." J. Cell Biol. **102**: 24-36.
- Evans, W. H. (1980). "A biochemical dissection of the functional polarity of the plasma membrane of the hepatocyte." Biochem. Biophys. Acta **604**: 27-64.

- Gladhaug, I. P. and Christoffersen, T. (1987). "Kinetics of epidermal growth factor binding and processing in isolated intact rat hepatocytes. Dynamic externalization of receptors during ligand internalization." Eur. J. Biochem. **164**: 267-275.
- Gombotz, W. R., Guanghi, W., Horbett, T. A. and Hoffman, A. S. (1991). "Protein adsorption to poly(ethylene oxide) surfaces." J. Biomed. Mat. Res. **25**: 1547-1562.
- Grondin, P., Plantavid, M., Sultan, C., Breton, M., Mauco, G. and Chap, H. (1991). "Interaction of pp60c-src, phospholipase C, inositol-lipid, and diacylglycerol kinases with the cytoskeletons of thrombin-stimulated platelets." J. Biol. Chem. **266**: 15705-15709.
- Gronowski, A. and Bertics, P. J. (1993). "Evidence for the potentiation of epidermal growth factor receptor tyrosine kinase activity by association with the detergent-insoluble cellular cytoskeleton: analysis of intact and carboxy-terminally truncated receptors." Endocrinology **133**: 2838-2839.
- Haigler, H. T., Maxfield, F. R., Willingham, M. C. and Pastan, I. (1980). "Dansylcadaverine inhibits internalization of  $^{125}\text{I}$ -epidermal growth factor in BALB 3T3 cells." J. Biol. Chem. **255**: 1239-1241.
- Haigler, H. T., McKanna, J. A. and Cohen, S. (1979). "Direct visualization of the binding and internalization of a ferritin conjugate of epidermal growth factor in human carcinoma cells A-431." J. Cell. Biol. **81**: 382-395.
- Hatai, M., Hashi, H., Mogi, A., Soga, H., Yokota, J. and Yaoi, Y. (1994). "Stimulation of tyrosine- and serine-phosphorylation of focal adhesion kinase in mouse 3T3 cells by fibronectin and fibroblast growth factor." FEBS Lett **250**(1): 113-116.
- Herschfield, M. S., Buckley, R. H., *et al.* (1987). "Treatment of adenosine deaminase deficiency with polyethylene glycol-modified adenosine deaminase." N. Engl. J. Med. **316**(10): 589-596.
- Hershko, A., Mamont, P., Shields, R. and Tomkins, G. M. (1971). "Pleiotypic Response." Nature New Biol. **232**: 206-211.
- Higashiyama, S., Abraham, J. A., Miller, J., Fiddes, J. C. and Klagsbrun, M. (1991). "A heparin-binding growth factor secreted by macrophage-like cells that is related to EGF." Science **251**: 936-939.
- Holmes, W. E., Sliwkowski, M. X., *et al.* (1992). "Identification of heregulin, a specific activator of p185<sup>erbB2</sup>." Science **256**: 1205-1210.
- Holt, S. J., Alexander, P., Inman, C. B. and Davies, D. E. (1994). "Epidermal growth factor induced tyrosine phosphorylation of nuclear proteins associated with translocation of epidermal growth factor receptor into the nucleus." Biochem. Pharmacol. **47**: 117-126.
- Holt, S. J., Alexander, P., Inman, C. B. and Davies, D. E. (1995). "Ligand-induced translocation of epidermal growth factor receptor to the nucleus of NR6/HER fibroblasts is serum dependent." Exp. Cell Res. **217**: 554-558.

- Horwitz, J. I., Toner, M., Tompkins, R. G. and Yarmush, M. L. (1993). "Immobilized IL-2 preserves the viability of an IL-2 dependent cell line." Mol. Immun. **30**(11): 1041-1048.
- Hoschuetzky, H., Aberle, H. and Kemler, R. (1994). " $\beta$ -Catenin mediates the interaction of the cadherin-catenin complex with epidermal growth factor receptor." J. Cell Biol. **127**(5): 1375-1380.
- Houck, K. A. and Michalopoulos, G. (1985). "Proline is required for the stimulation of DNA synthesis in hepatocyte cultures by EGF." In Vitro Cell. and Dev. Biol. **21**(2): 121-124.
- Ichii, S., Yoshida, A. and Hoshikawa, Y. (1988). "Binding sites for epidermal growth factor in nuclear fraction from rat liver." Endocrinol. Jpn. **35**: 567-575.
- Ishigami, A., Reed, T. D. and Roth, G. S. (1993). "Effect of aging on EGF stimulated DNA synthesis and EGF receptor levels in primary cultured rat hepatocytes." Biochem. Biophys. Res. Comm. **196**: 181-186.
- Ito, Y., Inoue, M., Liu, S. Q. and Imanishi, Y. (1993). "Cell growth on immobilized growth factor. 6. enhancement of fibroblast cell growth by immobilized insulin and/or fibronectin." J. Biomed. Mat. Res. **27**: 901-907.
- Ito, Y., Liu, S.-Q., Nakabayashi, M. and Imanishi, Y. (1992). "Cell growth on immobilized cell-growth factor II." Biomaterials **13**(11): 789-794.
- Ito, Y., Zheng, J., Imanishi, Y., Yonezawa, K. and Kasuga, M. (1996). "Protein-free cell culture on an artificial substrate with covalently immobilized insulin." PNAS **93**: 3598-3601.
- Jeon, S. I., Lee, J. H., Andrade, J. D. and de Gennes, P. G. (1991). "Protein-surface interactions in the presence of polyethylene oxide. I. Simplified theory." J. Coll. Int. Sci. **142**: 149-158.
- Jiang, L.-W. and Schindler, M. (1990). "Nucleocytoplasmic transport is enhanced concomitant with nuclear accumulation of epidermal growth factor binding activity in both 3T3-1 and EGF receptor reconstituted NR-6 fibroblasts." J. Cell. Biol. **110**: 559-568.
- Johnson, G. R., Saeki, T., Gordon, A. W., Shoyab, M., Salomon, D. S. and Stromberg, K. (1992). "Autocrine action of amphiregulin in a colon carcinoma cell line and immunocytochemical localization of amphiregulin in human colon." J. Cell. Biol. **118**: 741-751.
- Johnson, L. K., Volodavsky, I., Baxter, J. D. and Gospodarowicz (1980). "Nuclear accumulation of epidermal growth factor in cultured rat pituitary cells." Nature **287**: 340-343.
- Juliano, R. (1996). "Cooperation between soluble factors and integrin-mediated cell anchorage in the control of cell growth and differentiation." BioEssays **11**: 911-917.

- Katre, N. V., Knauf, M. J. and Laird, W. J. (1987). "Chemical modification of recombinant interleukin 2 by polyethylene glycol increases its potency in the murine Meth A sarcoma model." PNAS **84**: 1487-1491.
- Kimura, H. (1993). "Schwannoma-derived growth factor must be transported into the nucleus to exert its mitogenic activity." PNAS **90**: 2165-2169.
- Kimura, H., Fischer, W. H. and Schubert, D. (1990). "Structure, expression, and function of a schwannoma-derived growth factor." Nature **348**: 257-260.
- Knauer, D. J., Wiley, H. S. and Cunningham, D. D. (1984). "Relationship between epidermal growth factor receptor occupancy and mitogenic response: quantitative analysis using a steady state model system." J. Biol. Chem. **259**: 5623-5631.
- Knoche, H. W. (1991). Radioisotopic Methods for Biological and Medical Research. New York, Oxford.
- Knusli, C., Delgado, C., Malik, F., Domine, M., Tejedor, M. C., Irvine, A. E., Fisher, D. and Francis, G. E. (1992). "Polyethylene glycol modification of granulocyte-macrophage colony stimulating factor enhances neutrophil activity but not colony stimulating activity." Brit. J. of Haematol. **82**: 654-663.
- Komoriya, A., Hortsch, M., Meyers, C., Smith, M., Kanety, H. and Schlessinger, J. (1984). "Biologically active synthetic fragments of epidermal growth factor: localization of a major receptor-binding region." PNAS **81**: 1351-1355.
- Lauffenburger, D. A. and Linderman, J. L. (1993). Receptors: Models for Binding, Trafficking, and Signaling. New York, Oxford University Press.
- Lawrence, W. T. and Diegelmann, R. F. (1994). "Growth Factors in Wound Healing." Clinics in Dermatology **12**: 157-169.
- Leach, K. L., Ruff, V. A., Jarpe, M. B., Adams, L. D., Fabbro, D. and Raben, D. M. (1992). "a-Thrombin stimulates nuclear diglyceride levels and differential nuclear localization of protein kinase C isozymes in IIC9 cells." J. Biol. Chem. **267**: 21826-21822.
- Lee, J. H., Kopeček, J. and Andrade, J. D. (1989). "Protein-Resistant Surfaces Prepared by PEO-Containing Block Copolymer Surfactants." J. Biomed. Mat. Res. **23**: 351-368.
- Li, W., Park, J. W., Nuijens, A., Sliwkowski, M. X. and Keller, G. A. (1996). "Heregulin is rapidly translocated to the nucleus and its transport is correlated with c-myc induction in breast cancer cells." Oncogene **12**: 2473-2477.
- Li, Y., Sattler, G. L. and Pitot, H. C. (1993). "Oxaloacetate induces DNA synthesis and mitosis in primary cultured rat hepatocytes in the absence of EGF." Biochem. Biophys. Res. Comm. **193**(3): 1339-1346.
- Lindon, J. N., McManama, G., Kushner, L., Merrill, E. W. and Salzman, E. W. (1986). "Does the conformation of adsorbed fibrinogen dictate platelet interactions with artificial surfaces?" Blood **68**(2): 355-362.

- Liu, S.-Q., Ito, Y. and Imanishi, Y. (1992). "Cell growth on immobilized cell growth factor I." Biomaterials **13**(1): 50-57.
- Liu, Y., Guyton, K. Z., Gorospe, M., Xu, Q., Kokkonen, G. C., Mock, Y. D., Roth, G. S. and Holbrook, N. J. (1996). "Age-related decline in mitogen-activated protein kinase activity in epidermal growth factor-stimulated rat hepatocytes." J. Biol. Chem. **271**(7): 3604-3607.
- Lopina, S. T. 1995. Carbohydrate-derivatized poly(ethylene oxide) hydrogels for hepatocyte adhesion. Chemical Engineering. Cambridge, MIT: 167.
- Lowenstein, E. J., Daly, R. J., *et al.* (1992). "The SH2 and SH3 domain-containing protein GRB2 links receptor tyrosine kinases to ras signaling." Cell **70**: 431-442.
- Lowry, O. H., Rosebrough, N. J., Farr, A. L. and Randall, R. J. (1951). "Protein measurement with the folin phenol reagent." J. Biol. Chem. **193**: 265-275.
- Lutz, P. and Rempp, P. (1988). "New developments in star polymer synthesis. Star-shaped polystyrenes and star-block copolymers." Makromol. Chemie **189**: 1051-1060.
- Mainiero, F., Pepe, A., Yeon, M., Ren, Y. and Giancotti, F. G. (1996). "The intracellular functions of  $\alpha 6\beta 4$  integrin are regulated by EGF." J. Cell Biol. **134**(1): 241-253.
- Marengere, L. E. M. and Pawson, T. (1992). "Identification of residues in GTPase-activating protein src homology-2 domains that control binding to tyrosine phosphorylated growth factor receptors and p62." J. Biol. Chem. **267**: 22779-22786.
- Massia, S. and Hubbell, J. (1991). "Human endothelial cell interactions with surface-coupled adhesion peptides on a nonadhesive glass substrate and two polymeric biomaterials." J. Biomed. Mat. Res. **1991**: 223-42.
- Mayo, K. H., Nunez, M., Burke, C. and Starbuck, D. (1989). "Epidermal growth factor receptor binding is not a simple one-step process." J. Biol. Chem. **264**: 17838-17844.
- McMillin, C. R. and Walton, A. G. (1974). "Circular dichroism technique for study of adsorbed protein structure." J. Colloid Interface Sci. **48**: 345-349.
- Merrill, E. W. (1993). "Poly(ethylene oxide) star molecules: synthesis, characterization, and applications in medicine and biology." J. Biomater. Sci. Polymer Ed.
- Meyer-Ingold, W. (1993). "Wound therapy: growth factors as agents to promote healing." Trends in Biotech **11**: 387-392.
- Mitaka, T., Sattler, C. A., Sattler, G. L., Sargent, L. M. and Pitot, H. C. (1990). "Multiple cell cycles occur in rat hepatocytes cultured in the presence of nicotinamide and epidermal growth factor." Hepatology **13**(1): 21-30.

- Miyamoto, S., Teramoto, H., Gutkind, J. S. and Yamada, K. M. (1996). "Integrins can collaborate with growth factors for phosphorylation of receptor tyrosine kinases and MAP kinase activation: roles of integrin aggregation and occupancy of receptors." J. Cell Biol. **135**(6, Part 1): 1633-1642.
- Mooney, D. J., Langer, R. and Ingber, D. E. (1995). "Cytoskeletal filament assembly and the control of cell spreading and function by extracellular matrix." J. Cell Sci. **108**: 2311-2320.
- Payraastre, B., van Bergen en Henegouwen, P. M. P., Breton, M., den Hartigh, J. C., Plantavid, M., Verkleij, A. J. and Boonstra, J. (1991). "Phosphoinositide kinase, diacylglycerol kinase and phospholipase C activities associated to the cytoskeleton: effect of epidermal growth factor." J. Cell Biol. **115**: 121-128.
- Peterson, G. L. (1979). "Review of the folin phenol quantitation method of Lowry, Rosebrough, Farr, and Randall." Anal. Biochem. **100**: 201-220.
- Plopper, G. E., McNamee, H. P., Dike, L. E., Bojanowski, K. and Ingber, D. E. (1995). "Convergence of integrin and growth-factor receptor signaling pathways within the focal adhesion complex." Mol. Biol. Cell **6**(10): 1349-1365.
- Rakowicz-Szulczynka, E. M., Rodeck, U., Herlyn, M. and Koprowski, H. (1986). "Chromatin binding of epidermal growth factor, nerve growth factor, and platelet-derived growth factor in cells bearing the appropriate surface receptors." PNAS **83**: 3728-3732.
- Remp, P., Lutz, P. and Merrill, E. W. (1990). Anionically Polymerized Star Macromolecules Having Divinyl Benzene Cores with Grafted Poly(Ethylene Oxide) Arms as Biomaterials. American Chemical Society, Polymer Division, Symposium, Boston.
- Rotin, D., Margolis, B., *et al.* (1992). "SH2 domains prevent tyrosine dephosphorylation of the EGF receptor: Identification of Tyr992 as the high-affinity binding site for SH2 domains of phospholipase-C $\gamma$ ." EMBO J. **11**: 559-567.
- Ruoslahti, E. and Yamaguchi, Y. (1991). "Proteoglycans as modulators of growth factor activities." Cell **64**: 867-869.
- Schlessinger, J. and Geiger, B. (1981). "Epidermal growth factor induces redistribution of actin and  $\alpha$ -actinin in human epidermal carcinoma cells." Exp. Cell Res. **134**: 273-279.
- Shoyab, M., Plowman, G. D., McDonald, V. L., Bradley, J. G. and Todaro, G. J. (1989). "Structure and function of human amphiregulin: a member of the epidermal growth factor family." Science **243**: 1074-1076.
- Simpson, R. J., Smith, J. A., *et al.* (1985). "Rat epidermal growth factor: complete amino acid sequence." Eur. J. Biochem. **153**: 629-637.
- Sofia, S. J., Kuhl, P. R. and Griffith, L. G. (1997). Methods for the Preparation and Use of Tethered Ligands as Biomaterials and Tools for Cell Biology. Methods in Tissue Engineering. J. R. Morgan and M. L. Yarmush. Totowa, Humana Press.

- Starbuck, C. (1991). Quantitative Studies of Epidermal Growth Factor Receptor Binding and Trafficking Dynamics in Fibroblasts: Relationship to Cell Proliferation. Chemical Engineering. Philadelphia, University of Pennsylvania.
- Starbuck, C. and Lauffenburger, D. A. (1992). "Mathematical model for the effects of epidermal growth factor receptor trafficking dynamics on fibroblast proliferation response." Biotechnol. Prog. **8**: 132-143.
- Stenger, D. A., Georger, J. H., Dulcey, C. S., Hickman, J. J., Rudolph, A. S., Nielson, T. B., McCort, S. M. and Calvert, J. M. (1992). "Coplanar molecular assemblies of amino- and perfluorinated alkylsilanes: characterization and geometric definition of mammalian cell adhesion and growth." J. Am. Chem. Soc. **114**: 8435-8442.
- ten Dijke, P. and Iwata, K. K. (1989). "Growth factors for wound healing." Bio/Technology **7**: 793-798.
- Thomas, G., Martin-Perez, J., Siegmann, M. and Otto, A. M. (1982). "The effect of serum, EGF, PGF2 $\alpha$ , and Insulin on S6 phosphorylation and the initiation of protein and DNA synthesis." Cell **30**: 235-242.
- Thomas, G., Siegmann, M., Kubler, A. M., Gordon, J. and Jimenez de Asua, L. (1980). "Regulation of 40S ribosomal protein S6 phosphorylation in Swiss mouse 3T3 cells." Cell **19**: 1015-1023.
- Tomomura, A., Sawada, N., Sattler, G. L., Kleinman, H. K. and Pitot, H. C. (1987). "The control of DNA synthesis in primary cultures of hepatocytes from adult and young rats: interactions of extracellular matrix components, epidermal growth factor, and the cell cycle." J. Cell. Physiol. **130**: 221-227.
- Tsutsumi, Y., Kihira, T., Tsunoda, S., Kanamori, T., Nakagawa, S. and Mayumi, T. (1994). "Molecular design of hybrid tumor necrosis factor alpha with polyethylene glycol increases its anti-tumor potency." Brit. J. Cancer **71**(5): 963-968.
- Vaziri, C. and Downes, C. P. (1992). "Association of a receptor and G-protein-regulated phospholipase-C with the cytoskeleton." J. Biol. Chem. **267**: 22973-22981.
- Walton, G. M., Chen, W. S., Rosenfeld, M. G. and Gill, G. N. (1990). "Analysis of deletions of the carboxyl terminus of the epidermal growth factor receptor reveals self-phosphorylation at tyrosine 992 and enhanced in vivo tyrosine phosphorylation of cell substrates." J. Biol. Chem. **265**: 1750-1754.
- Wang, Q.-C., Pai, L. H., Debinski, W., FitzGerald, D. J. and Pastan, I. (1993). "Polyethylene glycol-modified chimeric toxin composed of transforming growth factor  $\alpha$  and *pseudomonas* exotoxin." Cancer Res. **53**: 4588-4594.
- Wells, A., Welsh, J. B., Lazar, C. S., Wiley, H. S., Gill, G. N. and Rosenfeld, M. G. (1990). "Ligand-induced transformation by a noninternalizing epidermal growth factor receptor." Science **247**: 962-964.
- Wen, D., Peles, E., *et al.* (1992). "Neu differentiation factor: a transmembrane glycoprotein containing an EGF domain and an immunoglobulin homology unit." Cell **69**: 559-572.

- Westermarck, K., Nilsson, M., Ebendal, T. and Westermarck, B. (1991). "Thyrocyte migration and histiotypic follicle regeneration are promoted by epidermal growth factor in primary culture of thyroid follicles in collagen gel." Endocrinology **129**: 2180-2186.
- Wiley, H. S. and Cunningham, D. D. (1981). "A steady state model for analyzing the cellular binding, internalization and degradation of polypeptide ligands." Cell **25**: 433-440.
- Wiley, H. S., Herbst, J. J., Walsh, B. J., Lauffenburger, D. A., Rosenfeld, M. G. and Gill, G. N. (1991). "The Role of Tyrosine Kinase Activity in Endocytosis, Compartmentation, and Down-regulation of the Epidermal Growth Factor Receptor." The Journal of Biological Chemistry **266**: 11083-11094.
- Wollenberg, G. K., Harris, L., Farber, E. and Hayes, M. A. (1989). "Inverse relationship between epidermal growth factor induced proliferation and expression of high affinity surface epidermal growth factor receptors in rat hepatocytes." Lab. Invest. **60**(2): 254-259.
- Yanai, S., Sugiyama, Y., Kim, D. C., Iga, T., Fuwa, T. and Hanano, M. (1991). "Kinetic analysis of receptor-mediated endocytosis of epidermal growth factor by isolated rat hepatocytes." Amer. J. Phys. **260**: C457-67.
- Yang, L. J., Rhee, S. G. and Williamson, J. R. (1994). "Epidermal growth factor-induced activation and translocation of phospholipase C- $\gamma$ 1 to the cytoskeleton in rat hepatocytes." J. Biol. Chem. **269**(10): 7156-7162.
- Young, B. R., Lambrecht, L. K. and Cooper, S. L. (1982). Plasma Proteins: Their Role in Initiating Platelet and Fibrin Deposition on Biomaterials. Biomaterials: Interfacial Phenomena and Applications. S. L. Cooper and N. L. Peppas. Washington, DC, American Chemical Society. **199**: 317-350.
- Zapf, A., Hsu, D. and Olefsky, J. M. (1994). "Comparison of the intracellular itinerary of insulin-like growth factor and insulin and their receptors in Rat-1 fibroblasts." Endocrinol. **134**: 2445-2452.
- Zheng, J., Ito, Y. and Imanishi, Y. (1994). "Cell growth on immobilized cell-growth factor." Biomaterials **15**(12): 963-968.